

Evolutionary Dynamics in Food Webs: Influence of Resources and Space

Von der Mathematisch-Naturwissenschaftlichen Fakultät
an der Carl von Ossietzky Universität Oldenburg
zur Erlangung des Grades und Titels eines

Doktors der Naturwissenschaften (Dr. rer. nat.)

angenommene Dissertation

von Herrn Daniel Ritterskamp
geboren am 30.07.1987 in Willich

1. Gutachter: Prof. Dr. Bernd Blasius
2. Gutachter: Prof. Dr. Frank Hilker
Tag der Disputation: 30.09.2015

Erklärung zur Dissertation

Hiermit versichere ich, dass ich diese Arbeit selbständig verfasst und keine anderen als die angegebenen Quellen und Hilfsmittel benutzt habe. Außerdem versichere ich, dass ich die allgemeinen Prinzipien wissenschaftlicher Arbeit und Veröffentlichung, wie sie in den Leitlinien guter wissenschaftlicher Praxis der Carl von Ossietzky Universität Oldenburg festgelegt sind, befolgt habe.

Daniel Ritterskamp
Oldenburg, im August 2015

Kurzzusammenfassung

Seit langem sind Ökologen an dem in der Natur zu beobachtendem Artenreichtum interessiert und folglich auch an der Entstehung ökologischer Gemeinschaften. Die ersten Untersuchungen der Arten und deren Interaktionen innerhalb solcher Gemeinschaften, welche als Nahrungsnetze bezeichnet werden, wurde auf das achtzehnte Jahrhundert zurück datiert. Seitdem hat die Bedeutung solcher Nahrungsnetze in der Ökologie zugenommen, da das Wohlergehen der Menschheit stark von den erbrachten Ökosystemdiensten dieser Nahrungsnetze abhängt.

Jedoch sind viele Nahrungsnetze heutzutage durch externe Umwelteinflüsse, welche durch den Menschen verursacht werden, stark gefährdet. Um dem Entgegenzuwirken und Nahrungsnetze zu stabilisieren und zu konservieren ist es notwendig zu verstehen, wie diese Entstehen und auf äußere Störungen reagieren. Dies soll in dieser Arbeit behandelt werden.

Dazu wird die Modellklasse der allometrischen evolutionären Nahrungsnetzmodelle verwendet. Diese Modelle erzeugen Nahrungsnetze indem evolutionäre Prozesse und Populationsdynamik miteinander kombiniert werden. Arten werden innerhalb dieser Modelle hauptsächlich durch ihre Körpergröße beschrieben. In einigen Modellen werden zusätzliche beschreibende Eigenschaften verwendet, welche jedoch meistens von der Körpergröße abhängig sind. Die Interaktion zwischen zwei Arten wird durch den Unterschied ihrer Eigenschaften bestimmt. In dieser Arbeit werden diese Modelle herangezogen, um drei konzeptuelle Fragen bezüglich der Entstehung von Nahrungsnetzen zu untersuchen. Dies geschieht in drei separaten Kapiteln:

Im ersten Kapitel untersuchen wir Evolution in Nahrungsnetzen und versuchen zu beantworten, ob die entstehenden Nahrungsnetze aus einem evolutionären Gesichtspunkt aus statisch oder dynamisch sind. In empirischen Studien werden Nahrungsnetze häufig als statisch behandelt, jedoch gibt es Belege dafür, dass evolutionäre Dynamiken in der Form von evolutionären Zyklen in ökologischen Gemeinschaften auftreten können. Unsere theoretischen Untersuchungen implizieren, dass Evolution in vielen Nahrungsnetzen gegenwärtig ist. Des Weiteren finden wir innerhalb des verwendeten Modells neue evolutionäre Zustände. In diesen unterliegen entweder einzelne Arten evolutionären Zyklen oder ganze Nahrungsnetze. Die Konkurrenz zwischen Arten und die Wechselwirkung mit der Ressource sind für diese Zyklen von großer Bedeutung.

Im zweiten Kapitel überprüfen wir den Einfluss von Ressourcen auf die Entstehung von Nahrungsnetzen mit Hilfe von allometrischen evolutionären Nahrungsnetzmodellen. Dies ist motiviert durch die Beobachtung, dass viele natürliche Nahrungsnetze mehrere Ressourcen unterschiedlicher Größe enthalten. Dies wird jedoch in vielen Modellen nicht berücksichtigt und die meisten Modelle berücksichtigen lediglich eine einzelne Ressource. Aus diesem Grund untersuchen wir wie zusätzliche Ressourcen die Entstehung von Nahrungsnetzen beeinflussen. Um dies zu tun, entwickeln wir ein allometrisches Nahrungsnetzmodell in dem Arten lediglich durch ihre Körpergröße beschrieben werden und schließen zwei Ressourcen unterschiedlicher Größe in die Modellbeschreibung ein. Unsere Ergebnisse zeigen, dass durch die zusätzliche Ressource Partitionen innerhalb des Nahrungsnetzes auftreten können. Die Interaktionen zwis-

chen diesen Partitionen beeinflusst signifikant das Nahrungsnetz. Es können Oszillationen in den Biomassen der Arten auftreten oder sogar evolutionäre Intermittenz. Hinzu kommt, dass die Vielfalt der auftretenden Nahrungsnetzstrukturen zunimmt, da der Einfluss von hierarchischen Körpergrößenzusammenhängen verringert wird.

Im dritten Kapitel wird der Einfluss von einem höher dimensionalen Eigenschaftsraum auf die Entstehung von Nahrungsnetzen untersucht. Dies wird durch aktuelle Studien motiviert, die ergeben haben, dass Interaktion zwischen Arten nicht durch eine einzige Größe beschrieben werden können, sondern dass dazu ein höher dimensionaler Eigenschaftsraum notwendig ist. Dies wird jedoch von den meisten allometrischen evolutionären Nahrungsnetzmodellen nicht berücksichtigt, da in diesen die Artbeschreibung lediglich auf Körpergröße basiert. Aus diesem Grund führen wir ein allometrisches evolutionäres Nahrungsnetzmodell in einem zwei dimensionaligen Eigenschaftsraum ein, der von der Körpergröße und einer abstrakten Eigenschaft aufgespannt wird. Unsere Untersuchungen ergeben, dass die zusätzliche unabhängige Eigenschaft die Vielfalt der möglichen evolutionären Zustände als auch in der Nahrungsnetzstrukturen erhöht. Es treten evolutionär statische und auch dynamische Zustände auf, sowie Netzwerke mit einer hohen und niedrigen Ordnung.

Alle durchgeführten Studien zeigen, dass Evolution ein allgegenwärtiger Faktor in Nahrungsnetzen ist, der sich in vielfältiger Art und Weise manifestieren kann. Außerdem konnten wir beobachten, dass die verwendeten minimalistischen Modelle eine hohe Erklärungskraft haben, da diese Strukturen und Phänomene, welche in der Natur zu beobachten sind, reproduzieren können.

Abstract

Ecologists have long been interested in species diversity and thus, the emergence of ecological communities. The first study describing species and their interactions within such a community, summarised by food webs, dates back to the eighteenth century. Since then, the importance of food webs for ecology has increased, because humanity strongly depends on the provided ecosystem services. However, nowadays many food webs are endangered by environmental changes that are mainly caused by human impact. To stabilise and conserve these food webs, it is necessary to investigate how they react to perturbations and to understand their emergence. Therefore, the scope of this thesis is to study the emergence of food webs.

We use the framework of allometric evolutionary food web models, which generates food web topologies by combining evolution with population dynamics. In these models, the key trait to characterise a species is bodysize, additional traits are linked to the latter. The interaction strength between species is determined by their pairwise distances. We use this framework to face three conceptual questions regarding food web assembly, in three independent research chapters:

In the first chapter, we consider evolution in food webs and ask whether assembled food webs are evolutionarily static or if evolution is always present. Food webs in empirical and theoretical studies are mostly treated as evolutionary static, but empirical evidence exists for evolutionary cycling in ecological communities. Our studies reveal that evolution is present in many food webs and novel states are introduced: cycling of single morphs and complex food webs. For these, the competition range between species and feedback with the resource have proven to be important factors.

In the second chapter, we take a closer look at the importance of resources in allometric evolutionary food web models. Many empirical food webs contain multiple resources, but many models neglect this fact by considering a single resource only. Therefore, we study how additional resources influence food web assembly. To address this issue, we set up an allometric evolutionary food web model with species characterised by bodysize and include two resources of different sizes. Our finding shows that the additional resource can cause to the emergence of partitions, which also occurs in empirical food webs. Interactions between these partitions significantly influence the network. They give rise to biomass oscillations and evolutionary intermittence and increase the structural variety of food webs, since hierarchical bodysize interactions are weakened.

In the third chapter, we investigate the influence of higher dimensional trait space on food web assembly. This is motivated by recent findings, which state that a higher dimensional trait space is necessary to describe species interactions. However, most allometric evolutionary food web models solely base their species description on bodysize as a single trait. We introduce an allometric evolutionary food web model with species description based on bodysize and a second independent trait. We find that the additional dimension allows for various behaviours in evolution and network structures: evolutionary static and dynamic states, as well as ordered and

unordered food webs.

All our studies show that evolution is present in food webs and can manifest in various ways. In addition, the introduced minimalistic models have proven to have a high explanatory power, since they are able to reproduce structures and phenomena that are observed in empirical food webs.

Contributions to the chapters of this thesis

Throughout this thesis, I will use **we**, instead of **I** for two reasons. First, I want to include the reader and lead her or him through this work. Second, I did not write the research chapters, completely on my own. The contributions of all authors for these chapters is listed below:

Chapter 5:

Evolutionary cycles in an evolutionary food web model

Authors: Daniel Ritterskamp, Daniel Bearup, Bernd Blasius*

DR wrote the program and performed the study, which was supervised by BB. All authors contributed to the manuscript.

Chapter 6:

Evolutionary food web models: effects of an additional resource

Authors: Daniel Ritterskamp, Daniel Bearup, Christoph Feenders, Bernd Blasius*

DR, DB and BB developed the model set up. DR wrote the program and performed the study. DR and CF contributed to the manuscript.

Chapter 7:

A New Dimension: Evolutionary Food Web Dynamics in two Dimensional Trait Space

Authors: Daniel Ritterskamp, Daniel Bearup, Bernd Blasius*

DR, and BB developed the model. DR wrote the program and performed the study. All authors contributed to the manuscript. It was submitted to the Special Issue “Models in Evolution” of the “Journal of Theoretical Biology”.

In addition, the appendix contains one chapter presenting preliminary results (chapter appendix A) performed by myself, and a chapter (appendix B) introducing an already published paper “*Evolutionary food web model based on body masses gives realistic networks with permanent species turnover*” in “*Scientific Reports*” (doi: 10.1038/srep10955), with myself as an co-author.

Contents

Contributions to the chapters of this thesis	vi
I. Introduction	5
1. Motivation	7
1.1. Outline	7
2. Food webs	9
3. Evolutionary food web models	9
3.1. The allometric evolutionary food web model by Loeuille and Loreau (2005) . .	13
3.1.1. Population dynamics	13
3.1.2. Evolutionary dynamics	15
3.1.3. Classical network structure	15
3.1.4. Critical revision	17
3.2. An allometric evolutionary food web model in two dimensional trait space . . .	18
3.2.1. Population dynamics	18
3.2.2. Evolutionary dynamics	22
4. Objectives	23
II. Research chapters	25
5. Evolutionary cycles in an evolutionary food web model	27
5.1. Introduction	28
5.2. Model	30
5.2.1. Population dynamics	30
5.2.2. Evolutionary dynamics	31
5.2.3. Parameter values, implementation, and cycle detection	32
5.3. Results	32
5.3.1. Numerical simulations, revealing four dynamics regions	32
5.3.2. Invasion analysis	37
5.4. Discussion	42
5.A. Appendix	45

Contents

6. Evolutionary food web models: effects of an additional resource	46
6.1. Introduction	47
6.2. Multi-resource model	48
6.2.1. Population dynamics	49
6.2.2. Evolutionary Dynamics	50
6.2.3. Parameter values	50
6.3. Results	50
6.4. Discussion	57
6.A. Appendix	59
7. A new dimension: evolutionary food web dynamics in two dimensional trait space	61
7.1. Introduction	62
7.2. Model	64
7.2.1. Population dynamics	65
7.2.2. Evolutionary dynamics	67
7.2.3. Initialization and parameter values	67
7.2.4. Data evaluation	68
7.3. Results	68
7.3.1. Communities with no trophic structure (Region I)	69
7.3.2. Communities with trophic structure	71
7.3.3. Transitions between community types	76
7.3.4. Drivers of variation in structure	78
7.3.5. Comparison to empirical data	79
7.4. Discussion	81
7.A. Appendix	85
III. Discussion	89
8. Summary	91
9. Future work and open questions	93
IV. Appendix	97
A. Spatial sampling: Influence on the measured food web	99
A.1. Introduction	99
A.2. Model	100
A.3. Initialization and parameter values	100
A.4. Results	100
A.5. Discussion, shortcomings and future work	103

B. Evolutionary food web model based on body masses gives realistic networks with permanent species turnover	105
Bibliography	119
Curriculum vitae	127
Danksagung	129

Part I.

Introduction

1. Motivation

“There’s something that doesn’t make sense. Let’s go and poke it with a stick.”

— 5th Doctor —
Doctor Who, BBC ONE

Species diversity and thus the emergence of ecological communities is one of the major topics in ecology (Dunne, 2009; Darwin, 2011). These communities have been investigated for a long time with the first study dating back to the eighteenth century, which describes fish consuming each other in a pond (see Egerton (2007)). Since then, the interest of ecologists in these communities has increased further, since human well-being is strongly linked to the ecosystem services provided by them (Guo et al., 2010; Millennium Ecosystem Assessment, 2003). The provided services strongly depend on the stability of these ecological communities, since each change alters the provided ecosystem services (Dirzo et al., 2014; Dobson et al., 2006).

Thus, it is necessary to conserve these communities and keep them in their current state. To figure out the necessary steps, one has to understand the assembly of ecological communities and their reactions to perturbations. This gives rise to the following questions: How do ecological communities assemble and how do they react to invasive species (Brännström and Johansson, 2012; Lurgi et al., 2014)? What is the influence of resources on ecological communities (Huisman and Weissing, 1999; Wardle et al., 2004)? How many traits are necessary to characterise interactions between species in a community (Eklöf et al., 2013; Cohen, 1977)? Which mechanisms make assembled ecological communities stable and persistent (McCann, 2000; May, 1972)?

Therefore, the scope of this thesis is to study the assembly of ecological communities, also referred to as food webs. For this purpose, we use the framework of allometric evolutionary food web models. We examine the influence of environmental conditions on food web assembly, such as resource size distributions or spatial structure in a habitat. In addition, a focus is on the mechanisms that give rise to food web structures and evolutionary phenomena, which are observed in empirical data.

1.1. Outline

In this chapter, we introduce the general framework used in this thesis: first, we state the definition of food webs in chapter 2 and afterwards, we present the theoretical model class to describe food web assembly in chapter 3: allometric evolutionary food web models. We consider two explicit model versions, but also state ecological drawbacks within these. After this, we instigate each of the research chapters in Part II by motivating questions and stating their objectives (chapter 4).

1. Motivation

Each research chapter (chapter 5–7) represents one of three independent studies, each focuses on a different aspect of food web assembly. The first research chapter "Evolutionary cycles in an evolutionary food web model" (chapter 5) examines the presence of evolution in food webs, which is motivated by the fact that these are often treated as evolutionary static in empirical and theoretical studies. The second research chapter "Evolutionary food web models: effects of an additional resource" (chapter 6), considers the influence of additional resources on the assembly of food webs. The third research chapter "A new dimension: evolutionary food web dynamics in two dimensional trait space" (chapter 7), investigates the assembly of food webs in a two dimensional trait space.

In Part III, we answer the motivating questions of each research chapter and the main findings are summarised. Furthermore, the implications of each research chapter are brought into relation with each other and open questions and potential future work are presented.

In addition, two additional chapters are included in the appendix. Chapter appendix A entitled "Spatial sampling: influence on the measured food web" introduces preliminary results on the influence of the spatial sampling size on the observed food web. Additional work is necessary to complete this study and therefore it is only included in the appendix. Chapter appendix B contains an already published study introducing an allometric evolutionary food web model with three evolutionary traits, which is able to produce ecological realistic food webs. This paper is included in the appendix, since it is not in the main focus of this thesis, but gives additional inside into the assembly of food webs.

2. Food webs

“It is interesting to contemplate an entangled bank, clothed with many plants of many kinds, with birds singing in the bushes, with various insects flitting about, and with worms crawling through the damp earth, and to reflect that these elaborately constructed forms, so different from each other, and dependent on each other in so complex manner, have all been produced by laws acting around us.”

— Charles Darwin —
Concluding remarks, The Origin of Species

Within ecological communities species consume each other. These feeding interactions – trophic links – are summarised in networks; these are called **food webs** (Dunne, 2009). The food web is provided with energy by basal taxa ("self feeding"; e.g. autotrophs, detritus), which are species that do not feed on any other species. An overview over the history of food webs is given by Dunne (2009), which is briefly summarised in the following.

The first descriptions of food webs date back to Carl Linnaeus in 1749 and Charles Darwin in 1832 (Egerton, 2007). The first diagrams that depict food webs appeared in the beginning of the 19th century, but quickly became common in scientific literature. Within these diagrams (see Fig. 2.1 for an example), species are represented by nodes, while edges denote feeding links between them. These links are considered as directed, since energy flows from prey to predator (arrowheads point in this direction). Species are often aligned along a trait axis, such as bodysize or trophic level (see caption of Fig. 2.1 for a definition of trophic level).

The first comparative study compiling thirty food webs was published by Cohen (1977, 1997). To standardise the collected data, he transformed the food web diagrams into binary matrices, called **adjacency matrices**. In the following work, we consider adjacency matrices as quadratic matrices of size S , with S being the number of species contained in a food web. Each species has an assigned row and column, representing their incoming links (row, feeding input) and outgoing links (column, predation losses). A one denotes the presence of a link, while zero denotes the absence. Note that this is not the original definition of Cohen (1977).

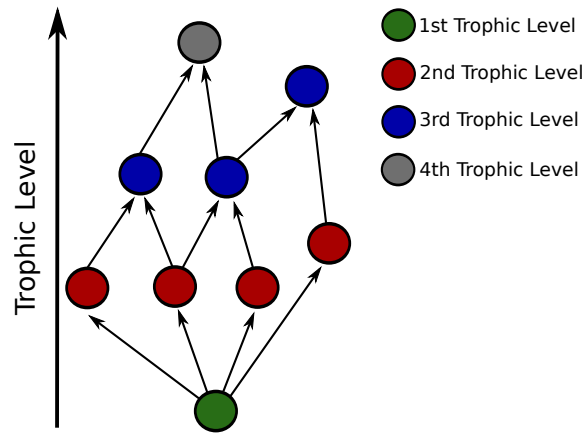


Figure 2.1.: Schematic food web representation. Arrows depict trophic links with arrowheads pointing into the direction of the energy flow (from prey to predator). Species are aligned according to their trophic level. Throughout this thesis, the flow based trophic level is used (Williams and Martinez, 2004). Therefore, the **trophic level** of species i is given by $t_i = 1 + \sum_{j, \text{Prey}} v_{ij} \cdot t_j$ with v_{ij} being the fraction of prey j on the total diet of species i . Resources have per definition a trophic level of one. Species are coloured according to their integer trophic level.

3. Evolutionary food web models

“Many were increasingly of the opinion that they’d all made a big mistake in coming down from the trees in the first place. And some said that even the trees had been a bad move, and that no one should ever have left the oceans.”

—Douglas Adams —
The Hitchhiker’s Guide to the Galaxy (1979 novel)

The assembly of food webs and their reaction to perturbations is an important aspect of ecological research. However, empirical data that consider the assembly is sparse, since the driving processes – invasion and evolution – occur on large time scales. To study evolution in small species, microorganisms were used (Mortlock, 2012), but for larger species theoretical models have to be applied. A various range of models exist that describe food web assembly, each focuses on different aspects. An elaborated overview can be found in (Brännström and Johansson,

2012; Loeuille and Loreau, 2009). In the following, we focus on three main classes: webworld models, matching models and allometric evolutionary food web models.

The matching model was introduced by Rossberg et al. (2006). Each species is characterised by two binary sequences of length n , one describes its vulnerability and the other its foraging ability. Each binary trait can represent oppositions, such as benthic and pelagic, nocturnal and diurnal, or sessile and vagile. The interaction strength between two species is given by the matching between the predator's foraging string and its prey's vulnerability string. The model itself considers random extinctions, invasions and speciation processes, but does not include any resources and population dynamics. Thus, only the presence or absence of species in a community is described. The resulting food webs have proven to be in good agreement with empirical food web data.

The webworld model was introduced by Caldarelli et al. (1998) and extended by Drossel et al. (2001). Similar to the matching model, each species is described by a binary string, representing the presence or absence of features, which affects interspecific interactions. New species are introduced by modifying existing species. In contrast to the matching model, the webworld model includes population dynamics.

Allometric evolutionary food web models characterise species, in contrast to the matching and webworld model, by continuous traits, with bodysize as the key trait. Therefore, these models are easy to interpret. In addition, resource dynamics are included. The fact that resources are explicitly considered and species description is based on bodysize, allows to integrate multiple different sized resources, a bodysize spectrum within species or an additional continuous traits (e.g. a spatial dimension). For this reason, we use the evolutionary food web formalism in this work.

An early predecessor of allometric evolutionary food web models are character displacement models, which describe the assembly of solely competing communities (Roughgarden, 1972). Species are characterised by a single continuous trait, which can be interpreted as bodysize, and determines their resource consumption and competition with other species. It is assumed that competition is stronger if traits are similar. The assembly itself is described by successively applying invasion and population dynamics. Within character displacement models, different kind of assembly algorithms were studied, which gave rise to different assembly dynamics (Rummel and Roughgarden, 1985; Taper and Case, 1992).

By extending character displacement models to describe the assembly of trophic communities, Loeuille and Loreau (2005) introduced the first allometric evolutionary food web model. It is well investigated and several studies exist, which investigated for instance the energetic equivalence rule (Loeuille and Loreau, 2006) or the mechanisms allowing stable food web structures to arise (Loeuille and Loreau, 2009; Allhoff and Drossel, 2013) within the model. Extensions of this model were also developed, to study the emergence of diversification by incorporating gradual evolution (Brännström et al., 2011), and to investigate how trade-offs in resource consumption influence the network structure (Ingram et al., 2009). In addition, to produce more realistic food webs, a recent study introduced additional feeding traits for each species (chapter appendix B). We refer the reader to Brännström and Johansson (2012) for an extensive overview.

3. Evolutionary food web models

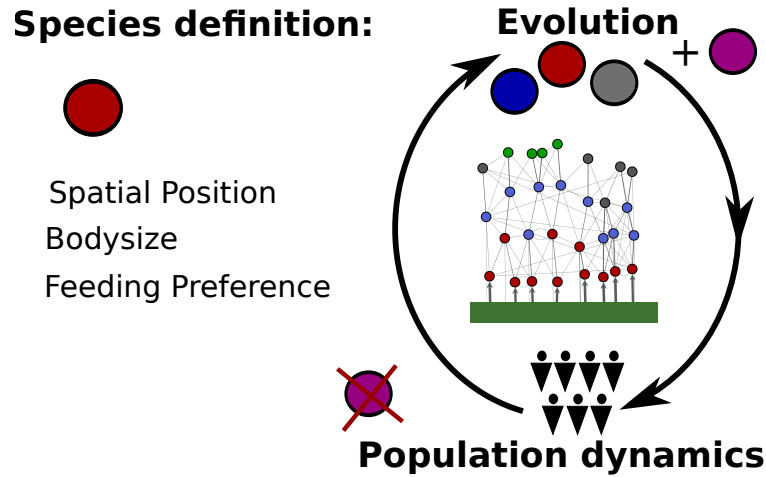


Figure 3.1.: Main idea of allometric evolutionary food web models. Species are characterised by evolutionary traits, e.g bodysize. Evolution and population dynamics are applied repeatedly. The first adds new species, which are similar to already existing species to the food web, and the second changes species biomasses and determines their survival. By doing this time and again complex food webs emerge.

In allometric evolutionary food web models, species are characterised by their biomass B_i , as a state variable, and a set of evolutionary traits. Thereby, the key trait is bodysize, but models exist that include additional evolutionary traits, which however are limited in their evolution. Independent evolving traits are considered in chapter 7. The emergence of food webs is described by the interplay of two components: evolution and population dynamics (Fig. 3.1).

Evolution is applied to the evolving traits. Via mutation events, new species are added to the food web, which are similar in traits to already existing species. These mutation events occur with a certain rate ω . Following such an event, population dynamics is applied, changing the biomasses B_i of all present species, to determine their survival. The biomass changes due to feeding interactions and competition between species. The respective interaction strength is determined by the relative distance of species in trait space. If the biomass B_i of a given species falls below a defined extinction threshold θ , it goes extinct and is removed from the food web. By applying evolution and population dynamics repeatedly, large and complex food webs emerge.

It is assumed that population dynamics and evolution are separated by time scales. Therefore, the population dynamics have to reach a static fixpoint between mutation events. To guarantee this, the mutation probability ω has to be sufficiently small. It is evident that this assumption is not fulfilled if biomass oscillations or chaotic behaviour occurs. However, within the original model (Loeuille and Loreau, 2005) and most successors only static fixpoints are reached. This is due to the fact that these are based on chemostat resource dynamics (Novick and Szilard, 1950) with linear functional responses and destabilisation is only possible if time delays between consumers (Ruan and Wolkowicz, 1996; MacDonald, 1976; Wolkowicz and Xia, 1997) or non-

3.1. The allometric evolutionary food web model by Loeuille and Loreau (2005)

linear functional responses (Fussmann et al., 2000) are included. However in chapter 6, we show that weak indirect feedback links between predator-prey pairs can lead to biomass oscillations within a food web. In this case, the interpretation of the model changes, since population dynamics and evolution occur on similar time scales, which can be applied to bacterial food webs (Fussmann et al., 2007).

The energy supply in this models is guaranteed by resources, which are not subject to evolution. In this work the term **resource** refers to any kind of energy input into the food web, e.g. light, nutrients, phytoplankton. Most allometric evolutionary food web models base the assembly on a single resource, despite the fact that empirical food webs can contain multiple resources (Dunbar, 1953). This problem is addressed in chapter 6.

The evolutionary algorithms used in most allometric evolutionary food web models do not consider speciation processes. Therefore we use the term **morph** instead of species in the following. The evolutionary algorithm itself should be interpreted as an evolutionary based assembly algorithm, since evolution is not considered on a genetic level and the bodysize difference between ancestor and mutant can be relatively large. Thus, the evolutionary algorithm describes mutation and invasion of morphs that are similar to existing ones.

3.1. The allometric evolutionary food web model by Loeuille and Loreau (2005)

The model by Loeuille and Loreau (2005) is the first allometric evolutionary food web model. The mechanism allowing the emergence of food web structure is well studied (Loeuille and Loreau, 2009). We use the classical model by Loeuille and Loreau (2005) in chapter 5 and an extended multi resource version in chapter 6, to investigate evolution in food webs and the influence of additional resources on food web assembly. Therefore, we present this classical model here in more detail. It considers one resource ($i = 0$) and a variable number of evolving morphs ($i = 1, \dots, N$). Each morph is described by its population biomass density B_i , as a state variable, and its bodysize m_i . The resource is associated with a fixed bodysize of $m_0 = 0$.

3.1.1. Population dynamics

The change of biomass B_i of morph i is given by the Lotka-Volterra equation, accounting for reproduction, intrinsic mortality, and losses due to predation and interference competition

$$\frac{dB_i}{dt} = B_i \left(\underbrace{f(m_i) \sum_{j=0}^N \gamma(m_i - m_j) B_j}_{\text{reproduction}} - \underbrace{\lambda(m_i)}_{\text{mortality}} - \underbrace{\sum_{j=0}^N \gamma(m_j - m_i) B_j}_{\text{predation}} - \underbrace{\sum_{j=1}^N \alpha(|m_i - m_j|) B_j}_{\text{competition}} \right). \quad (3.1)$$

Here, the intrinsic mortality $\lambda(m_i) = \lambda_0 m_i^{-0.25}$ and the production efficiency $f(m_i) = f_0 m_i^{-0.25}$ scale according to allometric relations with bodysize (Peters, 1986). The feeding kernel $\gamma(\cdot)$ describes the feeding rate exerted by predator i on prey j (Fig. 3.2). It is modelled as a one tailed

3. Evolutionary food web models

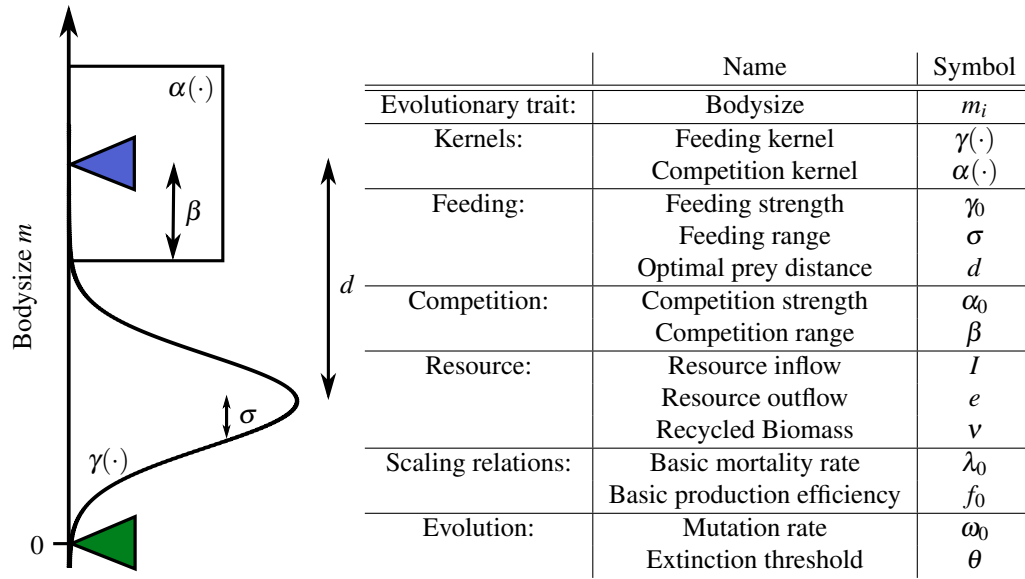


Figure 3.2.: Interaction kernels and model parameters. **Left:** One morph is positioned along the bodysize axis (blue triangle) and its feeding $\gamma(\cdot)$ and competition kernel $\alpha(\cdot)$ are plotted. In addition, the resource (green triangle) is shown. **Right:** Names and symbols of interaction kernels and parameters of the Loeuille and Loreau (2005) model.

Gaussian function of bodysize differences

$$\gamma(m_i - m_j) = \begin{cases} \frac{\gamma_0}{\sigma\sqrt{2\pi}} \exp\left(-\frac{(m_i - m_j - d)^2}{\sigma^2}\right), & m_i > m_j \\ 0, & \text{otherwise,} \end{cases} \quad (3.2)$$

where γ_0 can be used to scale the maximal feeding strength, and σ corresponds to the feeding range of a morph (i.e., the Gaussian function has standard deviation of $\sigma/\sqrt{2}$) and d is the optimal predator-prey bodysize distance. The feeding kernel reaches a maximum for a bodysize distance d . This follows from empirical observations, which have shown that morphs typically consume prey smaller than themselves (Vucic-Pestic et al., 2010; Brose et al., 2008; Riede et al., 2011). The cut-off for $m_i \leq m_j$ in the feeding kernel implies that a predator is only able to consume prey with a strictly smaller bodysize. This causes an asymmetry in trophic interactions: if two morphs that are nearly identical are considered, the larger one has a slightly larger reproduction growth (first term in Eq. (3.1)), since it can consume the smaller morph, while the reverse is not possible. This leads to an intrinsic evolutionary increase in bodysize of morphs, which will be discussed in chapter 5.

3.1. The allometric evolutionary food web model by Loeuille and Loreau (2005)

The competition kernel $\alpha(\cdot)$ describes interference competition between two morphs i and j (Fig. 3.2). It is modelled as a symmetric rectangular function of bodysize differences

$$\alpha(|m_i - m_j|) = \begin{cases} \alpha_0, & |m_i - m_j| < \beta \\ 0, & |m_i - m_j| \geq \beta, \end{cases} \quad (3.3)$$

where α_0 is the competition strength and β the competition range.

The biomass change of the resource $i = 0$ follows a chemostat equation

$$\begin{aligned} \frac{dB_0}{dt} = & I - eB_0 - \sum_{j=1}^N \gamma(z_j) B_j B_0 + v \sum_{j=1}^N \sum_{i=1}^N \alpha(|m_j - m_i|) B_j B_i \\ & + v \sum_{j=1}^N \lambda(m_j) B_j + v \sum_{j=1}^N \sum_{i=1}^N (1 - f(m_j)) \gamma(m_j - m_i) B_j B_i, \end{aligned} \quad (3.4)$$

consisting of a constant resource inflow I , a relative outflow of rate e , losses due to consumption by morphs, and three terms describing the recycling of a certain fraction v of dead biomass due to interference competition, intrinsic mortality, and preyed biomass that is not converted to predator biomass. The latter is expressed by $1 - f(m_j)$.

3.1.2. Evolutionary dynamics

The system is initialised with the resource (bodysize $m_0 = 0$ and initial biomass $B_0 = I/e$) and a single evolving morph of bodysize $z_1 = d$, corresponding to the maximal feeding strength on the resource. Each evolving morph mutates with a rate of ω_0 per unit biomass and unit time. At each mutation event of morph k , a new morph M is added to the system with bodysize m_M that is randomly chosen from the mutation interval $[0.8m_k, 1.2m_k]$. This interval is centred around, and increases linearly with, the bodysize of the mutating morph m_k . The new morph is introduced with an initial biomass of θ , which is also the extinction threshold. If due to the population dynamics the biomass B_k of a morph falls below this threshold θ , it is considered to be extinct and removed from the system.

3.1.3. Classical network structure

The food web structures, which were introduced in the original paper (Loeuille and Loreau, 2005), are evolutionary static, which denotes that the morph composition does not change any more, after the initial build up phase. These classical food web structures consist of several trophic level, each containing several morphs. Each morph consumes all morphs in the trophic level below, which is independent of the used parameters, since the feeding relations of the model are fixed (Allhoff and Drossel, 2013).

An example of the temporal evolution of a classical food web and its respective time averaged biomass-bodysize distribution is shown in Fig. 3.3. The network consists of several clearly separable bodysize compartments that keep a bodysize distance d to each other, corresponding to the optimal feeding distance. These compartments are analogous to trophic levels. The morphs in the same trophic level are separated by a bodysize distance of β , allowing morphs to avoid

3. Evolutionary food web models

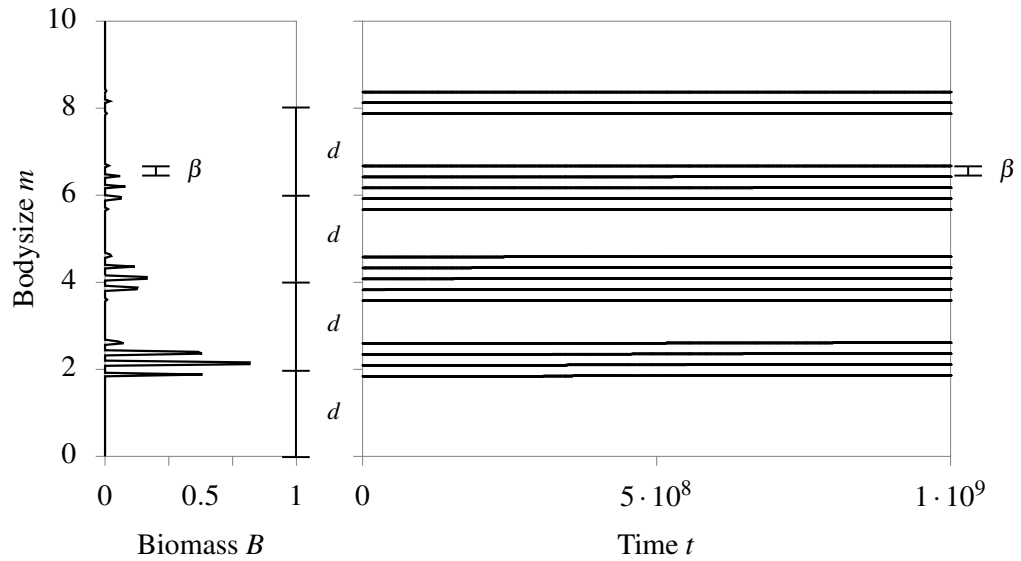


Figure 3.3.: Evolutionary food web dynamics, showing the time averaged biomass-bodysize histogram of all morphs (left) and the bodysizes of all morphs over time (right). An evolutionarily static food web emerges, as introduced in the original paper (Loeuille and Loreau, 2005). It consist of three distinct bodysize compartments, each representing a trophic level. Trophic levels appear at bodysizes that are multiples of d . Morphs in the same bodysize compartment keep a distance of β . The parameters were set to: $f_0 = 0.3$, $\lambda_0 = 0.1$, $\gamma_0 = 1$, $d = 2$, $I = 10$, $e = 0.1$, $v = 0.5$, $\omega_0 = 1e-05$, $\sigma = 1$, $\alpha_0 = 0.3$ and $\beta = 0.2$.

exclusive competition. The time averaged biomass-bodysize distribution is composed of single peaks indicating that the morph composition is nearly static after the initial build up of the network.

The distinctness of the bodysize compartments strongly depends on the parameters. For weak competition strengths α_0 and small feeding ranges σ , these compartments are distinct (see example Fig. 3.3), for increasing parameters the bodysize compartments merge and become indistinguishable. The resource parameters (I, e, v), the feeding strength γ_0 and the competition range β are kept fixed in the classical studies. The latter parameter is set to small values, imposing that only morphs with very similar bodysizes interact with each other.

3.1.4. Critical revision

Since the assembly of food webs is highly complex and due to the fact that the model of Loeuille and Loreau (2005) was the first allometric evolutionary food web model, some ecological facts are simplified. We are going to address a few of them in the following:

Allometric scaling describes the dependency of morph specific traits (e.g. intrinsic mortality, conversion efficiency) on bodysize, which was studied in great detail by Peters (1986). The model of Loeuille and Loreau (2005) is one of the first that incorporated allometric relationships into the morph description, but the used allometric scaling is incomplete. An additional allometric factor of $m_i^{-0.25}$ should be included in the predation losses in Eq. (3.1) (see box in chapter 3.2). Besides, the allometric factor has only a small influence in the model, since all bodysizes are within a small range [2 : 15]. Therefore, the allometric factor $m_i^{-0.25}$ ranges between [0.84 : 0.5] and does not lead to different time scales between morphs of different sizes.

The feeding kernel describes the ability of morphs to consume each other. The function used by Loeuille and Loreau (2005) has an optimum at a certain distance to its own bodysize, as supported by empirical data, since the energy gained by a predator of a given size increases with prey bodysize, while the probability for a successful attack decreases (Peters, 1986). However, it is known that the feeding kernel should be asymmetric and therefore a Riekers function is a ecological more accurate description (Vucic-Pestic et al., 2010).

The functional response used in the original model is linear, which assumes that the time a predator spends consuming or foraging for prey is negligible. For very large prey populations, this is ecologically inaccurate, since the predator growth rate is unrealistic high. This can be corrected by using a Holling type functional response (Holling, 1959), which incorporates saturation.

Competition in the model causes direct biomass losses. However, competition is rather a time consuming factor, since empirical studies showed that competition seldom results in death of individuals. Thus, an alternative way to model competition is to incorporate it into the functional response (Beddington–DeAngelis functional response; (Beddington, 1975)).

In the model by Loeuille and Loreau (2005), competition is based on interference competition, described by a boxed shape competition kernel. Thus, competition is either present or absent, which is an oversimplification. Therefore, the box-function should be substituted by a smooth function. Competition can also be based on link overlap (similarity of diets), which occurs between two predators that share the same prey. In this case, the competition kernel is given by the overlap of the feeding kernels of both competing morphs (MacArthur and Levins, 1967; Scheffer and van Nes, 2006), resulting in similar sizes of competition and feeding range. As mentioned above, in the classical study of the model by Loeuille and Loreau (2005) the competition range was kept small. Motivated by this, we consider the effect of larger competition ranges in chapter 5.

Recently, an ecologically more accurate food web model was introduced, which considered most of the above mentioned points and also incorporated individual feeding ranges and feeding centres for each morph (chapter appendix B). In addition to bodysize, the feeding centre and feeding range evolve within certain preimposed intervals. This model produces network structures

3. Evolutionary food web models

that are in good agreement with empirical data. However, due to the interdependent morph traits, the behaviour of the model is highly complex and novel phenomena occur. This hinders the investigation of specific effects. Therefore, the more minimalistic model by Loeuille and Loreau (2005) is used in chapter 5 and a multi resource version in chapter 6.

3.2. An allometric evolutionary food web model in two dimensional trait space

The model of Loeuille and Loreau (2005) characterises morphs solely by their bodysize. Other studies considered more traits, but these were either limited in their evolutionary range (Ingram et al., 2009, chapter appendix B). However, recent studies stressed that a higher dimensional trait space is necessary to describe morph interactions within a food web (Allesina et al., 2008; Eklöf et al., 2013). Therefore, additional independent evolutionary traits have to be considered in allometric evolutionary models.

To investigate the effect of this higher dimensional space, we set up an allometric evolutionary food web model in an two dimensional trait space. For this purpose, we start with the model of Loeuille and Loreau (2005), complete the allometric scaling, use a more realistic feeding kernel, base competition on link overlap (see previous section); and add an additional trait dimension to characterise morphs. The interactions along the additional dimension are motivated by the model of MacArthur and Levins (1967): morphs interact stronger with decreasing distance along this axis. However, we decided to keep the additional trait abstract, using only neutral assumptions. Therefore, the abstract trait can describe space, but also water column height, time of activity or resource requirements. It may also be interpreted as an underlying gradient, such as temperature, salinity, day length, rainfall.

The model considers a variable number of evolving morphs ($i = 1, \dots, N$), each characterised by two evolutionary traits – logarithmic bodysize z_i and an abstract trait x_i – and a population biomass density B_i , which varies due to interactions with other morphs. The resource has a bodysize $z_R = 0$ and is continuously distributed along the abstract trait axis, which has a length of L . However, we use periodic boundary conditions to simulate an infinite range.

It is to mention that the parameter notation used in the Loeuille and Loreau (2005) model and this model differ. For instance, the feeding kernel is now referred to as $\alpha(\cdot)$ and the competition kernel as $c(\cdot)$, see Table 3.1 for a list of all parameters. More important is that this model considers the **logarithmic bodysize z** instead of *normal bodysize*. Therefore, the feeding kernel becomes asymmetric and the allometric scaling gains influence, since bodysize now spans a range of $[10 : 10^9]$ (see section 3.1.4).

3.2.1. Population dynamics

The change of biomass B_i of morph i is given by Lotka-Volterra equations, accounting for reproduction by consuming other morphs and the resource, intrinsic mortality, and losses due to

3.2. An allometric evolutionary food web model in two dimensional trait space

	Name	Symbol
Evolutionary traits:	Logarithmic bodysize	z_i
	Abstract trait	x_i
Kernels:	Feeding kernel	$\alpha(\cdot)$
	Competition kernel	$c(\cdot)$
	Distribution abstract trait	$u(\cdot)$
	Abstract trait interaction strength	$I(\cdot)$
Feeding:	Attack strength	α_0
	Feeding range	σ_z
	Optimal prey distance	d
	Abstract trait range	σ_x
Competition:	Competition strength	c_0
Resource:	Resource input	I
	Resource outflow	e
Scaling relations:	Basic mortality rate	λ_0
	Basic production efficiency	f_0
Evolution:	Time between mutations	t_m
	Extinction threshold	θ

Table 3.1.: Interaction kernels and parameters of the allometric evolutionary food web model in two dimensional trait space. Scaling relations and evolutionary parameters are kept fixed. Note that this model does not have an explicit parameter for the competition range, since feeding and competition ranges are interdependent due to link overlap competition. This reduces the number of free parameters.

predation and competition, similar to Loeuille and Loreau (2005),

$$\begin{aligned}
 \frac{dB_i}{dt} = B_i & \left(\underbrace{f_0 a(z_i) \sum_{j=1, i \neq j}^N \alpha(z_i, z_j, x_i, x_j) B_j}_{\text{reproduction}} + \underbrace{f_0 a(z_i) \int_0^L dx \alpha(z_i, z_R, x_i, x) R(x)}_{\text{mortality}} - \lambda_0 a(z_i) \right. \\
 & \left. - \underbrace{\sum_{j=1}^N a(z_j) \alpha(z_j, z_i, x_j, x_i) B_j}_{\text{predation}} - \underbrace{\sum_{j=1}^N c(z_i, z_j, x_i, x_j) B_j}_{\text{competition}} \right), \quad (3.5)
 \end{aligned}$$

where f_0 is the conversion efficiency and λ_0 is the basic mortality rate. Feeding interactions, predation and consumption, and the intrinsic mortality scale according to allometric relations with bodysize (Peters, 1986), which is expressed by $a(z_i) = 10^{-0.25z_i}$. Morphs feed on the continuously distributed resource, which gives rise to the integral expression in equation (3.5).

The feeding kernel $\alpha(\cdot)$ describes the ability of predator i to consume prey j . We assume that the feeding kernel is a product of two functions, describing the bodysize and abstract trait interactions,

$$\alpha(z_i, z_j, x_i, x_j) = \alpha_0 \alpha_z(z_i, z_j) I(x_i, x_j), \quad (3.6)$$

3. Evolutionary food web models

with α_0 being the attack strength (Fig. 3.4c). The bodysize dependency of the feeding kernel is similar to Loeuille and Loreau (2005) of Gaussian shape, but only along the logarithmic bodysize axis. Regarding the *normal* bodysize axis the feeding kernel is asymmetric as proposed by Vucic-Pestic et al. (2010). The bodysize dependency of the feeding kernel is given by

$$\alpha_z(z_i, z_j) = \frac{1}{\sigma_z \sqrt{2\pi}} \exp\left(-\frac{(z_i - z_j - \log(d))^2}{2\sigma_z^2}\right), \quad (3.7)$$

where d is the optimal predator-prey bodysize distance and σ_z corresponds to the feeding range of a morph.

The dependency of the feeding kernel (and the general interaction between two morphs) on the abstract trait is calculated following MacArthur and Levins (1967). It is assumed that a given morph utilises a certain range around its abstract trait value x_i , described by the utilisation function

$$u_i(x) = \frac{1}{\sigma_x \sqrt{2\pi}} \exp\left(-\frac{(|x_i - x|)^2}{2\sigma_x^2}\right), \quad (3.8)$$

with a range σ_x (Fig. 3.4a). The interaction strength between two morphs is then given by the normalised integral of the product of their utilisation functions (Scheffer and van Nes, 2006):

$$I(x_i, x_j) = \frac{\int_{-\infty}^{\infty} dx u_i(x) u_j(x)}{\int_{-\infty}^{\infty} dx u_i^2(x)} = \frac{1}{\sigma_x \sqrt{4\pi}} \exp\left(-\frac{(|x_i - x_j|)^2}{4\sigma_x^2}\right), \quad (3.9)$$

which has a width of $\sqrt{2}\sigma_x$ (Fig. 3.4b).

The function $c(\cdot)$ describes the link overlap competition between two morphs i and j . Competition is therefore based on two morphs sharing potential prey (having a similar diet), and is determined by their overlap in the abstract trait (Eq. (3.9)) and the potential prey they have in common. The latter is calculated from the overlap of the morphs' feeding kernel in bodysize

$$c_z(z_i, z_j) = \frac{\int_{-\infty}^{\infty} dz \alpha_z(z_i, z) \alpha_z(z_j, z)}{\int_{-\infty}^{\infty} dz \alpha_z(z_i, z)} = \frac{1}{\sigma_z 2\sqrt{\pi}} \exp\left(-\frac{(z_i - z_j)^2}{4\sigma_z^2}\right). \quad (3.10)$$

The link overlap competition is then obtained by taking the product of these two overlaps,

$$c(z_i, z_j, x_i, x_j) = c_0 c_z(z_i, z_j) I(x_i, x_j), \quad (3.11)$$

where c_0 is the competition strength (Fig. 3.5b). In contrast to the classical model by Loeuille and Loreau (2005) (section 3.1), the competition ranges in bodysize and abstract trait space are now related to the ranges of the utilisation function $u_i(x)$ and the bodysize feeding kernel $\alpha_z(\cdot)$ and are therefore no independent parameters.

3.2. An allometric evolutionary food web model in two dimensional trait space

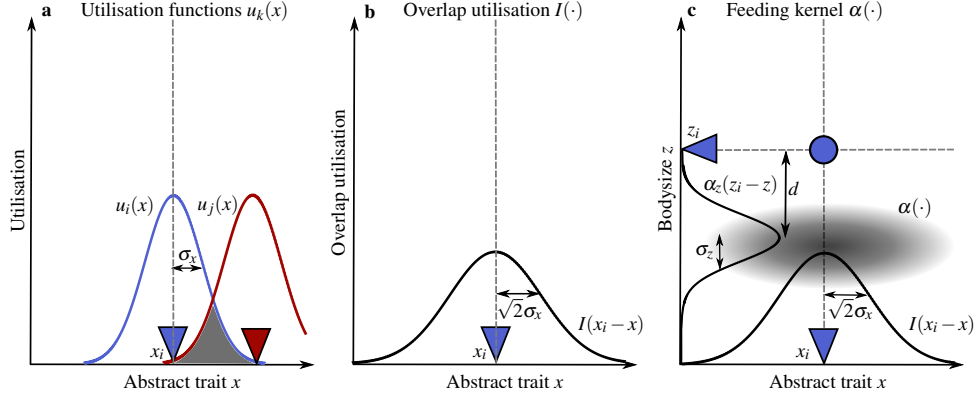


Figure 3.4.: Derivation of the utilisation overlap $I(\cdot)$ and feeding kernel $\alpha(\cdot)$. **a:** Utilisation function $u_k(x)$. Following MacArthur and Levins (1967), we assume that a morph k utilises a certain range σ_x around its abstract trait value x_k , described by its utilisation function (see Eq. 3.8). **b:** Utilisation overlap $I(\cdot)$ between two morphs (Eq. (3.9)). It is given by the normalised overlap of their utilisation functions (grey area in **a**) and has a width of $\sqrt{2}\sigma_x$. **c:** Feeding kernel $\alpha(\cdot)$, which is composed of the utilisation overlap $I(\cdot)$ and the bodysize feeding kernel $\alpha_z(\cdot)$ (Eq. 3.7). The latter has a maximum at a logarithmic bodysize of $z_i - \log(d)$ and a width of σ_z .

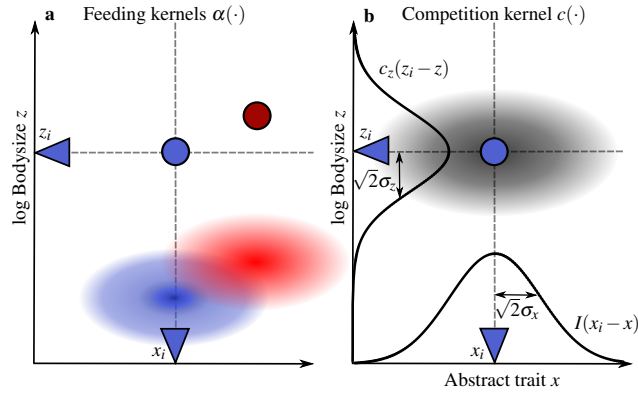


Figure 3.5.: Derivation of the competition kernel $c(\cdot)$. **a:** Overlap of the feeding kernels $\alpha(\cdot)$ of two morphs. **b:** Competition kernel $c(\cdot)$, composed of the utilisation overlap $I(\cdot)$ and the overlap of the bodysize feeding kernels of the competing morphs $c_z(\cdot)$. The latter has a width of $\sqrt{2}\sigma_z$. Therefore, the competition ranges in bodysize and the abstract trait depend on the ranges of the bodysize feeding kernel and the utilisation function and are no independent parameters.

3. Evolutionary food web models

Annotation: The competition term in Eq. (3.5) has no allometric factor in the biomass representation of the population sizes, while the reproduction and predation terms include an allometric factor ($a(z_i) = 10^{-0.25z_i}$). This is due to the fact that we ignore the allometric factors in the individual based feeding kernel, when calculating the similarity of the diets of two morphs:

If starting from the individual representation (Number of individual N_i), the feeding kernel scales with bodysizes of the prey and predator ($\alpha(z_i, z_j, x_i, x_j) 10^{0.75z_i} 10^{z_j}$). In the biomass representation this results in the allometric factor $a(z_i)$ in the predation and growth term. However, when calculating link overlap competition (Eq. (3.10)), we neglect these factors, since the similarity of their diets (prey they have in common) should not be affected by this. Therefore, the competition term has another allometric factor than the predation and growth terms.

The resource has a constant bodysize and is continuously distributed along the abstract trait axis. The dynamics of the resource is given by the following chemostat equation

$$\frac{dR(x)}{dt} = I - eR(x) - \sum_{j=1}^N \alpha(z_j, z_R, x_j, x) B_j R(x) \quad (3.12)$$

where the first and second terms represent a constant input I and an outflow e relative to the resource biomass respectively. The final term describes losses due to consumption by the morphs in the system.

3.2.2. Evolutionary dynamics

The evolutionary algorithm differs from the model of Loeuille and Loreau (2005), since we introduce a fixed mutation period $t_m = 10^5$ after that we allow one mutation. A morph k is randomly picked and a mutant M is added to the food web, with a new abstract trait $x_M \in [x_k - 0.8, x_k + 0.8]$ and logarithmic bodysize $z_M \in [z_k - \log(2), z_k + \log(2)]$. In comparison, the model by Loeuille and Loreau (2005) assigned each morph an individual mutation probability and therefore mutation events could occur close to each other, which is not possible with a fixed mutation period. A mutant is introduced with an initial biomass of $\theta = 10^{-10}$, which is also the extinction threshold. If the biomass B_k of any morph falls below this threshold it is considered extinct and removed from the food web.

4. Objectives

Albert grunted. "Do you know what happens to lads who ask too many questions?" Mort thought for a moment. "No," he said eventually, "what?" There was silence. Then Albert straightened up and said, "Damned if I know."

— *Mort, Discworld Novels* —
Terry Pratchett

The previous chapters have highlighted that food web assembly is of high complexity. Consequently, theoretical descriptions have to use approximations and are to a certain extent incomplete. Therefore, many unanswered conceptual questions exist. Some of them we consider in the following research chapters.

1) Question: How static is static? Food webs in empirical and theoretical studies are mostly considered as evolutionary static. This idea is also represented in the study of Loeuille and Loreau (2005), which focused on evolutionary static food webs and did not investigate evolutionary dynamics. However, empirical evidence exist that ecological communities are subject to evolutionary cycling. A common example are taxon cycles (Roughgarden and Pacala, 1989), during which an island community consisting of a single resident is invaded by a similar but slightly larger morph. Invader and resident coevolve with each other until the resident goes extinct. The bodysize of the invader adapts to the size of the former resident and the cycle resets. The underlying evolutionary process is driven by competition and therefore, it is to expect that taxon cycles also occur in larger communities, such as food webs (continental taxon cycles (Ricklefs and Bermingham, 2002)).

Thus, the objective of chapter 5 is to investigate taxon cycles in food webs and by doing so, demonstrate that evolution is present in food webs. For this purpose, we use the model by Loeuille and Loreau (2005) and study an extended competition parameter range (section 3.1.3), since taxon cycles are driven by competition. We reveal novel states in the model: cycling of single morphs and complex food webs. For these, the feedback with the resource has proven to be an important driver.

2) Question: How do resources of different sizes influence food webs? Many empirical food webs contain multiple resources, such as seaweed, salt, nutrients and dendritus (Dunbar, 1953), or they include resources that can be divided into size classes, such as phytoplankton (Sommer et al., 2002; Downing et al., 2014). Morphs can specialise on resources of different sizes, which leads to the emergence of partitions within a food web, as observed in soil food webs (Wardle et al., 2004;

4. Objectives

Fukami et al., 2006; Larios and Suding, 2014). Despite these empirical observations, allometric evolutionary food web models neglect the fact that food webs can be based on multiple resources by considering a single resource only. Therefore, the objective of chapter 6 is to emphasise the importance of additional resources, when describing the assembly of food webs. For this purpose, we extend the model of Loeuille and Loreau (2005) by an additional resource of various size and investigate the emerging structures and their influence on evolution and population dynamics. We find that additional resources can describe the emergence of partitions, which increases the structural variety and can also destabilise the population dynamics, leading to biomass oscillations.

3) Question: How does a higher dimensional trait space influence food web assembly?

Ongoing discussions are taking place about how many dimensions are necessary to determine morph interactions. Cohen (1977) stated that one dimension is enough, but contradicting studies were published, which stressed the necessity of a higher dimensional trait space (Allesina et al., 2008; Eklöf et al., 2013). Nonetheless, it is not only essential to use the right number of dimensions, but also to consider the correct traits.

Recent empirical studies emphasised the influence of space on food webs (Dunne, 2009; Amarasekare, 2008): biodiversity patterns are found along latitudinal and longitudinal gradients (Stomp et al., 2011), network characteristics scale with spatial range of the community (Brose et al., 2004) and migration processes can stabilize food webs (Holt, 2002).

However, allometric evolutionary food web models focus on bodysize and parameters that depend on it. Thus, little is known about the influence of space, or more generally an additional independent trait axis, on food web assembly. Therefore, the objective of chapter 7 is to investigate food web assembly in higher dimensional trait space and to study the phenomena that occur due the higher dimensionality. We start exploring the higher dimensional trait space, by constructing the minimal model in two dimensional trait space, which was introduced in chapter 3.2. In addition, to demonstrate the ecological accuracy of the higher dimensional food webs, we compare them to empirical data. Our results show that the additional trait axis allows the emergence of communities with a great range of network structures and evolutionary dynamics. For these the relative importance of competition and predation has proven to be a key determinant.

Part II.

Research chapters

5. Evolutionary cycles in an evolutionary food web model

Evolutionary cycles in an evolutionary food web model

Daniel Ritterskamp¹, Daniel Bearup, Bernd Blasius

CvO University Oldenburg, ICBM, Carl-von-Ossietzky-Strasse 9-11, 26111 Oldenburg, Germany

Abstract

The interplay of population dynamics and evolution within ecological communities has been of long-standing interest for ecologists and can give rise to evolutionary cycles, e.g. taxon cycles. Evolutionary cycling was intensely studied in small communities with asymmetric competition; the latter drives the evolutionary processes. Here we demonstrate that evolutionary cycling arises naturally in larger species communities if trophic interactions are present, since these are intrinsically asymmetric. To investigate the evolutionary dynamics of a trophic community, we use an allometric food web model. We find that evolutionary cycles emerge naturally for a large parameter ranges. The origin of the evolutionary dynamics is related to an intrinsic asymmetry in the feeding kernel which creates an evolutionary ratchet, driving species towards larger bodysize. We reveal different kind of cycles: single morph cycles, and coevolutionary and mixed cycling of complete food webs. The latter denotes that each trophic level can have a different evolutionary dynamic. We discuss the generality of our findings and conclude that ongoing evolution in food webs may be more frequent than commonly believed.

Keywords: Community cycling, Taxon Cycles, Coevolution, Red-Queen Dynamic, Large community-evolution models

5.1. Introduction

One of the most striking characteristics of ecological communities is their rich structure and variety among different habitats (Strong, 1992; Persson et al., 1992; Polis, 1991). To explain this large observed diversity, one of the main goals of evolutionary ecology is to gain a complete understanding of community assembly. It is known that the assembled community is determined by the interplay of population dynamics, driven by species interactions (e.g. competition and feeding relationships), and evolutionary processes, which change the phenotypic traits of populations within the community and may give rise to emergence of new species by speciation events. The outcome of such eco-evolutionary processes is not easy to understand from first principles and it may result in static or dynamic community structures.

The appearance of dynamic structures and cycles has been well-studied for the case of competitive interactions on a niche axis, such as bodysize (MacArthur Levins 1972). Thereby, a

¹Corresponding author

particularly important role has been attributed to the asymmetry of species interactions, which may be caused for instance by allometric scaling of consumption rates with bodysize. As suggested by Rummel and Roughgarden (1983), the joint effect of colonization and asymmetric competition favours the occurrence of evolutionary cycles, e.g. taxon cycles. These describe a scenario where a local habitat, which is occupied by a single resident species, is sequentially colonized by a new invading species of larger bodysize. This forces the smaller resident to evolve to even smaller bodysizes, to reduce competition with the larger invader. The larger invader follows this evolutionary movement and converges in bodysize towards the resident. In this coevolutionary arms-race towards smaller bodysizes, the resident eventually is driven out of its fundamental niche range and becomes extinct, leading to a single species community. This can again be invaded by a larger species and the cycle repeats itself. It was shown that this simple mechanism is able to describe empirical data for *Anolis* lizards (Roughgarden and Pacala 1989) and was subsequently investigated in a series of further studies (e.g., Rummel and Roughgarden 1985, Taper and Case 1992, Matsuda and Abrams 1994). In these studies, it was found that evolutionary cycles are a robust model outcome, but the details of the cycles depend on the specific model assumptions. In particular, it is possible that the bodysize change of the cycle operates in the reverse direction, so that species are driven towards larger bodysizes.

While evolutionary cycles have been studied intensely for competitive interactions, not much is known about their relevance in trophically structured communities. This is quite astonishing, given the striking structural similarity of allometric evolutionary food web models (Brännström and Johansson, 2012) to the above mentioned competition models. One of the first allometric evolutionary food web models, was introduced by Loeuille and Loreau (2005). In this model, similar to (Rummel and Roughgarden 1983, 1985, Taper and Case 1992, Matsuda and Abrams 1994) each species is characterized by its bodysize and feeding and competitive interactions between species are determined by their difference in bodysize. In addition, allometric relations are explicitly considered (Peters, 1986). The model, and several variants, were studied in great detail (Loeuille and Loreau, 2006, 2005; Allhoff and Drossel, 2013; Brännström et al., 2011; Allhoff et al., 2015a). Given that predator-prey interactions are naturally asymmetric, one would expect that evolutionary cycles are a typical outcome in evolutionary food web models. However, all these studies focused mainly on evolutionary static food web structures, whereas evolutionary cycles have not been considered (Loeuille and Loreau, 2005; Brännström et al., 2011). To our knowledge only one recent study, investigating a variant of the Loeuille and Loreau (2005) model with three evolving traits, introduced robust not-static evolutionary behaviour in the form of irregular extinction avalanches (Allhoff et al., 2015a) - however, such dynamics are quite different from the regular dynamics of the above described taxon cycles.

In this study, we revisit the well-studied evolutionary allometric food web model by Loeuille and Loreau (2005). We show that this model indeed can produce evolutionary cycles in a large parameter range and that the possibility of evolutionary cycles is related to the competition between species. When Loeuille and Loreau (2005) introduced this model, they found food webs that are relatively invariant over time. While these results proved to be robust to a broad range of feeding ranges and competition strength, the rest of the parameter space was relatively unexplored. In particular, the parameter governing the bodysize distance over which morphs can compete, the competition range, was limited to rather small values. While some biological justification for this

5. Evolutionary cycles in an evolutionary food web model

range was given, here we argue that this range may be too small. If competition between species arises from niche overlap (*sensu* MacArthur and Levins (1967)), we should expect a competition range that is significantly broader and is of the same order as the feeding range of a species. This would allow inter-species competition to have a much more significant effect on the evolutionary dynamics.

Motivated by this observation, we numerically investigate the evolutionary behaviour in the model (Loeuille and Loreau, 2005), by systematically varying the strength and range of the competition between species. Our simulations show that evolutionary cycling, where species are driven towards larger bodysizes, is naturally present in the considered model – not only between single species but also in large trophic communities. Thereby, we observe a plethora of dynamics regimes. Beside static food webs, we observe evolutionary single morph cycles, complex community cycles where different trophic levels undergo separate coevolutionary cycles, as well as transient dynamics. Using invasion analysis and Pairwise Invasibility Plots (PIPs) we are able to support the numerical observations, which allows us to explain the mechanism underlying the evolutionary cycles. Our findings imply that ongoing evolution in food webs may be more frequent than commonly believed.

5.2. Model

We follow the evolutionary food web model by Loeuille and Loreau (2005). The model considers one basal resource, such as an inorganic nutrient, ($i = 0$) and a variable number of evolving morphs ($i = 1, \dots, N$). We use the term morph, rather than species, since we are not considering the speciation process. Each morph is described by its population biomass density B_i and bodysize z_i . The resource has a total density B_0 and is associated with a non-evolving ‘bodysize’, which is fixed to the value $z_0 = 0$. The model consists of a population dynamics and an evolutionary dynamics component, both of which operate on different time scales. The population dynamic describes the trophic interactions among morphs and determines their respective growth, survival or extinction. On a larger time-scale, usually after the population dynamics has reached an attractor, new morphs are added to the community by an evolutionary-algorithm.

5.2.1. Population dynamics

The change of biomass B_i of morph i is given by the Lotka-Volterra equations, accounting for reproduction, intrinsic mortality, and losses due to predation and interference competition (Loeuille and Loreau, 2005)

$$\frac{dB_i}{dt} = B_i \left(\underbrace{f(z_i) \sum_{j=0}^N \gamma(z_i - z_j) B_j}_{\text{Reproduction}} - \underbrace{m(z_i)}_{\text{Mortality}} - \underbrace{\sum_{j=0}^N \gamma(z_j - z_i) B_j}_{\text{Predation loss}} - \underbrace{\sum_{j=1}^N \alpha(|z_i - z_j|) B_j}_{\text{Competition}} \right). \quad (5.1)$$

Here, the intrinsic mortality $m(z_i) = m_0 z_i^{-0.25}$ and the production efficiency $f(z_i) = f_0 z_i^{-0.25}$ scale according to allometric relations with bodysize (Peters, 1986). The function $\gamma(z_i - z_j)$

describes the consumption rate exerted by predator i on prey j . The model assumes that the feeding efficiency decays with the bodysize difference as a one tailed Gaussian function

$$\gamma(z_i - z_j) = \begin{cases} \frac{\gamma_0}{\sigma\sqrt{2\pi}} \exp\left(-\frac{(z_i - z_j - d)^2}{\sigma^2}\right), & z_i > z_j \\ 0, & z_i \leq z_j, \end{cases} \quad (5.2)$$

where d is the optimal predator-prey bodysize distance, γ_0 can be used to scale the maximal consumption strength, and σ describes the feeding range of a morph (i.e., the Gaussian function has standard deviation of $\sigma/\sqrt{2}$). The cut-off for $z_i \leq z_j$ in the feeding kernel implies that a predator is only able to consume prey with a strictly smaller bodysize. This causes an asymmetry in trophic interactions, wherein the larger of two similar sized morphs has a small advantage since it can consume, but cannot be consumed by, the smaller one.

The function $\alpha(|z_i - z_j|)$ describes interference competition between two morphs i and j . It is modelled as a symmetric rectangular function (the competition kernel) of bodysize differences

$$\alpha(|z_i - z_j|) = \begin{cases} \alpha_0, & |z_i - z_j| < \beta \\ 0, & |z_i - z_j| \geq \beta, \end{cases} \quad (5.3)$$

where α_0 is the competition strength and β the competition range.

The change in the density of the resource $i = 0$ follows a chemostat equation

$$\begin{aligned} \frac{dB_0}{dt} = & I - eB_0 - \sum_{j=1}^N \gamma(z_j) B_j B_0 + \nu \sum_{j=1}^N \sum_{i=1}^N \alpha(|z_j - z_i|) B_j B_i \\ & + \nu \sum_{j=1}^N m(z_j) B_j + \nu \sum_{j=1}^N \sum_{i=1}^N (1 - f(z_j)) \gamma(z_j - z_i) B_j B_i, \end{aligned} \quad (5.4)$$

consisting of a constant resource inflow I , a relative outflow of rate e , losses due to consumption by morphs, and three terms describing the recycling of a fraction ν of dead biomass from interference competition, intrinsic mortality, and consumption.

5.2.2. Evolutionary dynamics

The system is initialized with the resource (trait value $z_0 = 0$ and initial biomass $B_0 = I/e$) and a single evolving morph of bodysize $z_1 = d$, corresponding to a maximal consumption rate on the resource. Each evolving morph mutates with a rate of ω_0 per unit biomass and unit time. At each mutation event of a morph k , a new morph is added to the system with bodysize z_M that is randomly chosen from the mutation interval $[0.8 z_k, 1.2 z_k]$. This interval is centred around, and increases linearly with, the bodysize of the mutating morph z_k . The new morph is introduced with an initial biomass of θ , which is also the extinction threshold. If due to the population dynamics the biomass B_k of any morph falls below this threshold θ , it is considered extinct and removed from the system.

5.2.3. Parameter values, implementation, and cycle detection

We varied the range β and the strength α_0 of the competition kernel as our main control parameters. The other model parameters are fixed to: $f_0 = 0.3$, $m_0 = 0.1$, $\gamma_0 = 1/\sqrt{2}$, $d = 2$, $I = 10$, $e = 0.1$, $v = 0.5$, and $\sigma = \sqrt{2}$. In contrast to Loeuille and Loreau (2005) we increased the extinction threshold from $\Theta = 10^{-20}$ to $\Theta = 10^{-10}$ (see also Allhoff and Drossel (2013)) and the mutation rate from $\omega_0 = 10^{-6}$ to $\omega_0 = 10^{-5}$. Our robustness tests showed that these deviations from the original model formulation have no effect on the model outcome, but they allowed us to substantially increase the considered evolutionary time of our simulation runs. If not stated elsewhere, the simulations were carried out over 10^9 time-units. Numerical simulations were performed by using a Runge-Kutta-Fehlberg method 4/5 (Press et al., 2007) which was implemented in C++. To ensure the generality of our results, we performed 5 simulation runs with a different sequence of random numbers for each parameter set. We define a simulated time series as an evolutionary cycle, if it contains at least one whole period after an initial build up phase of 10^8 time-units. Therefore, the maximal observable period length is limited by the remaining $9 \cdot 10^8$ time-units. If the period length of a cycle is close to this limit, cycling is difficult to determine and may depend on the realization of the random numbers in the evolutionary algorithm. Here, we say that a parameter set shows cycling, if any of the five simulation runs does. By this criteria the distinction between static and cycling food webs depends on the considered time interval, especially in the transition regions.

5.3. Results

5.3.1. Numerical simulations, revealing four dynamics regions

We used numerical simulations to study the evolutionary dynamics of the food web model in dependence of the inter-species competition. Exploring the parameter space (β, α_0) of the competition kernel, we identified four distinct behavioural regimes (regions I - IV). The regions in which each of these behaviours occur are presented graphically in Fig. 5.1 and exemplary time series for all regimes are shown in Figs. 5.2 and 5.A.1. Region I is characterized by the build-up of evolutionary and convergence stable food webs, as introduced by Loeuille and Loreau (2005). Region II exhibits single morph cycles. In this region the community is composed of the resource and a monomorphic consumer with a bodysize that is not constant but undergoes evolutionary cycles within a narrow range. Region III features complex community dynamics. This region is characterized by co-occurring single morph and polymorphic coevolutionary cycles that cover several trophic layers. Region IV is a transition area in which single morph cycles can be observed that eventually become polymorphic. The resulting polymorphisms can be evolutionary static or dynamic. Our numerical simulations showed that the map of evolutionary outcomes in Fig. 5.1 is generic. If other model parameters (e.g. σ , γ_0) are altered, the transition lines between the four regions are changed. However, as long as the parameters chosen allow trophic structure, each of these types of behaviour can be found. In the following we consider each state, and the transition between states, in more detail.

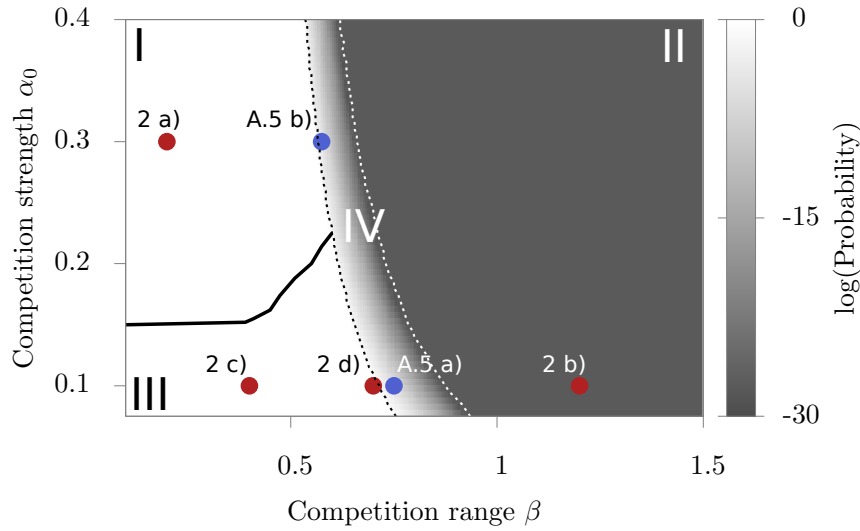


Figure 5.1.: Map of the evolutionary dynamics in dependence of the competition parameters. The map splits into four regions of distinct dynamic behaviour: Static food webs (region I), single morph cycles (region II), complex community dynamics (region III), and a transition regime in which single morph cycles occur but the system eventually becomes polymorphic (region IV). The black solid line separates the regions of static (region I) and cyclic (region III) polymorphic food webs and is obtained from numerical simulations. The grey scale indicates the probability P for a monomorphic system to become dimorphic during one cycle period and is calculated by analysis of the invasion fitness in a monomorphic system (see section 5.3.2). The black dotted line shows the isocline of $P = 1$. To the right of this line single morph cycles can occur. The white dotted line indicates the isocline of $\log P = -30$ and separates regions II and IV. The red dots correspond to the examples shown in Fig. 5.2 and the blue dots to the transition states shown in Fig. Appendix 5.A.1.

Static food webs: region I For small competition ranges β and high competition strengths α_0 (region I) we obtain food webs that are close to an evolutionarily and convergence stable state. This is exactly the behaviour observed by Loeuille and Loreau (2005). Fig. 5.2a shows an exemplary time series of a static food web and its distribution of biomass relative to bodysize. After an initial build-up (not shown), the network structure and morph composition of the food web is practically static. It consists of several distinct bodysize clusters, each centred at a bodysize which is a multiple of the optimal feeding distance d . These clusters are analogous to trophic levels. In particular, a morph in a given cluster predominantly consumes morphs in the cluster immediately below it and, similarly, is mainly consumed by morphs in the cluster immediately above it. These trophic levels are further separated into sharp bodysize layers. That is, morphs in the same trophic level are separated by a bodysize distance of β , which allows them to avoid

5. Evolutionary cycles in an evolutionary food web model

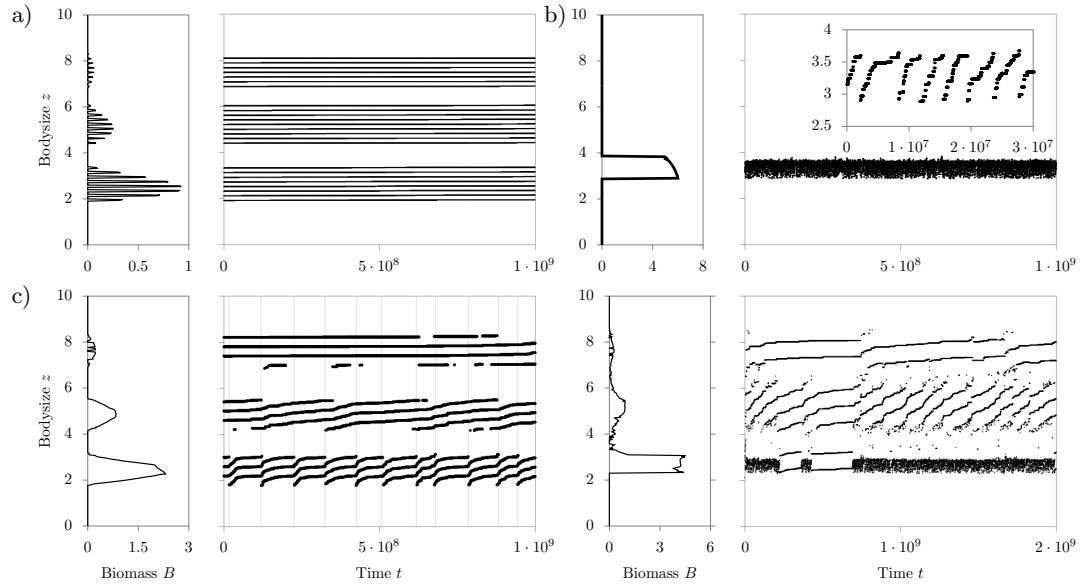


Figure 5.2.: Evolutionary food web dynamics for different competition parameters β and α_0 . Each subplot (a-d) corresponds to the parameter combination of a red point in Fig. 5.1 and shows the time evolution of bodysizes of all morphs after the initial build-up phase (right) and the corresponding biomass-bodysize histograms (left). **a)** Static food web, as in Loeuille and Loreau (2005), for $\alpha_0 = 0.3$ and $\beta = 0.2$. **b)** Single morph cycles ($\alpha_0 = 0.1$ and $\beta = 1.2$). The inset shows a close-up of the simulated cycle in bodysize for a shorter time range. **c)** Complex community dynamics, showing different coevolutionary cycles in each trophic level ($\alpha_0 = 0.1$ and $\beta = 0.4$). The vertical lines mark time-points at which the two largest morphs in the lowest trophic level are within competition range. **d)** Mixed evolutionary cycle, showing the coexistence of a single morph cycle in the lowest trophic level and coevolutionary cycles in the higher trophic levels ($\alpha_0 = 0.1$ and $\beta = 0.7$).

interference competition (note that here β is much smaller than the optimal feeding distance d). In the left panel of Fig. 5.2a, we plot the average biomass of morphs of a given bodysize throughout the simulation. This distribution is composed of single peaks indicating that the morph composition is static after the initial build up of the network. The envelope of all peaks within a trophic level is bell shaped. This arises due to differences in growth rate within the trophic level; morphs close to the centre of a trophic level are at the optimal feeding distance to the centre of the trophic level below and thus are able to grow faster. The total biomass of a trophic level decreases with increasing bodysize, due to efficiency losses. Thus, species in higher trophic level, in general, have smaller bodysize.

In the example given, the trophic levels are distinct. Increasing the feeding range σ , or competition strength α_0 causes the trophic levels to widen until the trophic levels merge. As the competition range β increases, the bodysize distance between morphs within a trophic level increases and fewer morphs can coexist in each level. For sufficiently large β only a single morph can exist in the system and we enter region II.

Single morph cycles: region II For large competition ranges β (region II) we observe a new dynamic regime for this model, which we term single morph cycles. This regime is characterized by a dynamic monomorphic community that consists of the basal resource (of bodysize $z_0 = 0$) and a single consumer morph with a bodysize that is not constant but undergoes an evolutionary cycle within a small range, see Fig. 5.2b. The inset shows a close-up of the time series which displays the bodysize cycle more clearly. In addition, a close-up of the temporal evolution of the bodysize and biomass over four complete periods of the cycle is shown in the Appendix (Fig. 5.A.2). In the beginning of a cycle, starting with a small initial bodysize, the resident is repeatedly replaced by a slightly larger morph. As the resident's bodysize increases, its biomass decreases, as seen in the trapezoidal structure of the biomass-bodysize distribution in the left panel of Fig. 5.2b and in Fig. 5.A.2b in the Appendix. At the end of a cycle, the now large resident is invaded and outcompeted by a small mutant and the single morph cycle resets. The mechanism underlying this behaviour is discussed in Section 5.3.2. The biomass-bodysize distribution is in contrast to region I continuous and not composed of single peaks, because morphs occur in the whole bodysize range of a cycle.

With increasing competition strength α_0 the frequency and amplitude of the cycle decrease (not shown). The amplitude also decreases with decreasing feeding range σ . This decrease is very rapidly, but cycles are still present for $\sigma < 0.5$. We note that the competition range β always spans the entirety of the bodysize range of a single morph cycle. As β decreases we eventually reach a threshold where the system can support a polymorphic food web and enter either region I or region III.

Complex community dynamics and coevolutionary cycles: regions III and IV For low competition strength α_0 and small to intermediate competition range β we obtain a regime of complex community dynamics (region III), characterized by polymorphic food webs which are evolutionarily dynamic. Example time series for this region are plotted in Figs. 5.2c and d. In this regime, each trophic level within the food web undergoes an evolutionary cycle. In some cases this is a single morph cycle, as described in the previous section (e.g., the lowest trophic level in Fig. 5.2d); in other, the trophic level consists of multiple morphs which undergo a coevolutionary cycle (e.g., the lowest trophic level in Fig. 5.2c).

A close-up of the temporal dynamics of bodysizes and biomasses during a coevolutionary cycle is shown in Fig. 5.3. At the beginning of the cycle, the bodysizes of all morphs within the trophic level increase gradually in successive interdependent mutational steps, while maintaining a constant separation. Initially this increase is gradual until, eventually, the largest morph goes extinct. The remaining morphs then rapidly increase their bodysize to fill this vacated niche. This effect cascades down to each of the smaller morphs allowing them to increase their bodysizes at a similar rate. This upwards movement also leaves a niche at small bodysize which a new morph

5. Evolutionary cycles in an evolutionary food web model

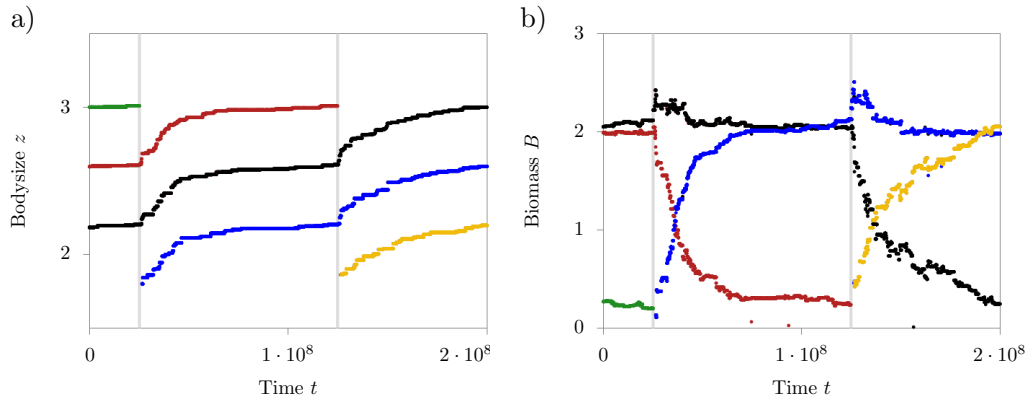


Figure 5.3.: Evolutionary dynamics during a coevolution cycle. **a)** Close-up of the time evolution of morph bodysizes $z_i(t)$ within one trophic layer, here shown for the first trophic level of Fig. 5.2c. **b)** Corresponding time evolution of morph biomasses $B_i(t)$. Identical colours denote evolutionary akin morphs. The vertical lines mark time instances at which the two largest morphs in this trophic layer have a bodysize distance smaller than β . At these points the largest morph goes extinct and a new morph with smaller bodysize can invade the system.

can invade, which functionally resets the cycle to its initial state. The biomasses of the larger two morphs decrease as their bodysize increases (e.g. red curve in Fig. 5.3). This is because as their bodysize increases they move away from the optimal distance at which to feed on the next lowest trophic level. In contrast, the biomass of the smallest morph increases (e.g. blue or yellow curves), as it approaches the optimal feeding distance. The biomass of the intermediate morph (e.g. black or blue curves) stays relatively constant, as its bodysize moves from one side of the optimal feeding distance to the other.

While this describes the coevolutionary cycle within a trophic layer, different trophic levels within a food web undergo independent cycles. Fig. 5.2c, for example, shows a food web in which only coevolutionary cycles occur. The network has basically the same structure as in the static case, consisting of three trophic levels (Fig. 5.2a), but it is evolutionarily dynamic. Within a trophic level, morphs coevolve with each other and increase their bodysize together. But this coevolutionary dynamics seems to be independent from the cycling within other trophic levels. In particular, the trophic levels cycle at different frequencies that decrease with the trophic level; about two or three cycles of the lowest trophic level occur for every single cycle of intermediate trophic level. The highest trophic level is nearly static. This implies that the evolutionary process in each trophic level is independent of the other trophic levels. Similar to the static case (region I), the biomass of each successive trophic level is less than that of the previous one. But the cycling causes the biomass-bodysize distribution to become continuous, in contrast to the static case which had clearly defined peaks.

Coevolution cycles arise in food webs when the competition strength α_0 and the competition range β are low (see Fig.5.1). As for single morph cycles, when α_0 increases the frequency and amplitude of a coevolution cycle decreases, until at sufficient large values of α_0 the different

trophic layers of the food web become evolutionary static in a series of successive infinite period bifurcations. Finally, when a critical threshold is passed the system enters region I. On the other hand, starting again in region III, with increasing β fewer morphs can exist in a trophic level (in an analogous way to that described in Section 5.3.1). As a consequence, the frequency of these cycles slightly increases with β because with decreasing number of morphs but constant nutrient input, each morph can acquire a higher biomass, which increases the mutation rates and the evolutionary speed. Finally, for sufficiently large β we observe the collapse of the whole polymorphic system into a single morph cycle (region II).

For intermediate values of β , it is also possible for the lowest trophic level to transition to single morph cycles, while the other trophic levels are unaffected, see Fig. 5.2d. We call such cases mixed evolutionary cycles. Food webs undergoing mixed evolutionary cycling have clear similarities to those displaying purely coevolutionary cycling. In Fig. 5.2d we still see three distinct trophic levels with continuous biomass-bodysize distributions. However, the upper two trophic levels are much closer together than in the purely coevolutionary case. In addition, while the biomass-bodysize distributions of these levels remain bell shaped the distribution for the lower trophic level is approximately rectangular, a clear precursor to the trapezoidal form obtained for single morph cycles, see Fig. 5.2b. Note that the lower trophic level can occasionally support a second resident, see Fig. 5.2d at time $t = 5 \cdot 10^8$. The single morph cycle stops and both residents increase in bodysize. Eventually the bigger morph goes extinct, as in a coevolution cycle, and the single morph cycle starts again. The origin of mixed evolutionary cycles can be made plausible by the observation that the lowest trophic level is subject to especially strong predation pressure because its residents can be consumed by morphs in all higher trophic levels. Predation and competition strength, α_0 , have the same structure, so the effect of higher predation is reminiscent to that of higher value of α_0 for the lowest trophic level. As a consequence, by comparison with Fig. 5.1, the lowest trophic level can collapse into a single morph cycle already a value of β for which the higher trophic levels still undergo a coevolutionary cycle.

The transition into region II, by further increase of β , is characterized by a region of transient single morph cycles (region IV). In this regime, we can observe single morph cycles that persist only for a finite time and eventually become polymorphic. The resulting polymorphism can be either evolutionary static or dynamic, depending on the competition strength α_0 . If decreasing β returns the system to region III, as above, we obtain a mixed evolutionary cycle (see example time series in Fig. 5.A.1a). Alternatively, if decreasing β returns the system to region I then we will obtain a static food web (see Fig. 5.A.1b). As β increases, the probability that a polymorphic state emerges from these single morph cycles declines, eventually reaching zero as the system enters region II.

5.3.2. Invasion analysis

Anatomy of a Single Morph Cycle

The existence of evolutionarily dynamic food webs has not previously been observed in this model. In this section we seek to develop an understanding of these dynamic states. We start by considering single morph cycles, which are characterized by a monomorphic system that undergoes a sequence of replacements of a resident, z_R , by a slightly larger mutant, z_M . Eventually

5. Evolutionary cycles in an evolutionary food web model

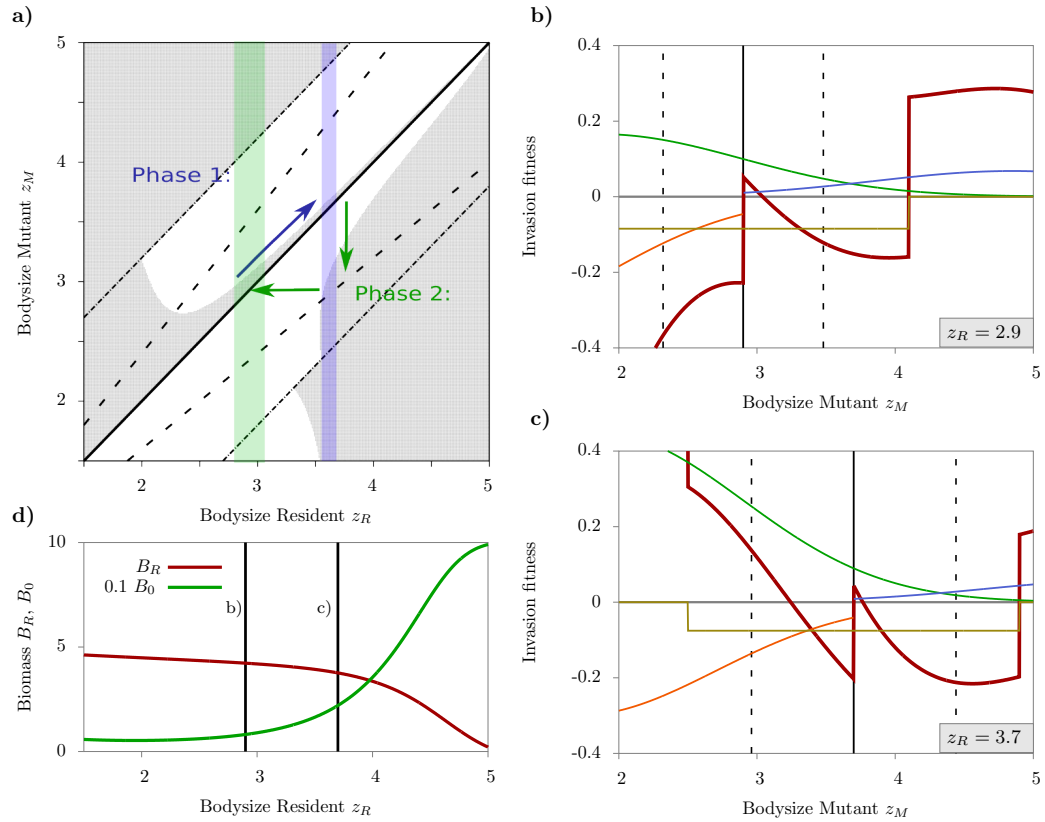


Figure 5.4.: Invasion analysis of a single morph cycle. **a)** Pairwise Invasibility Plot (PIP) in dependence of the bodysize of the resident z_R and of the mutant z_M . Regions with negative invasion fitness, $s(z_M, z_R) < 0$, are marked in white and regions with $s(z_M, z_R) > 0$ in grey. The bold line designates the points at which mutant and resident have identical bodysizes ($z_M = z_R$), dashed lines enclose the mutation interval ($0.8z_R$ and $1.2z_R$), and dashed-dotted lines the competition range ($z_R \pm \beta$). The arrows outline trajectories during a single morph cycle. The shaded areas delineate the variance of bodysizes during a cycle, where a resident may exceed the jump point (blue shaded area) or have varying initial bodysize (green shaded area). **b), c)** Fitness landscape as a function of the mutant's bodysize z_M , at the beginning of a cycle for $z_R = 2.9$ (**b**) and close to the end for $z_R = 3.7$ (**c**). The plot shows the invasion fitness (red) and its composition by growth due to resource consumption (green) and predation (blue) and by losses due to predation (orange), and interference competition (grey), according to Eq. (5.5). For visualization all growth terms are rescaled by a factor of 0.2. The vertical solid line marks the bodysize z_R of the resident and the two dashed lines border the mutation interval. **d)** Equilibrium biomass of the resident, B_R , and of the resource, B_0 , as a function of z_R . The vertical lines mark the values of z_R corresponding to panels b) and c). Parameter values are $\beta = 1.2$, $\alpha = 0.1$, corresponding to Point 2b in Fig. 1.

this gradual increase in resident bodysize ends when a small morph is able to invade and the cycle resets (Fig. 2b). To gain insight into this process, we consider the invasion fitness $s(z_M, z_R)$ of a mutant z_M in a monomorphic system of bodysize z_R (Geritz et al., 1998). The invasion fitness $s(z_M, z_R)$ can be derived from Eq. (5.1) and is given by:

$$\begin{aligned} s(z_M, z_R) = & f(z_M) \gamma(z_M) B_0 + f(z_M) \gamma(z_M - z_R) B_R - m(z_M) \\ & - \gamma(z_R - z_M) B_R - \alpha(|z_M - z_R|) B_R. \end{aligned} \quad (5.5)$$

Here, B_0 and B_R denote the equilibrium biomasses of the resource and the resident in the monomorphic system and are given by Eqs. (5.1) and (5.4). To gain analytically tractable expressions for the invasion fitness, we neglect the nutrient recycling terms in Eq. (5.4), that is we take v equal to zero.

A positive invasion fitness $s(z_M, z_R) > 0$ indicates that the mutant is able to invade and establish itself. Assuming that the population stays monomorphic, we can use Eq. (5.5) to construct the bodysize ranges which characterize a viable mutant for a given resident bodysize. These ranges can be summarized graphically using Pairwise Invasibility Plots (PIP) (Geritz et al., 1998). In Fig. 5.4a we plot a PIP for the parameter set used to obtain Fig. 5.2b. Using this PIP we find that the evolutionary cycle can be split into two phases as follows. Phase 1: For small resident bodysizes ($z_R < 3.54$) only mutants with larger bodysizes have positive fitness. Thus, the resident's bodysize increases over evolutionary time via a series of replacements by a larger mutant (blue arrow in Fig. 5.4a). Phase 2: When the resident's bodysize reaches a critical value ($z_R \geq z_J = 3.54$), a second positive fitness region emerges corresponding to mutants which are smaller than the resident. At this point a jump to a smaller bodysize becomes possible (green arrows in Fig. 5.4a). Such a jump can produce a resident morph small enough to return the cycle to its initial state. Having outlined the cycle we now consider its two phases in more detail.

In Fig. 5.4b we plot the invasion fitness (i.e., a cross-section of the PIP) for a typical point ($z_R = 2.9$) in Phase 1 of the cycle. The dependence of the invasion fitness $s(z_M, z_R)$ on the bodysize of the mutant z_M (red curve) shows a non-monotonic behaviour, which can be explained by the way in which $s(z_M, z_R)$ is composed by different gain and loss terms in Eq. (5.5). We see that the effects of intrinsic mortality (purple) and competition (grey) are relatively constant with respect to mutant bodysize, at least within the mutation interval. Note though, that the competition loss disappears for $z_M > z_R + \beta$, giving rise to the upward jump of the invasion fitness at $z_M = 4.1$. Here, this region of increased invasion fitness is out of the mutation interval and does not interfere with the single morph cycle. Growth due to resource consumption (green) declines gradually with mutant size, as larger morphs have lower resource feeding efficiency (the size difference becomes larger than the optimal feeding distance $z_M - z_0 > d$). The most significant factor is the effect of asymmetry in the predation interactions. In particular, mutants that are larger than the resident are able to gain in growth due to feeding on it (blue), while mutants smaller than the resident suffer from predation by the resident (orange). This, effectively results in an upward jump of the invasion fitness at $z_M = z_R$, which is sufficient to off-set the moderated decay in feeding efficiency creating a region of positive invasion fitness for increased bodysizes $z_M > z_R$. Consequently, the only viable evolutionary path in Phase 1 is increasing bodysize (blue arrow).

With increasing bodysize of the resident z_R , the decline in the feeding efficiency on the resource

5. Evolutionary cycles in an evolutionary food web model

becomes more severe because the deviation from the optimal feeding distance to the resource increases. As a consequence, the invasion fitness is increasingly dominated by the relative contribution of the feeding efficiency (green). In contrast, the jump in the invasion fitness at $z_M = z_R$ due to the asymmetry of predation remains largely independent of z_R . As a consequence, the region of positive fitness for larger mutants, $z_M > z_R$, shrinks with increasing z_R (see Figs. 5.4a and c). Using analytical and numerical calculations (not shown) we found that this region finally disappears for a resident bodysize of $z_{max} = 5.09$ (independent of the competition parameters α_0 and β). As such z_{max} is the maximal achievable bodysize of a morph in a monomorphic system for the given parameter values. Furthermore note that the probability of an evolutionary change, and hence the speed of the evolutionary dynamics, is proportional to the ratio of the positive fitness interval to the mutation interval. Thus, as the fitness interval for larger morphs shrinks, the rate of increase in resident bodysize decreases, going to zero as $z_R \rightarrow z_{max}$.

These effects stem from the apparently paradoxical observation that, while increasing bodysize is evolutionarily favoured, it results in a less fit resident. In particular, a mutant with a larger bodysize than the resident is able to invade by preying on the resident. However, once the resident is driven to extinction, the new resident's lower feeding efficiency results in it being less able to exploit the remaining resource at z_0 . Consequently, as resident bodysize, z_R , increases, resident biomass and utilization of the resource decline. This effect can be seen clearly by plotting resident and resource biomass against resident bodysize, see Fig. 5.4d.

The increased availability of the resource is responsible for the emergence of a second positive fitness interval found in Phase 2 of the cycle. A typical invasion fitness profile is plotted in Fig. 5.4c. The contributions of most growth factors are similar to those obtained in Phase 1 (Fig. 5.4b). However, now the growth due to resource consumption depends more strongly on mutant size and its maximum contribution is much higher. For sufficiently small mutants the extra growth gained from greater feeding efficiency is able to off-set the increased losses from predation, allowing a smaller mutant to displace the resident (green arrows). We refer to the smallest resident bodysize for which this is possible as the jump point z_J (for the chosen parameter values $z_J = 3.54$). When a mutant with bodysize less than this threshold successfully invades the system, the system resets to Phase 1.

Note that, since mutational steps are random, the range of bodysizes during an evolutionary cycle varies. The resident's bodysize can exceed the jump point before the smaller mutant invades (blue shaded area in Fig. 5.4a). Furthermore, the smaller mutant can occur anywhere within the positive region of the fitness cross-section obtained for a given resident. The combination of these two effects allows the smaller mutant to emerge in a relatively wide range (green shaded area in Fig. 5.4a).

We observed previously that the frequency of single morph cycles was related to the competition strength α_0 . This can now be explained as follows. Note first that once the jump point is reached the cycle can be reset in a single step. Furthermore, such a reset is has a high probability, since the positive fitness region for the smaller mutant is bigger than that for a larger mutant. Thus, the system is unlikely to spend a significant amount of evolutionary time in Phase 2. Consequently, the length of a cycle is primarily determined by the number of evolutionary steps required to produce a resident with bodysize greater than z_J . The region of positive fitness larger than the resident, which is responsible for the upwards movement (see Figs. 5.4a and c), narrows with

increasing competition strength α_0 (because the fitness landscape is shifted downwards within the competition range). Therefore increasing the competition strength reduces the evolutionary speed and thus the frequency of the cycle.

In summary, the intrinsic asymmetry in the feeding kernel $\gamma(\cdot)$ in Eq. (5.3) creates an evolutionary ratchet, which results in an increase in the resident's bodysize. However, the concomitant decrease in resident feeding efficiency generates a nutrient environment which ultimately allows the invasion of a small mutant. The interplay between these two processes results in a single morph evolutionary cycle.

Transition region to dimorphic states While in single morph cycles the mutant always replaces the resident, we observed that in region IV single morph cycles can become polymorphic. While the dynamics of such a polymorphic state are analytically intractable (at least using the techniques outlined above), we are able to determine conditions under which a dimorphic state can form. In particular, in this model two species are able to coexist only if they do not compete directly; that is if the distance between their bodysizes is greater than the competitive range, β . Thus a dimorphism becomes possible when the mutation interval, $[0.8z_R, 1.2z_R]$, contains the competition interval, $[z_R - \beta, z_R + \beta]$. We call the smallest resident bodysize where this condition holds the dimorphic point, z_D , and note that it is related to the competition range as follows, $z_D = 5\beta$. With this in mind the transitory single morph cycles found in region IV can be explained by the random nature of the mutational steps. In particular, when $z_D > z_J$ the resident bodysize must increase past z_J in order to reach the dimorphic point. Consequently the system must enter Phase 2 and thus the possibility of the cycle resetting before the system becomes polymorphic exists. The further above z_D is from z_J the more likely it becomes that the cycle resets before it becomes dimorphic. This intuition is justified formally below.

In Fig. 5.1, we plotted the probability of a single morph cycle becoming dimorphic during a single cycle. This probability was estimated as follows. For a fixed resident bodysize, the probability for a given mutational step attaining a particular evolutionary outcome (dimorphism, upwards or downwards movement in bodysize) is given by the range in the invasion fitness that leads to the evolutionary event divided by the whole positive fitness area. The negative fitness area is not considered since an unsuccessful invasion does not alter the system. We start with a resident of a bodysize of z_J and calculate the probability of each evolutionary outcome (transition probability) for that resident bodysize. In the next step, we increase the resident bodysize by the expected mutational step-size of the upwards movement. (This is given by the centre of the positive fitness responsible for upwards movement.) Thus we calculate the transition probabilities at each of the expected bodysizes between z_J and z_{max} and by doing this consecutively we consider all possible evolutionary trajectories. These trajectories terminate when a dimorphism emerges or the cycle resets (which is assumed to happen via a downwards movement). The probability to become dimorphic along a given trajectory is equal to the product of the transition probabilities of the steps in that trajectory. The overall probability of reaching a dimorphic state is then given by summing over all trajectories which reach this state.

5. Evolutionary cycles in an evolutionary food web model

Complex Community Dynamics In region III we observe food webs that contain coevolutionary, and occasionally single morph, cycles. We have previously observed that the cycles in distinct trophic levels are independent. As such the behaviour of single morph cycles, even in a polymorphic system, can be adequately understood in a monomorphic context, see above. Moreover, the dynamic patterns of coevolutionary cycles can be made plausible by the evolutionary behaviour of morphs in a single trophic level. The increase of a morph's bodysize in a coevolution cycle is due to the same mechanism as in single morph cycles. The asymmetry in the feeding kernel $\gamma(\cdot)$ (Eq. (5.3)), creates an evolutionary ratchet, which drives the morphs to higher bodysizes (see Fig. 5.3). However, the evolution of the morphs is limited by interference competition. Each morph, except the largest and the smallest morph, have two neighbours at a bodysize distance slightly bigger than the competition range β . Therefore mutants of the intermediate morphs inevitably compete with these neighbours and can not invade. While the smallest morph has only a larger neighbour, smaller mutants are not viable due to the decreasing ability to feed on the lower trophic level and high intra trophic level predation. The largest morph in an coevolution cycle has only a smaller neighbour, thus it can increase its bodysize through the evolutionary ratchet. All other morphs follow one after another, since they are not bounded upwards any more. Therefore coevolution is a top-down process in this model. However, just as in the single morph case, increasing bodysize results in the largest morph reaching an unstable state where it can be invaded and outcompeted by smaller mutants. This is analogous to the jump point of a single morph cycle.

In contrast to single morph cycles, the largest resident is not outcompeted by a new offspring of its own, but by a mutant of the second largest resident. The second largest resident is replaced by a slightly larger mutant, which is within competition range β of the largest resident. (Time-points, at which the two largest residents compete are marked by grey vertical lines in Figs. 5.2c and 5.3.) This mutant is close enough to the optimal feeding distance that it can outcompete, and thus replace, the largest resident. Thus the interference competition from above is removed, allowing each of the resident morphs to increase its bodysize. A new mutant, descended either from the smallest resident, or from a resident in a lower trophic level, can invade either close to the end, or at the beginning, of a cycle; when the interference competition from the smallest resident is lowest.

5.4. Discussion

The model introduced by Loeuille and Loreau (2005) is well known for evolutionarily static food webs. We investigated a larger range of competition parameters, and found novel evolutionary states: cycling of single morphs (region II), cycling of complete food webs (region III), and transitory states from single morph cycles to polymorphic food webs (region IV). We want to focus on four main results:

First, the observed evolutionary cycles are based on coevolution, which is driven by competition and trophic interactions between resident morphs and also the invader. These coevolutionary processes are observed in empirical studies, where they can also be driven by competition (Connell, 1980; MacArthur, 1957) or trophic interactions (Abrams, 2000). However, it is difficult to study coevolution in larger communities, since the identification of the evolutionary dynamics and the

coevolving traits is difficult, due to the high number of complex interactions (Rothstein, 1990). Our findings show, that the number of interactions can be reduced by dividing morphs in smaller groups in which interactions are considered, since each trophic level coevolves independently.

Second, we found that food web characteristics are remarkably robust towards evolution. The network structure, number of morphs and links are mainly constant during evolution. In addition, the network structures of solely coevolving food webs and static food webs are similar. Therefore they are not distinguishable on the time scale of the population dynamics. However for mixed evolutionary food webs the network structure changes: the number of species contained in each trophic level and the distance between each level loses its regularity.

Third, our results are a good demonstration of the Cope's rule (Cope, 1896.): During an evolutionary cycle, morphs increase their bodysize, since a slightly larger morph has a higher fitness than a smaller morph. In addition, our study suggests a more natural solution for the "Endless trends to gigantism" paradigm (Hone and Benton, 2005), than mass extinction (Kingsolver and Pfennig, 2004). Large bodysizes are advantageous over a wide range, especially towards similar sized morphs, but result in a lower ability to consume the original resource, which finally increases the vulnerability towards invasion of better adapted morphs.

Fourth, single morph cycles have similar characteristics to taxon cycles (Roughgarden and Pacala, 1989; Wilson, 1961) and suggest that the downgrade of the environment for the resident (decreasing resource consumption) is also responsible for the arising evolutionary cycling: the increase in bodysize of the resident, due to coevolution with invaders results in morphs that are progressively less suited to their environment and morphs that are better adapted to the environment can invade. In addition, we propose that taxon cycles might be a transitory phase of island colonisation: we observe that single morph cycles can be transitory states, after which the community becomes polymorphic and large food webs emerge. These webs can be either static or dynamic. The latter can be a possible representation of cycling of larger communities –continental taxon cycles – which are hypothesised, but hard to study empirically, due the intertwining of the invasion processes (Ricklefs et al., 2014). Note that within the model used, the estimation of the time scale considered is not possible without relating it to empirical data, since all variables are treated as dimensionless.

As mentioned above, evolutionary cycling was studied extensively in competing communities. (Rummel and Roughgarden (1983); Taper and Case (1992); Matsuda and Abrams (1994)). They showed that for evolutionary cycles an asymmetry in the (competition) interactions is necessary. In our study an asymmetry is introduced naturally via trophic interactions and therefore we suggest that evolutionary cycling is an intrinsic phenomenon in the model of Loeuille and Loreau (2005) and might also be a general phenomenon in allometric evolutionary food web models. However, before transferring our results to other models, one has to consider the simplifications used in the model of Loeuille and Loreau (2005) in more detail, to show the generality of our findings. We consider the most influential ones: the competition $\alpha(\cdot)$ and the feeding kernel $\gamma(\cdot)$.

First, the interference competition is box-shaped with a competition range β and it has a strict cut-off (Eq. (5.3)). Therefore, morphs either compete with a single strength, or competition is absent. However, competition should change continuously in strength with bodysize distance. A more realistic form of competition is based on link overlap (MacArthur and Levins, 1967), as applied by (Allhoff et al., 2015a; Ritterskamp et al., 2015b). The link overlap competition range is

5. Evolutionary cycles in an evolutionary food web model

linked to the feeding range σ of the competing morphs ($\propto \sqrt{2}\sigma$). If the box-shaped interference competition is replaced by link overlap competition, evolutionary cycling still occurs. Comparing link overlap competition with box-shaped competition shows that link overlap competition occurs over a wider bodysize distance. This justifies the investigated competition range β in our studies.

Second, the feeding kernel $\gamma(\cdot)$ consists of a truncated Gaussian. This cut-off influences the evolutionary dynamic as shown in section 5.3.2. Without the cut-off evolutionary cycling is not visible anymore and static food webs lose evolutionary stability. However, evolutionary cycling still occurs, if we replace the feeding kernel by a more ecologically accurate function, e.g. the Ricker function (Vucic-Pestic et al., 2010).

Evolutionary cycling is robust towards variation of the feeding kernel $\gamma(\cdot)$ and the shape of competition $\alpha(\cdot)$. In addition, we have validated the competition range β used in our studies. Therefore, we suggest that evolutionary cycling in food webs may be found in other food web models and also in empirical data. The next obvious step is therefore to investigate evolutionary cycling in other ecologically more accurate models e.g. (Allhoff et al., 2015a; Ritterskamp et al., 2015b).

We have shown that evolutionary cycles occur in the evolutionary food web model used and can manifest in various ways. However, the underlying mechanism, leading to evolutionary cycling, is not restricted to the applied model. Therefore, we suggest that evolutionary cycles might be a general phenomenon in evolutionary food web models and also empirical food webs and therefore conclude that ongoing evolution in food webs may be more frequent than commonly believed.

5.A. Appendix

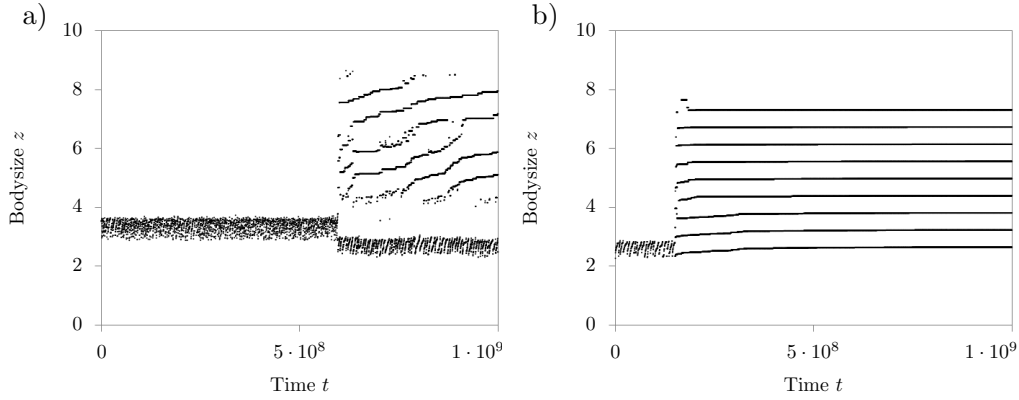


Figure 5.A.1.: Transient dynamic. After a transient of single morph cycles the system becomes polymorphic. **a:** Mixed evolutionary behaviour of a food web is visible after the transition. The competition parameters are set to $\alpha_0 = 0.1$ and $\beta = 0.75$. **a:** A static food web emerges after the transition. The competition parameters are set to $\alpha_0 = 0.3$ and $\beta = 0.58$.

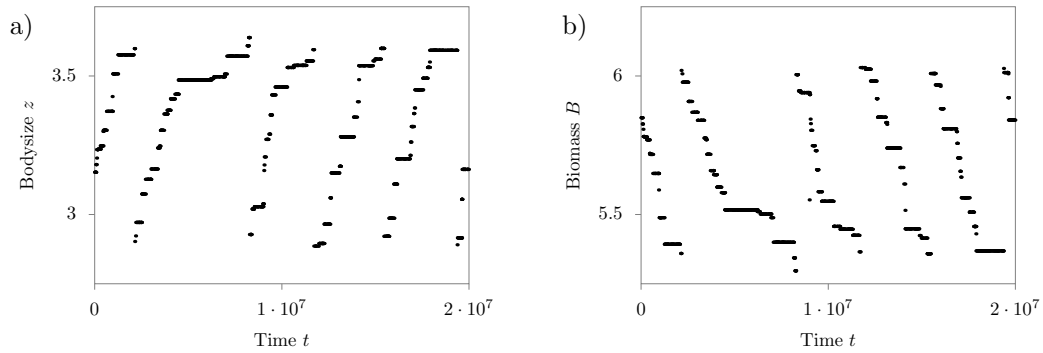


Figure 5.A.2.: Evolutionary temporal behaviour of a single morph cycle (Fig. 5.2b)). **a, b:** Close-up of the biomass B and body size z during an single morph cycle shown in Fig. 5.2b.

6. Evolutionary food web models: effects of an additional resource

Evolutionary food web models: effects of an additional resource

Daniel Ritterskamp¹, Daniel Bearup, Christoph Feenders, Bernd Blasius

CvO University Oldenburg, ICBM, Carl-von-Ossietzky-Strasse 9-11, 26111 Oldenburg, Germany

Abstract

Many empirical food webs contain multiple resources, which can lead to the emergence of sub-communities – partitions – in a food web that are weakly connected with each other. These partitions interact and affect the complete food web. However, the fact that food webs can contain multiple resources is often neglected when theoretically describing food web assembly, by considering a single resource only. We present an allometric, evolutionary food web model and include two resources of different sizes. Simulations show that an additional resource can lead to the emergence of partitions, i.e. groups of species that specialise on different resources. For certain arrangements of these partitions the interactions between them alter the food web properties: first, they increase the variety of emerging network structures, since hierarchical bodysize relationships are weakened. Therefore, they have the potential to explain the variety of food web structures that is observed in empirical data. Second, they can destabilise the population dynamics by introducing indirect interactions with a certain strength between predator and prey species. This leads to biomass oscillations and evolutionary intermittence.

Keywords: Subfood webs, Resource Distribution, Substructures, Partitioning, Intermittence, Destabilisation, Biomass Oscillations, Large community-evolution models

6.1. Introduction

Ecologists have long been interested in food webs, with the first study dating back to the eighteen century (see references within (Egerton, 2007)). Many of the investigated food webs contain multiple resources (energy inputs), such as seaweed, salt, nutrients, and dendritus (Dunbar, 1953), or they include resources that can be divided into size classes, such as phytoplankton (Sommer et al., 2002; Downing et al., 2014). Both can lead to the emergence of sub-communities, **partitions**, within a food web that are weakly connected with each other, e.g. soil food webs contain above and below ground communities (Wardle et al., 2004; Fukami et al., 2006; Larios and Suding, 2014).

When modelling the assembly of food webs however, the fact that food webs can be based on multiple resources of different size classes is often neglected. Within the variety of models that exist (see Brännström and Johansson (2012) for an overview) resources are either disregarded or

¹Corresponding author

6. Evolutionary food web models: effects of an additional resource

only a single one is incorporated. This also includes the three main classes of food web assembly models: matching models (Rossberg et al., 2006); webworld models (Caldarelli et al., 1998; Drossel et al., 2001); and allometric, evolutionary food web models (Loeuille and Loreau, 2005). The matching model does not include resources and the webworld model considers a single resource, but the resource biomass is not modelled explicitly. In contrast, allometric, evolutionary food web models incorporate resource population dynamics explicitly; nevertheless only a single resource is generally considered. This framework allows however, to study the influence of different resource sizes, since bodysize is the main trait to characterise species and therefore we focus on allometric, evolutionary food web models.

Allometric, evolutionary food web models were first introduced by Loeuille and Loreau (2005), with species properties following allometric bodysize scaling (Peters, 1986). Hence, species are solely characterised by bodysize and interactions between species are determined by their bodysize difference. An evolutionary based assembly algorithm is applied, which introduces new species to the community, while population dynamics determine which of the species survive. It is assumed that these processes occur on separated time scales. Several extensions of the original model have been used to study different aspects of food web assembly: to investigate the mechanism determining food web structure and to reproduce the variety of food web structures that is observed in empirical data, different feeding ranges and feeding centres for each species were introduced (Ingram et al., 2009; Allhoff et al., 2015a); to examine the spatial influence on food web assembly, an additional trait axis was imposed (Ritterskamp et al., 2015b); and to study diversification, gradual evolutionary change was incorporated (Brännström et al., 2011). However, we are not aware of any study that considers multiple resources.

In this paper, we present a multi-resource model, including only basic assumptions to keep its complexity minimal. We extend the model of Loeuille and Loreau (2005) by adding a second resource with an adjustable bodysize. Since the classical model is well studied, the dynamical behaviour and the mechanisms that determine the network structures are well understood (Loeuille and Loreau, 2005, 2009; Ritterskamp et al., 2015a), we can focus on effects that are caused by the additional resource. In this extended multi-resource model we expect to see more complex dynamics, since ecological communities can be destabilised by a small number of resources and exhibit oscillatory and chaotic population dynamics (Huisman and Weissing, 1999; Huisman et al., 2001; McCann, 2000). The objective of this paper is thus to investigate the role of additional resources in the assembly of food webs. Within the multi-resource model we (i) investigate the emerging partitions, (ii) consider their interaction and their influence on the food web structure and the population dynamics, and (iii) lay out the mechanism responsible for the occurring biomass oscillations.

6.2. Multi-resource model

The multi-resource model is based on the classical model of Loeuille and Loreau (2005), but the number of resources and their underlying dynamics are changed. The term resource refers, in the following, to any kind of energy input into the food web, for instance, nutrients, phytoplankton, plants or any kind of basal species, whose energy uptake is not described by the model. In addition, it is assumed that resources do not interfere with each other. The multi-resource model

considers two of these resources (R_1, R_2), instead of originally one, and a variable number of evolving species ($i = 1, \dots, N$). From now on, we use the term morph, rather than species, since we do not consider speciation processes.

Each morph and resource is described by its population biomass density B_i and bodysize z_i . The resources have a bodysizes of $z_{R_1} = 0$ and $z_{R_2} \geq 0$. The latter will be varied to investigate the effects of different resource sizes on the food web assembly. The model splits up into population dynamics and an evolutionary algorithm, each acting on a different time scale. The population dynamics describe the trophic interactions among morphs and determine their survival or extinction. On a longer time scale, usually after the population dynamics have reached an equilibrium, the evolutionary algorithm adds new morphs to the community and can be interpreted as a morph assembly-algorithm.

6.2.1. Population dynamics

The change of biomass B_i of morph i is given by the Lotka-Volterra equation, describing reproduction, intrinsic mortality, and losses due to predation and interference competition

$$\frac{dB_i}{dt} = B_i \left(\underbrace{f(z_i) \sum_{j \in \{R_1, R_2, 1, \dots, N\}} \gamma(z_i - z_j) B_j}_{\text{reproduction}} - \underbrace{m(z_i)}_{\text{mortality}} - \underbrace{\sum_{j=1}^N \gamma(z_j - z_i) B_j}_{\text{predation loss}} - \underbrace{\sum_{j=1}^N \alpha(|z_i - z_j|) B_j}_{\text{competition}} \right). \quad (6.1)$$

The intrinsic mortality $m(z_i) = m_0 z_i^{-0.25}$ and the production efficiency $f(z_i) = f_0 z_i^{-0.25}$ scale with bodysize according to allometric relations (Peters, 1986). The feeding kernel $\gamma(z_i - z_j)$ describes the predation pressure exerted by predator i on prey j . It is modelled as a one tailed Gaussian function of the bodysize differences

$$\gamma(z_i - z_j) = \begin{cases} \frac{\gamma_0}{\sigma\sqrt{2\pi}} \exp\left(-\frac{(z_i - z_j - d)^2}{\sigma^2}\right), & z_j < z_i \\ 0, & \text{otherwise,} \end{cases} \quad (6.2)$$

where d is the optimal predator-prey bodysize distance, γ_0 scales the maximal feeding strength, and σ corresponds to the feeding range of a morph. The cut-off for $z_i \leq z_j$ in the feeding kernel implies that a predator is only able to consume prey with a strictly smaller bodysize.

The competition kernel $\alpha(|z_i - z_j|)$ describes interference competition between two morphs i and j . It is modelled as a symmetric rectangular function of bodysize differences

$$\alpha(|z_i - z_j|) = \begin{cases} \alpha_0, & |z_i - z_j| < \beta \\ 0, & \text{otherwise,} \end{cases} \quad (6.3)$$

where α_0 is the competition strength and β is the competition range.

In contrast to the classical model (Loeuille and Loreau, 2005), we include two resources R_1 and R_2 , with their biomass change given by

$$\frac{dB_{R_i}}{dt} = I_{R_i} - e_{R_i} B_{R_i} - \sum_{j=1}^N \gamma(z_j - z_{R_i}) B_j B_{R_i} \quad i \in \{1, 2\}, \quad (6.4)$$

6. Evolutionary food web models: effects of an additional resource

consisting of a constant nutrient inflow I_{R_i} , a relative outflow e_{R_i} , and losses due to consumption by morphs. Since the recycling term that is contained in the classical model has only a minor influence on the food web assembly for a single resource (Allhoff and Drossel, 2013), it is omitted in the multi-resource version. The model can be easily extended by an arbitrary number of resources.

6.2.2. Evolutionary Dynamics

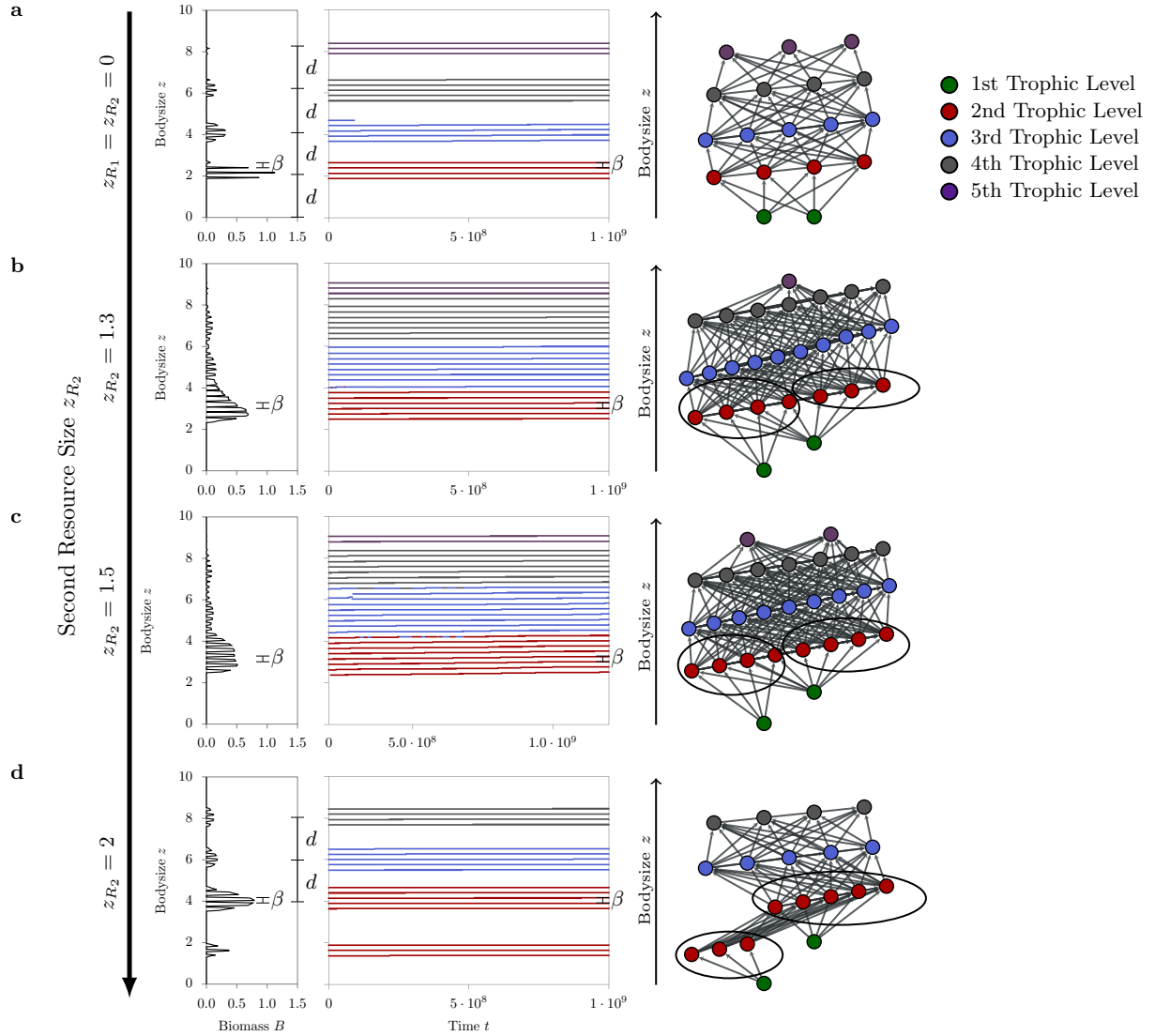
Each model run is initialised with both resources ($z_{R_1} = 0, z_{R_2}, B_{R_1} = I_{R_1}/e_{R_1}, B_{R_2} = I_{R_2}/e_{R_2}$) and a single evolving morph of bodysize $z_1 = d$, corresponding to a maximal feeding rate on resource R_1 . Each evolving morph mutates with a rate of ω_0 per unit biomass and unit time. At each mutation event of morph k , a new morph l is added to the system with bodysize z_l that is randomly chosen from the mutation interval $[0.8z_k, 1.2z_k]$. This interval is centred around the mutating morph z_k and increases linearly with bodysize. The new morph is introduced with an initial biomass of θ , which is also chosen as the extinction threshold. If, due to the population dynamics, the biomass B_k of any morph falls below this threshold θ , it is considered extinct and removed from the food web.

6.2.3. Parameter values

To perform simulations we use the Runge-Kutta-Fehlberg method 4/5 (Press et al., 2007) provided by the GNU Scientific Library in C++ (Gough, 2009). We varied the size of the second resource z_{R_2} for different simulations as our main control parameter. The size of the other resource $z_{R_1} = 0$ remains unchanged. Both resources are interchangeable and their absolute bodysize values are of little importance, due to the weak influence of the allometric scaling (Allhoff and Drossel, 2013). All other parameters were set to $f_0 = 0.3, m_0 = 0.1, d = 2, I_{R_1} = I_{R_2} = 5, e_{R_1} = e_{R_2} = 0.1, \gamma_0 = 1, \sigma = 1, \beta = 0.25, \alpha_0 = 0.1$, such that two identical resources produce the structure introduced in Fig. 2A (Loeuille and Loreau, 2005) in the classical study. We kept the total biomass input I as in the classical study ($I = I_{R_1} + I_{R_2} = 10$), to focus on the influence of the additional resource and not on effects due to resource enrichment. Following Allhoff and Drossel (2013), we used an extinction threshold of $\theta = 10^{-10}$, rather than $\theta = 10^{-20}$ Loeuille and Loreau (2005). In addition, we applied a mutation rate of $\omega_0 = 10^{-5}$ (Ritterskamp et al., 2015a), which is larger by a factor of ten than the original value (Loeuille and Loreau, 2005).

6.3. Results

Size dependence To study the effect of different sized resources on food web assembly, we set up the model as explained above and vary the size z_{R_2} of the second resource. For representative resource settings, we consider the temporal evolution of bodysizes, the time averaged biomass-bodysize histogram, the final network structure (Fig. 6.1), and the biomasses of chosen morphs (Fig. 6.2 and 6.A.1).



6. Evolutionary food web models: effects of an additional resource

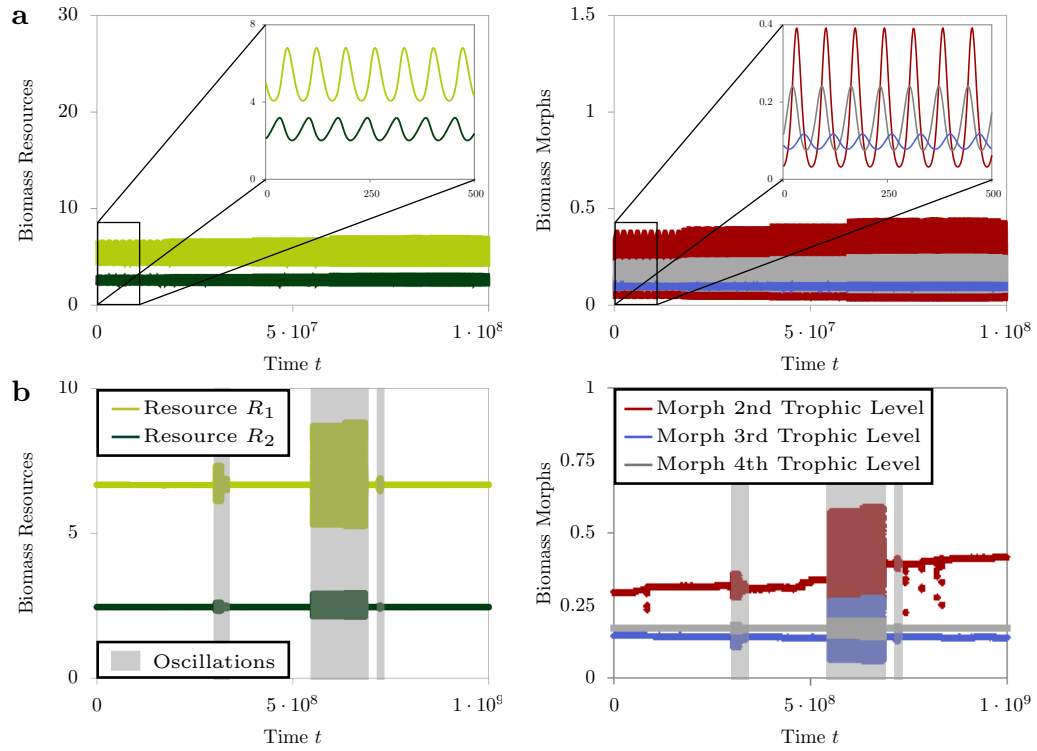


Figure 6.2.: Biomass dynamics of food webs in Fig. 6.1b,c. The left column shows the biomasses of resources R_1 and R_2 . The right column shows the biomasses of representative morphs at different trophic levels **a**: Biomasses of the food web presented in Fig. 6.1b ($z_{R_2} = 1.3$). Biomass oscillations occur. Their amplitude changes slightly with food web configuration. **b**: Biomasses of the food web presented in Fig. 6.1c ($z_{R_2} = 1.5$). Evolutionary intermittence occurs, i.e. intervals of stationary states are interrupted by biomass oscillations.

First, we consider the case of two identical resources ($z_{R_1} = z_{R_2} = 0$, Fig. 6.1a). Four clearly separated bodysize compartments occur at multiples of the optimal feeding range d . Each bodysize compartment represents one trophic level and comprises several morphs. Morphs in the same compartment keep a specific bodysize distance to each other, corresponding to the competition range β . All biomasses reach a static fixed point in this case (Fig. 6.A.1a,b) and the network is also evolutionary static; meaning the morph composition stays unchanged because new invading morphs are not viable. Each morph is represented in the averaged biomass-bodysize histogram as a single peak (Fig. 6.1a). The emerging network is identical to the preimposed structure (see Section 6.2.3) and we refer to it as classical structure. This consistency demonstrates that two identical resources act as a single one and that the division of one resource into two identical resources does not influence the food. Since we do not observe additional effects due to the artificial subdivision of the resource, we can focus on size effects of the second resource.

For a second resource size z_{R_2} in-between the size of the first resource ($z_{R_1} = 0$) and the optimal feeding distance d to the latter, only a single bodysize compartment occurs (Fig. 6.1b). Morphs in the second trophic level can be divided into two partitions, based on their effective resource consumption: one partition feeds on both resources and the second one exclusively consumes the bigger one. In addition to partitions, biomass oscillations of resources and all morphs throughout all trophic levels occur. (Fig. 6.2a). These biomass oscillations appear to be stable towards evolution.

For a second resource size z_{R_2} closer to the optimal feeding distance d , one large bodysize compartment emerges. Partitions, determined by their resource consumption, occur in the second trophic level (Fig. 6.1c). However in comparison to the previous case, the temporal evolution of biomasses now shows a more complex behaviour: time intervals of stationary biomasses are interrupted by oscillations (evolutionary intermittence, Fig. 6.2b). The behaviour of the population dynamics changes from static to oscillatory by small subsequent evolutionary mutations, each modifying the food web structure only slightly. Therefore, the food web configurations for the static and oscillatory regime have to be similar during the transition.

For a second resource z_{R_2} with a bodysize of d , which is the optimal bodysize distance to the first resource ($z_{R_1} = 0$), the emerging food web consists of four clearly separated bodysize compartments (Fig. 6.1d). Again, the second trophic level can be divided into two partitions, which are now nearly disconnected: the first partition consist of the lowest bodysize compartment that consumes only the smaller resource. The second partition includes the slightly larger bodysize compartment, which specialised on the larger resource. Upon the the second partition, higher trophic levels emerge. Note that the second trophic level is now represented by two separate bodysize compartments. For this configuration of completely disconnected, non interacting partitions the biomasses reach a stable fixed point (Fig. 6.A.1b,d). For even larger resource sizes, the partitions completely disconnect (see example in Fig 6.A.2) and each partition consists of several bodysize compartments, representing different trophic levels, and is solely based on one of the resources.

To investigate which resource sizes promote biomass oscillations and partitions within the food web, we continuously vary the size z_{R_2} of the second resource. We look at dynamical and structural properties: the extrema of the biomass of the larger resource; the fraction of time spent in an oscillatory state; the number of morphs; the total biomass of all morphs; and the relative densities of the bodysizes and trophic levels (Fig. 6.3). The biomass extrema (Fig. 6.3a) show that the considered parameter space splits up into two regimes: a static and an oscillatory regime.

Within the static regime, the biomass extrema overlap and food webs reach a static fixed point. Over the better part of the regime the bodysize compartments and also the trophic levels are separated, as shown by the standardised densities (Fig. 6.3d,e). For small z_{R_2} the network structures are similar to the classical result for identical resources (Fig. 6.1a). Four distinct bodysize layers occur, each representing a trophic level, and their bodysize centres increase with increasing z_{R_2} . For large resource sizes nearly disconnected partitions are visible (e.g. Fig. 6.1d) and the second trophic level is represented by the two lowest bodysize compartments, each specialised on one of the resources: the lowest bodysize compartment is slightly apart from the others and specialises on the smaller resource z_{R_1} , while the compartments above show the classical network structure (Fig. 6.1a). The separated partitions show an increase in total biomass,

6. Evolutionary food web models: effects of an additional resource

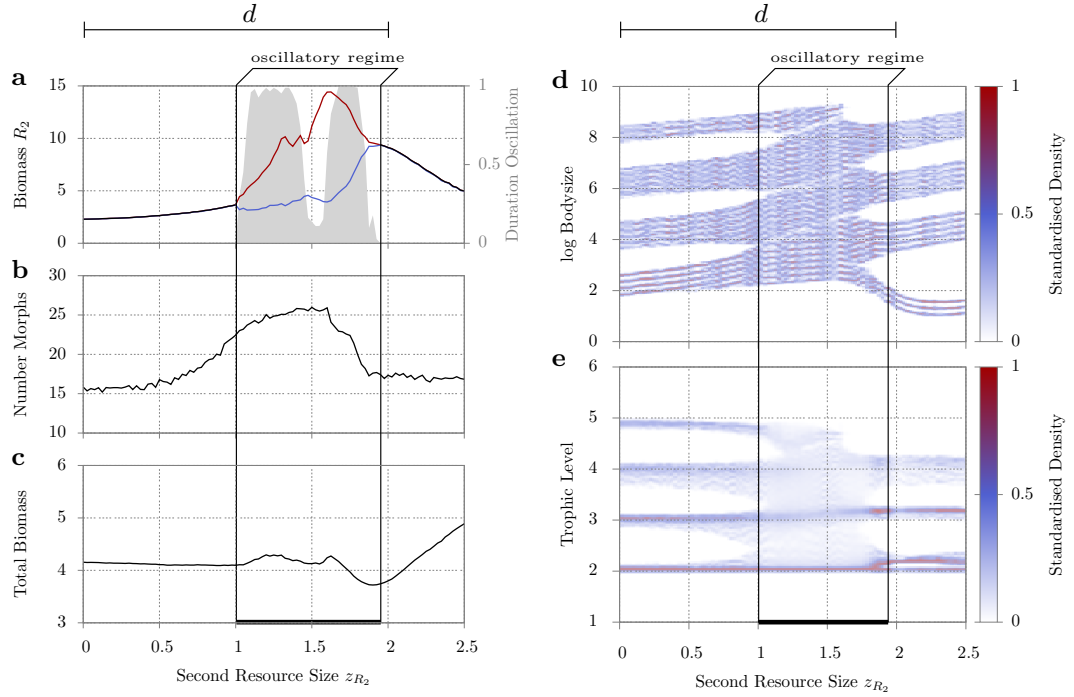


Figure 6.3.: Dependence of network characteristics on the second resource size z_{R_2} . **a:** Extrema of the biomass of the second resource R_2 and fraction of the total time spent in an oscillatory state (grey shaded area). If maxima and minima overlap, they are plotted in black, otherwise in red and blue, respectively **b:** Time-averaged number of morphs. **c:** Time-averaged total biomass. **d,e:** Standardised densities of the bodysizes and trophic levels. For each resource size z_{R_2} , 10 simulation runs were evaluated within the considered time interval (see caption Fig.6.1). Trophic levels and bodysizes were collected from all runs to create the standardised distributions. The extrema of the resource biomass were taken from the combined dataset consisting of all simulation runs.

since competition between them, and consequently biomass losses, are minimised. For resource sizes z_{R_2} close to $\frac{d}{2}$ the bodysize compartments and trophic level start to merge (Fig. 6.3d,e). The total number of morphs increases in this region, but apart from this the total number of morphs is nearly constant over the static regime.

The oscillatory regime starts for a second resource size of $\frac{d}{2}$ and ends for sizes slightly below d . Within this regime, the biomass extrema do not overlap and the system is in an oscillatory state (Fig. 6.3a). The fraction of time spent in an oscillatory state reaches two plateaus close to the borders of the regime, where it is close to one (deviations are due to inaccuracy in the identification of the oscillating state). In between, oscillations occur rarely, while the biomass extrema are not overlapping. This means that oscillations occur, which are interrupted by static behaviour: evolutionary intermittence (Fig. 6.1c and Fig. 6.2b). Within this intermittent region the total number of morphs reaches a maximum, while the total biomass is nearly constant

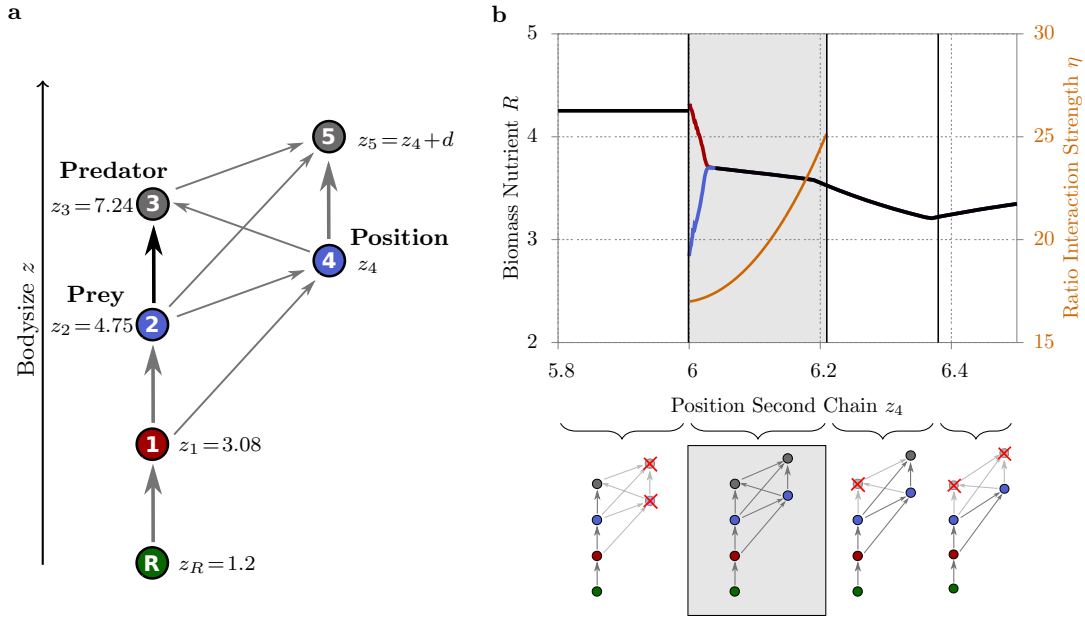


Figure 6.4.: Interaction between two food chains: two food chains are set up to investigate their interaction and the resulting population dynamics in dependency on their position relative to each other. Evolution is not considered, but only population dynamics. **a:** Set up of the two food chains: the longer chain is based on the resource R and contains three morphs (morph 1 – 3), while the second chain includes two morphs (morph 4 and 5), which have a bodysize distance of d to each other. The bodysize z_4 of morph 4 in the second chain is used to position the food chain and serves as a bifurcation parameter. Arrow width denotes link strength and black marks the **direct** feeding link between morph 2 (prey) and 3 (predator). We also consider the *indirect interaction* between the predator and prey via morph 4. The prey is consumed by morph 4, while morph 4 is consumed by the predator. Therefore there is an indirect biomass flow from prey to predator. **b:** Bifurcation diagram with bifurcation parameter z_4 , representing the position of the second food chain, showing the biomass extrema of the larger resource and the ratio η of the direct and indirect interaction between predator and prey. If the biomass extrema overlap, they are shown in black, otherwise maxima are plotted in red and minima in blue. In addition, the resulting networks are plotted (bottom). The region in which all morphs survive is marked in grey. The ratio of the direct feeding link and the indirect interaction between morph the predator and prey is given by $\eta = \frac{f(x_4)\gamma(z_4 - z_2)}{f(x_4)f(x_3)\gamma(z_4 - z_3)\gamma(z_3 - z_2)}$.

(Fig. 6.3b,c). In the oscillatory regime, the trophic levels are mainly indistinguishable and only one large bodysize compartment is visible (Fig. 6.3d,e), except for resource sizes z_{R_2} close to d . There the bodysize compartments start to separate slowly, while the system passes into the static regime. For these resource sizes the largest trophic level also ceases to exist, which reduces the maximal trophic level from five to four and a small bodysize compartment starts to emerge.

6. Evolutionary food web models: effects of an additional resource

Interaction of Partitions An additional resource can give rise to partitioned food web structures. The interactions between these partitions influence food webs in two ways:

First, the variety of possible food web structures increases: the classical food web structure disappears. The growth rate due to resource consumption over bodysize has now two maxima instead of original one: the first maximum, which is based on the original resource R_1 , occurs at a bodysize of $z_{max_1} = d$ and the new additional maximum, due to the second resource R_2 , has a bodysize of $z_{max_2} = z_{R_2} + d$. On each of these maxima, partitions with the classical structure emerge. However, feeding interactions and competitive exclusion occur between morphs in different partitions, which alters the overall food web structure. Therefore, the classical food web structure disappears for certain resource settings (e.g. Fig. 6.1b,c), despite initialising the model with parameters that lead to its emergence (section 6.2.3). In addition, the variety increases since one trophic level can be represented by bodysize compartments in each of the partitions (e.g. Fig. 6.1d).

Second, for intermediate resource sizes z_{R_2} ($d/2 \leq z_{R_2} \leq 1.95 < d$), partitions can destabilise the population dynamics: instead of reaching a static fixed point, biomass oscillations or evolutionary intermittence occurs. In the oscillatory regime, partitions are intertwined, each underlying the characteristics of the classical structure. However, gaps in bodysize between adjacent trophic levels of one partition are filled by the other one. This leads to indirect interactions between morphs of the same partition. In one partition, adjacent trophic levels are strongly connected, with subsequent levels representing predator and prey morphs. Now, weak indirect interactions occur between these trophic levels: a predator and a prey morph within the same partition can interact indirectly via a morph with an intermediate bodysize of the other partition, i.e. the morph is consumed by the predator and consumes the prey. These indirect connections are responsible for the destabilisation of the population dynamics, as we demonstrate in the following:

We consider the simplest form of partitioning: two interacting food chains. The first chain is based on the resource and contains three morphs, while the second one includes two morphs only. To study the influence of the relative position of the chains to each other and to systematically vary the indirect interaction strength between predator-prey pairs, we shift the position of the second chain, while keeping the position of the first one constant (see caption of Fig. 6.4). Note that this system contains only a single resource, but still explains the biomass destabilisation of the multi-resource model: resources do not participate in the above mentioned indirect interactions, but allow the evolutionary algorithm to create the necessary structure. Since we exclude evolution in this model set-up and put in the structure by hand, we do not lose any explanatory power, but are able to vary the indirect interaction strength systematically.

We examine the biomass extrema of the resource, the ratio η between the direct feeding link and the indirect interaction between a predator and its prey in the first chain (morph 2 and 3), and the resulting network of the surviving morphs as a function of the position of the second chain (Fig. 6.4b). We find that biomass oscillations occur for specific positions: Within a certain range all morphs survive (grey region). For smaller values of η , meaning that the biomass flow through the indirect link is relatively high, a phase shift between the predator-prey pair is induced (Fig. 6.A.3), which destabilises the complete population. This shows that indirect interactions between predator and prey can destabilise the population dynamic is supported.

The range of the oscillatory regime is broader for larger food webs, since due to the higher morph number the probability for a predator-prey pair to have the right ratio of indirect interactions increases. In addition, evolution can also cause a transition between an oscillating and non-oscillating system (evolutionary intermittence, see Fig. 6.1c), since, as mentioned above, the transitory networks for the static and oscillatory state are highly similar. Note that the second resource is not directly causing biomass oscillations, but it is crucial for the emergence of partitions in the food web, between which suitable feeding links cause the destabilisation.

6.4. Discussion

Most empirical food webs contain multiple resource (e.g. soil food webs (Wardle et al., 2004) or aquatic food web (Dunbar, 1953)) of different sizes, which is neglected in many existing models that describe the emergence of food webs. We expanded an allometric, evolutionary food web model by an additional resource and found three main results:

First, including an additional resource can lead to the partitioning of a food web. Each partition has a different resource specialisation and either focuses on a single resource or a mix of them. These partitions, or sub-food webs, can also be observed in empirical food webs with multiple resources (Wardle et al., 2004; Fukami et al., 2006). In addition, the emerging partitions result in a larger variety of food web structures: the preimposed distinct trophic levels of the classical food web structure can become interweaved by the interactions between partitions. In addition, hierarchical feeding interactions can be softened and the trophic level of a species does not strictly increase with body size. This variety is also observed in empirical food webs: freshwater ecosystems have a very hierarchical structure (Strong, 1992; Persson et al., 1992), while soil and marine food webs are more manifold (Polis, 1991).

Second, we found that the partitions, which emerge due to an additional resource, change the dynamical behaviour of the food web: the static fixed point becomes unstable and biomass oscillations occur. The underlying mechanism is the interplay of direct feeding link and indirect interaction (via an additional morph) between predator-prey pairs. For a certain ratio between both interactions, a phaseshift between predator and prey is induced, which destabilises the food web. This is in good agreement with other theoretical studies, which showed that either phase shifts (or time delays, (Ruan and Wolkowicz, 1996; MacDonald, 1976)) or weak interactions (Schwarzmüller et al., 2015; McCann, 2000) can lead to biomass oscillations. However, the additional resource is not itself destabilising, as for instance shown by Huisman and Weissing (1999), but allows the evolutionary algorithm to assemble the necessary partitioned structure.

Third, we observe that evolution can stabilise or destabilise the population dynamics of a food web, which is referred to as evolutionary intermittence: transitions between biomass oscillations and stationary behaviour occur that are induced by evolution. The transitions are therefore an intrinsic evolutionary behaviour and not necessarily an indicator for the endangerment or structural instability of a food web.

Already one additional resource has an enormous effect on the food web assembly. Therefore, the next steps are to include even more resources or an underlying continuous resource size distribution, which occurs in phytoplankton (Sommer et al., 2002; Downing et al., 2014), for example. Another promising step is also to incorporate the ability of morphs to consume different

6. Evolutionary food web models: effects of an additional resource

kinds of resources (e.g. light, nutrients, plants, dendritus, Dunbar (1953); Sommer et al. (2002)).

For our studies, we extended the model of Loeuille and Loreau (2005), which uses some approximations, e.g. in describing morph interactions. However, our findings do not depend on the particularities of the model by Loeuille and Loreau (2005) and therefore we expect them to be general features of food webs, which can be found in models that are ecologically more accurate. It seems likely that within such models, the complexity of the observed phenomena increases even further. For instance, if the linear functional response is substituted by a Holling Type functional response (Holling, 1959), the oscillatory regime might widen, since a simple food chain can already exhibit biomass oscillations (Fussmann et al., 2000; McCann et al., 1998). The complexity might also increase, if the allometric scaling is included in the reproduction and predation term in Eq. 7.1 (Brose et al., 2006; Binzer et al., 2011), since full allometric models can exhibit complex population dynamic Schwarzmüller et al. (2015); Binzer et al. (2011). However the structural variety is not affected by this.

Many empirical food webs have more than one resource and our studies indicate that it is worthwhile to include this fact in the description of food web assembly. Doing so, the simple multi-resource model gives rise to novel structures and dynamics that are lacking in single-resource models.

6.A. Appendix

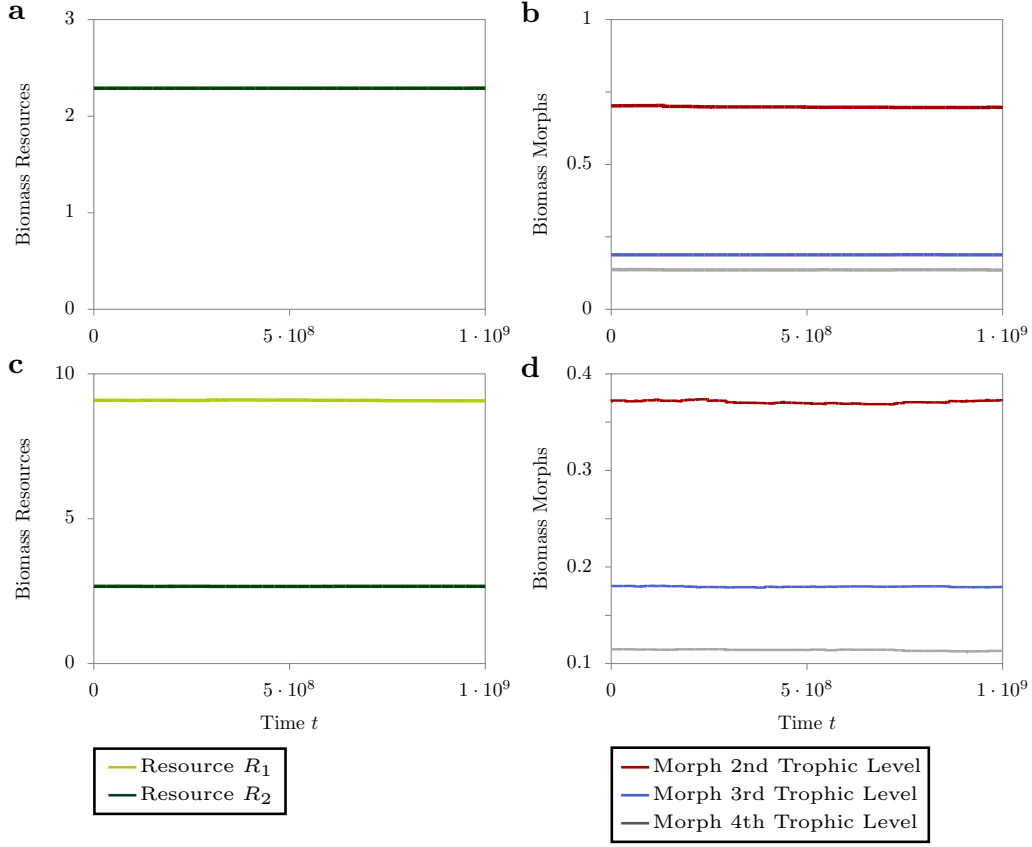


Figure 6.A.1.: Biomass evolution of the food webs shown in Fig. 6.1a (upper row) and d (bottom row). In the upper row, both resources have identical sizes $z_{R_1} = z_{R_2} = 0$. The resources in the bottom row have a size distance of d ($z_{R_1} = 0$ and $z_{R_2} = d$). **a,c:** Biomasses of both resources. Note that the curves in **a** overlap, since both resources have identical sizes. **b,d:** Biomasses of representative morphs of different trophic level. All biomasses of the resources and morphs reach a static fixed point. Small fluctuations are caused by evolutionary modification of the food web.

6. Evolutionary food web models: effects of an additional resource

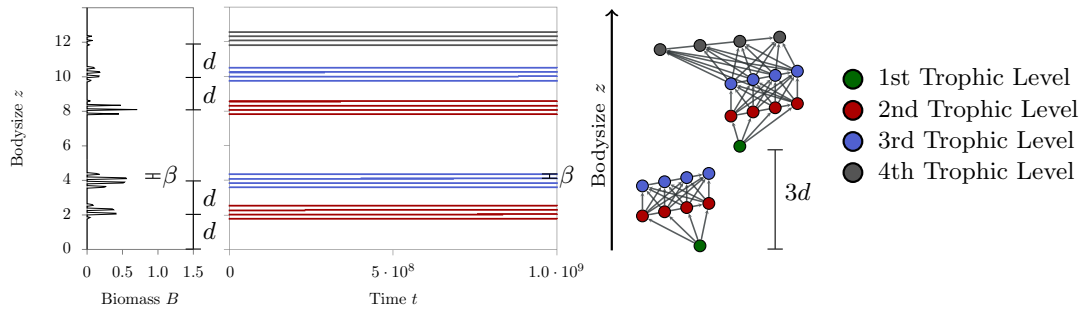


Figure 6.A.2.: Network time series and food web structure for a second resource of size $z_{R_2} = 6 = 3d$: time-averaged biomass-bodysize histogram (left), temporal evolution of bodysizes contained in the system (middle), and resulting network structure (right). The food web reaches an evolutionarily static state with two disconnected partitions each of which is based on one specific resource. The lower partition has a maximal trophic level of three, while the other has a maximal trophic level of four. Both exhibit the classical structure, but with distinct bodysize compartments.

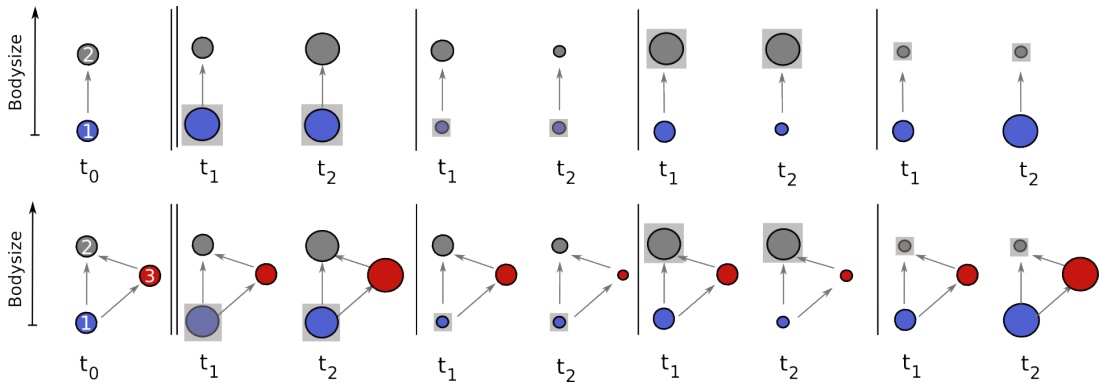


Figure 6.A.3.: Sketch of feeding interactions between morphs. The initial considered motifs (time t_0) are a predator (grey) and prey (blue) pair (top panel), and a triangle motif that contains an additional morph (red) (bottom panel). In both motifs the influence of the increase/decrease of the biomass of the prey/predator on the other morphs' biomasses is shown. The biomass of one of them is fixed to a higher/lower value (t_1 , underlined in grey) and sketch the reaction of the other morphs (t_2). The biomasses are indicated by the size of the nodes. **Top:** In a food chain, the biomass of the predator is proportional to the prey's biomass, while the prey's biomass is inversely proportional to the predators biomass. **Bottom:** Due to the additional morph, the biomass relationships are changed. For instance, the decrease in the prey's biomass still leads to an decrease of the predator's biomass, but due to the additional morph the decrease of the predator's biomass is buffered: the predator can consume the red morph. Similar effects can be seen for a change in the predator's biomass. If it decreases the prey's biomass does not increase linearly, since the red morph also increases in biomass and so does its consumption of the prey. Therefore the prey's biomass only increases slightly. The additional morph therefore induces a phaseshift between prey and predator.

7. A new dimension: evolutionary food web dynamics in two dimensional trait space

A new dimension: evolutionary food web dynamics in two dimensional trait space

Daniel Ritterskamp¹, Daniel Bearup, Bernd Blasius

CvO University Oldenburg, ICBM, Carl-von-Ossietzky-Strasse 9-11, 26111 Oldenburg, Germany

Abstract

Species within a habitat are not uniformly distributed. However this aspect of community structure, which is fundamental to many conservation activities, is neglected in the majority of models of food web assembly. To address this issue, we introduce a model which incorporates a second dimension, which can be interpreted as space, into the trait space used in evolutionary food web models. Our results show that the additional trait axis allows the emergence of communities with a much greater range of network structures, similar to the diversity observed in real ecological communities. Moreover, the network properties of the food webs obtained are in good agreement with those of empirical food webs. Community emergence follows a consistent pattern with spread along the second trait axis occurring before the assembly of higher trophic levels. Communities can reach either a static final structure, or constantly evolve. We observe that the relative importance of competition and predation is a key determinant of the network structure and the evolutionary dynamics. The latter are driven by the interaction – competition and predation – between small groups of species. The model remains sufficiently simple that we are able to identify the factors, and mechanisms, which determine the final community state.

Keywords: Spatial food webs, Higher dimensional trait space, Network structure, Evolutionary dynamics, Large community-evolution models

submitted to the Special Issue “Models in Evolution” of the “Journal of Theoretical Biology”

7.1. Introduction

Ecologists have long been interested in the complex structures exhibited by empirical food webs, the first studies dating back at least to the seventeenth century (see Egerton (2007); Dunne (2009)). Food webs describe the structure of ‘who-eats-whom’ in a community and constitute one of the most fundamental levels of biological organization. This structural richness has inspired theoretical approaches to capture food web topology and dynamics in terms of mathematical models. Most theoretical food web studies can be separated into two categories: generating food web structures or describing population dynamics. On the one hand, statistical models have been put forward that combine stochastic elements with simple link assignment rules and allow networks of trophic interactions between species that closely resemble empirical food webs to

¹Corresponding author

be synthesised (Dunne, 2009). The most prominent examples are the cascade model (Cohen and Newman, 1985), the niche model (Williams and Martinez, 2000) and the random model (Heckmann et al., 2012). While these models are able to provide detailed understanding of the structural complexity of food webs, they fail to predict the fine structure of complex food webs and intervality of a predator's diet (Stouffer et al., 2006; Williams and Martinez, 2008; Stouffer et al., 2007). Recently it was shown that the descriptive power of statistical food web models can be improved by incorporating multiple trait dimensions (Allesina et al., 2008). Notwithstanding, statistical food web models are fundamentally restricted in that they rely on ad hoc rules that can not explain the ecological mechanisms underlying the assembly of food webs and because they are, in principle, not able to capture the population dynamics.

A separate stream of research has focused on dynamical models, describing the temporal change of populations within a food web structure. Population dynamics models have proven to be able to capture a huge range of dynamic complexities, such as population cycles, multi-stability and chaotic dynamics. However at the same time they suffer from the problem of how to handle the variability of the model outcome with parametrisation in a high dimensional parameter space (Fussmann and Heber, 2002; Turchin, 2003). This problem is elegantly solved in allometric food web models, which were introduced by Yodzis and Innes (1992) and extensively studied since (Brose et al., 2006; Binzer et al., 2011). These models automatically determine the model parametrization using allometric scaling to determine how species dynamics vary with bodysize. However, just as statistical models cannot describe population dynamics, dynamical models cannot be used to generate food web structure, since the food web topology is required to initialize the model.

These two approaches are combined in evolutionary food web models, such as the webworld model (Caldarelli et al., 1998; Drossel et al., 2001), which generate food web topologies using an evolutionary algorithm and also describe population dynamics. One prominent case are niche based evolutionary food web models, which were introduced by Loeuille and Loreau (2005). In these models each species is characterised by a position, related to its bodysize, on a continuous niche axis. The strengths of interactions between species are then simply determined by their pairwise distances along the niche axis, taking additionally into account allometric scaling with bodysize. New species can be added to the community simply by assigning them a trait value, with the change in food web topology being determined automatically. As such they provide a simple mean to capture the combinatorial increase in possible food web structures that occurs as community size increases.

Niche based coevolutionary food web models were examined in great detail. Refinements of the original model (Loeuille and Loreau, 2005) studied, for example: the influence of trade-offs in resource consumption on the network structure (Ingram et al., 2009); the emergence of diversification by incorporating gradual evolution (Brännström et al., 2011); and evolvable shapes of the feeding interaction kernels to produce more realistic food webs (Allhoff et al., 2015a). These studies revealed a general difficulty of niche based evolutionary models to generate realistic food web structures (Allhoff and Drossel, 2013), which could be related to the fact that only a single evolutionary trait, bodysize, is considered. This observation is corroborated by analysis of empirical food web data which has shown that a higher number of traits is necessary to realistically describe species interactions (Eklöf et al., 2013).

7. A new dimension: evolutionary food web dynamics in two dimensional trait space

In this work we present an evolutionary food web model in a two dimensional trait space. We demonstrate that the second trait dimension can be incorporated naturally into the framework of niche based evolutionary food web models. By doing this, we unify the evolutionary food web model by Loeuille and Loreau (2005) with the seminal MacArthur and Levins model of competition along a niche axis (MacArthur and Levins, 1967). Thereby, in our model, species are described by their trait values in a two dimensional space and their interactions – feeding and competition – by the niche overlap in this space. The second trait can be interpreted in a variety of ways, for example as a vertical position in a water column, day time of activity, habitat preference, a hidden gradient (e.g. temperature, salinity, rainfall, day length) or it may simply be regarded as a spatial coordinate. Using the new model our objectives are to (i) investigate the population dynamics and evolutionary behaviour in the two dimensional trait space, (ii) characterise the transition between different evolutionary behaviours and structures in both dimensions of trait space, (iii) lay out the underlying mechanism producing these transitions, and (iv) verify the reasonability of the model by comparing it to empirical data.

7.2. Model

We develop an evolutionary food web model, describing the dynamics of one resource and a variable number of evolving morphs ($i = 1, \dots, N$). We use the term morph instead of species since we do not consider speciation processes. Each morph is characterised by two evolutionary traits, logarithmic bodysize z_i , and an abstract trait x_i , as well as a population biomass density B_i , which varies due to interactions with other morphs. Following MacArthur and Levins (MacArthur and Levins, 1967), the strength of morph interactions is determined by their pairwise distance in the two dimensional trait space: competitive interactions decrease with the distance between two morphs in either dimension; and so do feeding interactions with regard to their abstract traits, but they are maximized for a certain offset in the bodysize direction. This follows from empirical observations that species typically consume prey that is a certain fraction smaller than themselves (Vucic-Pestic et al., 2010; Brose et al., 2008). The resource of concentration R has a bodysize $z_R = 0$ and is continuously distributed along the abstract trait axis. The trait axis has a length of L , however we use periodic boundaries to simulate an infinite range (Scheffer and van Nes, 2006).

The model itself can be divided into two processes, the population dynamics of the community and an evolutionary algorithm, which occur on separated time scales. The population dynamics determine the variation in each morph's biomass B_i . The evolutionary algorithm operates on a slower time scale, introducing new morphs after the population dynamics have approached a steady state. We now consider each component in more detail.

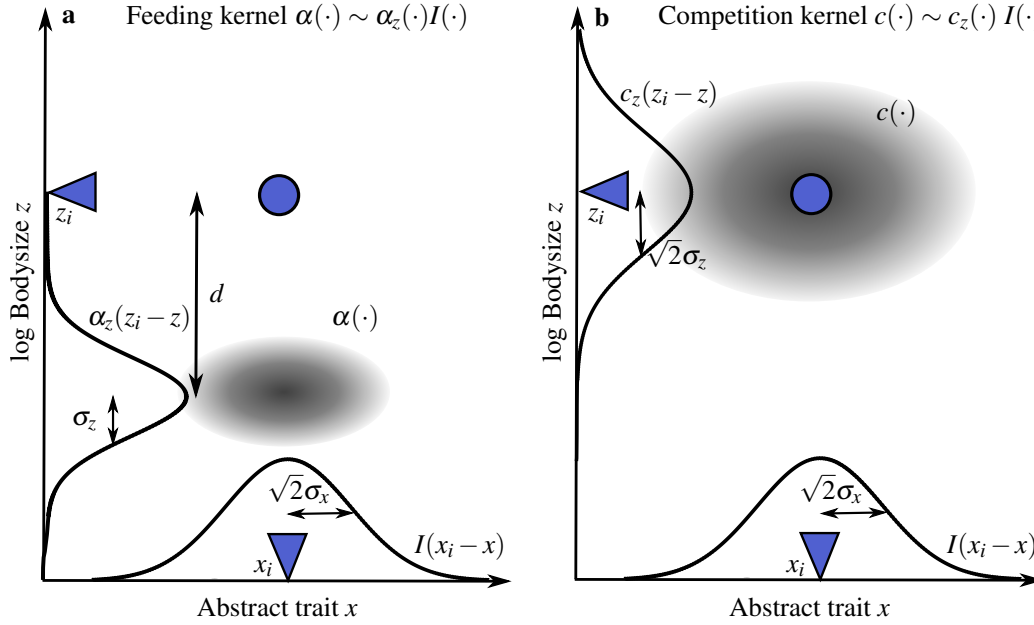


Figure 7.1.: Interaction kernels of the two dimensional food web model. The plots show the interaction strength described by two-dimensional Gaussian functions (ellipses) of a species with trait value x_i and bodysize z_i (indicated by blue circle and triangles). **a:** The feeding kernel $\alpha(\cdot)$ is modelled as the product of the bodysize feeding kernel $\alpha_z(z_i - z)$, with a maximum at $z = z_i - \log(d)$ and a width of σ_z , and the dependency on the abstract trait $I(x_i - x)$, centred around $x = x_i$ with a width of $\sqrt{2}\sigma_x$. **b:** The competition kernel $c(\cdot)$ is modelled as the product of $I(x_i - x)$ and the competition kernel in bodysize $c_z(z_i - z)$ with a width of $\sqrt{2}\sigma_z$, given by the overlap of the bodysize feeding kernels of the competing morphs. Since the competition kernel is determined by niche overlap the competition ranges are not independent parameters (see Fig. 7.A.3).

7.2.1. Population dynamics

The change of biomass B_i of morph i is given by Lotka-Volterra equations, accounting for reproduction by consuming other morphs and the resource, intrinsic mortality, and losses due to predation and competition

$$\begin{aligned}
 \frac{dB_i}{dt} = & B_i \left(\underbrace{f_0 a(z_i) \sum_{j=1, i \neq j}^N \alpha(z_i, z_j, x_i, x_j) B_j + f_0 a(z_i) \int_0^L dx \alpha(z_i, z_R, x_i, x) R(x)}_{\text{Reproduction}} \right. \\
 & \left. - \underbrace{m_0 a(z_i)}_{\text{Mortality}} - \underbrace{\sum_{j=1}^N a(z_j) \alpha(z_j, z_i, x_j, x_i) B_j}_{\text{Predation loss}} - \underbrace{\sum_{j=1}^N c(z_i, z_j, x_i, x_j) B_j}_{\text{Competition}} \right),
 \end{aligned} \tag{7.1}$$

7. A new dimension: evolutionary food web dynamics in two dimensional trait space

where f_0 is the conversion efficiency and m_0 is the basic mortality rate. Feeding interactions and the intrinsic mortality scale according to allometric relations with bodysize (Peters, 1986), which is expressed by $a(z_i) = 10^{-0.25z_i}$.

The feeding kernel $\alpha(\cdot)$ describes the ability of predator i to consume prey j . We assume that it is the product of two functions (Fig. 7.1a), describing the bodysize and abstract trait dependency,

$$\alpha(z_i, z_j, x_i, x_j) = \alpha_0 \alpha_z(z_i, z_j) I(x_i, x_j), \quad (7.2)$$

with α_0 being the attack strength.

Empirical studies suggest that feeding interactions depend on the logarithmic bodysize distances between morphs and are hump shaped (Vucic-Pestic et al., 2010; Brose et al., 2008). To represent this we express the bodysize dependency of the feeding kernel by a Gaussian function,

$$\alpha_z(z_i, z_j) = \frac{1}{\sigma_z \sqrt{2\pi}} \exp\left(-\frac{(z_i - z_j - \log(d))^2}{2\sigma_z^2}\right), \quad (7.3)$$

where d is the optimal predator-prey bodysize distance and σ_z corresponds to the feeding range of a morph. The dependency of the feeding kernel on the abstract trait is given by

$$I(x_i, x_j) = \frac{1}{\sigma_x \sqrt{4\pi}} \exp\left(-\frac{(|x_i - x_j|)^2}{4\sigma_x^2}\right), \quad (7.4)$$

which is of Gaussian shape with a width of $\sqrt{2}\sigma_x$ and states the interaction strength of two morphs along the abstract trait axis, see Fig 7.A.3 for its derivation.

Motivated by the model of MacArthur and Levins (MacArthur and Levins, 1967), the competition kernel $c(\cdot)$ is determined by the niche overlap between two morphs in the two dimensional trait space (Fig 7.1b), as the overlap in abstract space $I(\cdot)$ and the prey they have in common $c_z(\cdot)$,

$$c(z_i, z_j, x_i, x_j) = c_0 c_z(z_i - z_j) I(x_i, x_j), \quad (7.5)$$

where c_0 is the competition strength and

$$c_z(z_i - z_j) = \frac{1}{\sigma_z 2\sqrt{\pi}} \exp\left(-\frac{(z_i - z_j)^2}{4\sigma_z^2}\right). \quad (7.6)$$

The latter is calculated by the overlap of the bodysize feeding kernels $\alpha_z(\cdot)$ of both morphs, see Fig. 7.A.3 for more details. The width of the feeding and competition kernels in both dimensions are determined by the same parameters, with competition range being by a factor of $\sqrt{2}$ larger than the feeding range.

Unlike the evolving morphs, the resource has a constant bodysize and is continuously distributed along the abstract trait axis. The dynamics of the resource are given by the following chemostat equation

$$\frac{dR(x)}{dt} = I - eR(x) - \sum_{j=1}^N \alpha(z_j, z_R, x_j, x) B_j R(x). \quad (7.7)$$

Here, the first and second terms represent a constant input and an outflow relative to the resource biomass and the final term describes losses due to consumption by the morphs in the system.

Following the original formulation of these models by MacArthur and Levins (1967) and Loeuille and Loreau (2005), we intentionally keep our model as simple as possible. In particular, we describe predation rates using linear, rather than more realistic (Holling, 1959) functional responses. This allows us to truly unify both models. If all species have the same bodysize, our model reduces to the MacArthur and Levins model of competition along a niche axis (MacArthur and Levins, 1967). In contrast, if all species have the same value of their abstract trait our model reduces to the evolutionary food web model by Loeuille and Loreau (2005).

7.2.2. Evolutionary dynamics

Every t_m time units a randomly chosen morph k mutates, and a mutant m is added to the system, with a new abstract trait $x_m \in [x_k - \Delta_x, x_k + \Delta_x]$, and logarithmic bodysize $z_m \in [z_k - \Delta_z, z_k + \Delta_z]$. The mutant is introduced with an initial biomass of θ , which is also the extinction threshold. If the biomass B_k of any morph falls below this threshold, as a result of the population dynamics, it is considered to be extinct and is removed from the system.

7.2.3. Initialization and parameter values

Simulations are performed using the Sundials CVODE solver (Cohen and Hindmarsh, 1996) in C++ with absolute and relative errors per time step set to 10^{-12} . The abstract trait axis is discretised by one hundred grid points per unit length and periodic boundaries are applied. All simulations are initialized with the resource (logarithmic bodysize $z_R = 0$ and a concentration of $R(x) = I/e$) and a single evolving morph with an abstract trait of $x_1 = \frac{L}{2}$ and logarithmic bodysize $z_1 = \log(d)$.

Previous studies of evolutionary food web models have established reasonable parameter values for characterisations of morphs based on bodysize. Our extension to a two dimensional trait space has no effect on the interpretation of the majority of these parameters. Hence we take: $f_0 = 0.3$, $m_0 = 0.1$, and $d = 100$, following (Loeuille and Loreau, 2005); $\theta = 10^{-10}$, from (Allhoff and Drossel, 2013); and $\Delta_z = \log(2)$, as in (Allhoff et al., 2015a). The mutation time t_m is set to 10^5 , which is sufficiently high for the population dynamics to reach an equilibrium before the next mutation event.

Parameters describing interactions along the abstract trait dimension cannot be derived from existing literature. We fix these parameters as follows: $I = 1000$, $e = 0.1$, $\sigma_x = 0.05$, and $L = 1$. Tests of alternative values of these parameters found that they had no qualitative effect on our results (see Results). As discussed in Section 7.3 these parameters mainly influence the effective length of the abstract trait axis. Furthermore, we choose a relatively narrow mutation range in this direction, $\Delta_x = 0.08$, to ensure that mutants are similar to their parents. Finally, to reduce the number of free parameters, we set the attack strength, $\alpha_0 = 1.0$, and in the simulations presented in this work we vary the competition strength c_0 and feeding range σ_z as our main control parameters.

7.2.4. Data evaluation

Since the evolutionary outcome depends on the sequence of random numbers, we perform one hundred simulation runs for each parameter set, with different seeds. Each simulation runs for 10^{10} time units, if not stated otherwise. To calculate the network characteristics we collect 20 networks from each simulation run, each $5 \cdot 10^8$ time units, starting at a time of $5 \cdot 10^8$ to omit the initial assembly phase. This produces a total of 2000 networks for each parameter set. To calculate the network structure we follow Allhoff et al. (2015a) and remove all links that supply less than 75% of the biomass contributed by the average link. This cut-off criterion depends on the feeding kernel and the prey's biomass density and therefore mimics sampling limits in empirical data.

The emerging networks are compared to empirical data, in particular the 50 aquatic food webs in the Adirondack lake data set (Sutherland and of Environmental Conservation, 1989). Since the model can only produce networks with one resource, we treat all species in the first trophic level of the empirical food webs as a single species, as proposed by (Rossberg et al., 2006). The trophic level is calculated using the prey-averaged trophic level, for the empirical data, and the flow-based trophic level, for networks obtained from simulations (Williams and Martinez, 2004).

7.3. Results

We now investigate how morph interactions influence the emergence of the network structure and evolutionary behaviour. For this we systematically screen the parameter range of the competition strength c_0 and the feeding range σ_z . We find three distinct types of community and distinct regions of parameter space where each type dominates, which means that a type constitutes 80% of all simulated outcomes (Fig. 7.2). The first type of community is characterised by a complete absence of trophic structure. A single trophic level builds up, consisting of morphs that consume the resource, but no further trophic levels emerge. The areas of parameter space where such communities dominate are denoted Region I. The second type of community has trophic structure and is evolutionarily static. That is, after an initial dynamic phase of community assembly, the morphs, and the interactions between them, become fixed. Such food webs dominate in Region II. The third type of community has trophic structure and is evolutionarily dynamic. The morphs in the community, and their interactions, change constantly over time and leading to the temporary emergence of higher trophic levels – evolutionary outbursts – and cases where a given morph progressively decreases its bodysize. Region III is dominated by food webs of this type.

These regions are robust with respect to variation of the parameters governing interactions along the abstract trait dimension (see Section 7.2.3 for a specific list). Increasing the level of resources available, determined by I and e , (beyond the level necessary to support multiple bodysize layers) or the length of the abstract trait axis L , increases the number of morphs that can coexist, but does not change the food web type, whereas a larger value of σ_x is equivalent to a decrease in available resources or an increase in L .

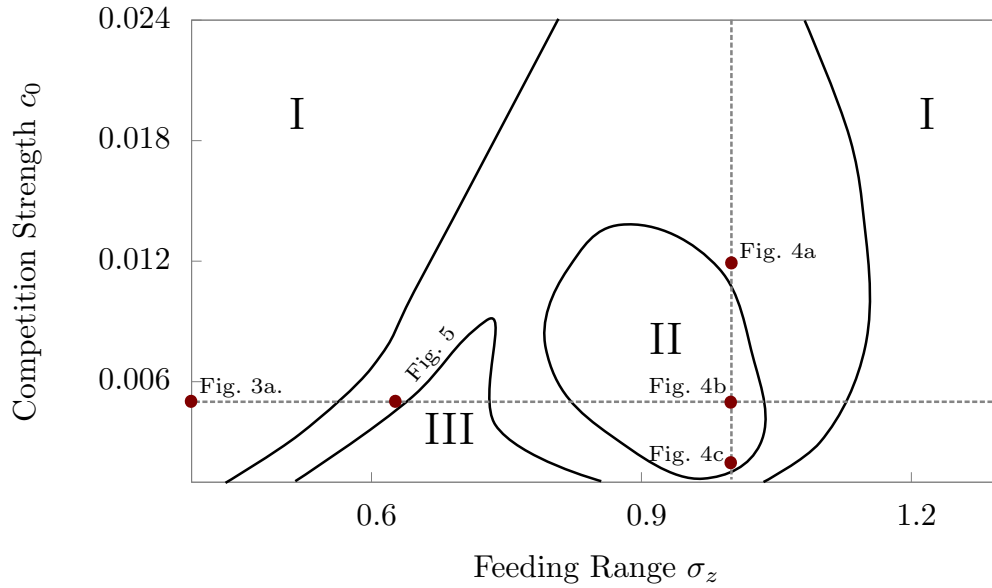


Figure 7.2.: Effect of feeding range σ_z and competition strength c_0 on the model outcome. Three regions in parameter space occur, each of which is dominated by a particular type of community: Region I is dominated by communities with no trophic structure; Region II by evolutionarily static food webs; and Region III by evolutionarily dynamic food webs. In between these regions, an unassigned area occurs that is not dominated by a specific community type (i.e., less than 80% of simulated communities correspond to a single state, see also Fig. 7.A.1 for the frequencies of each state). Points denote examples further analysed in Figs. 7.3-7.5 and dotted lines represent the cross sections shown in Figs. 7.6 and 7.7.

7.3.1. Communities with no trophic structure (Region I)

Region I is dominated by evolutionarily static communities with a single trophic layer of primary consumers. This region actually splits up into two sub-regions: For small feeding ranges σ_z , the single trophic level contains many morphs with nearly identical bodysizes (Fig. 7.3a). This can be explained by the fact that for small σ_z only morphs in a narrow bodysize interval can effectively feed on the resources. However due to the normalisation of the feeding kernel $\alpha(\cdot)$, resource consumption is relatively high, allowing morphs to coexist in relatively close proximity along the abstract trait axis. Consequently, the biomass distribution along the abstract trait axis is nearly uniform (Fig. 7.3c). As is shown in Fig. 7.2 the range of this sub-region in parameter space increases with competition strength. This is explained by the effect of competition strength on the emergence of food webs, see below.

7. A new dimension: evolutionary food web dynamics in two dimensional trait space

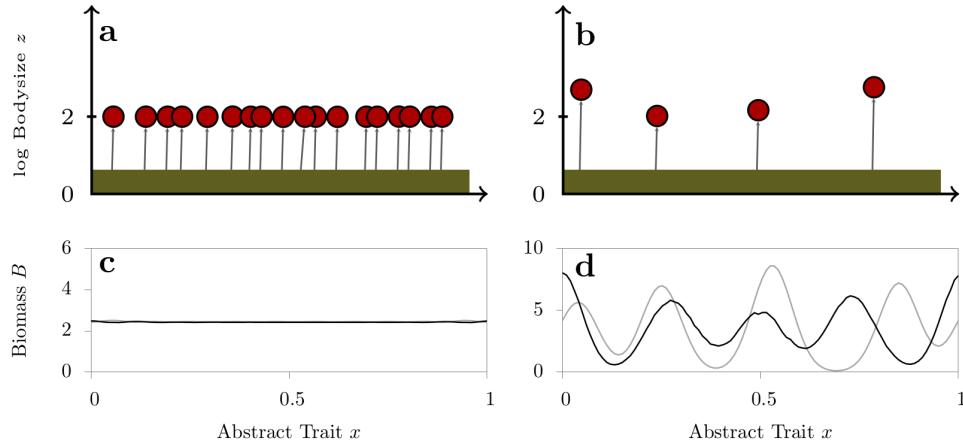


Figure 7.3.: Two characteristic patterns of static communities without trophic structure (Region I), emerging for the case of a narrow feeding range ($\sigma_z = 0.4$, left column) and a large feeding range ($\sigma_z = 1.5$, right column). **a,b:** Positioning of morphs (represented by red circles) in two dimensional trait space. The green bar illustrates the resource. **c,d:** Biomass distribution along the abstract trait axis of the presented network (grey). It is assumed that a morph's biomass is distributed around the abstract trait, x_i , according to a Gaussian of width σ_x (see Fig. 7.A.3). The black line denotes the average over 100 different simulated networks, whereby all biomass distributions are aligned by setting the maximum biomass value to an abstract trait value of zero. Therefore an artificial maximum and a subsequent minimum occur at the edges of the abstract trait axis. **Left column** ($\sigma_z = 0.4$): Dense morph packing along the abstract trait axis of morphs with similar bodysize. The biomass is continuously distributed along the trait axis, with the distributions of the single run and the average overlapping, since the interval between morphs is close to the distribution range along the abstract trait, σ_x . **Right column** ($\sigma_z = 1.5$): Food web wherein morphs keep a maximal characteristic distance to each other in trait space (see averaged distribution). Only four morphs are contained, which differ in bodysize, but are restricted to the same trophic level.

For large feeding ranges σ_z , the single trophic level contains only a few morphs with a higher variety in bodysize (Fig. 7.3b). In this case the feeding kernel is broad and morphs in a wider bodysize spectrum can feed on the resource. However, resource consumption is now low (due to the normalisation of the feeding kernel), meaning that only a lower level of competition between morphs can be sustained. Therefore morphs must maintain a larger distance in trait space in order to coexist. Consequently, in contrast to the case of small σ_z , the biomass distribution for these communities displays a rather regular, periodic, structure since neighbouring morphs are separated by trait intervals similar to the distribution range along the abstract trait axis σ_x . Thereby, the

structuring along the abstract trait axis paradoxically is explained by the interaction along the bodysize axis – even though the communities in Region I are characterised by the absence of trophic structure.

7.3.2. Communities with trophic structure

In our simulations, communities with trophic structure emerge only with high frequency for low to intermediate competition strengths c_0 and intermediate feeding ranges σ_z . This observation is consistent with the findings by Loeuille and Loreau (2009), who studied the emergence of trophic structures in niche based evolutionary food web models by evolutionary branching. For small feeding ranges, a small increase in bodysize leads to large losses in the feeding input from the resource and this, in combination with competition with the other morphs, means that larger mutants are rarely viable. As the feeding range increases, the losses in feeding input from the resource with increasing bodysize decrease. Thus, the gain in feeding input from smaller morphs becomes sufficient to offset this loss, and, if competition is not too high, larger mutants become viable. This ultimately allows additional trophic levels to form. Increasing the feeding range further ultimately leads to the region described above, where a large range of bodysizes can be sustained, but morphs have to maintain a large interval between them in trait space. While larger morphs are viable in this region, they tend to drive their prey to extinction (by a combination of feeding and competition interactions), and thus multiple trophic levels are unsustainable.

As noted above, in our model two types of food web emerge characterised by whether they are static or dynamic on evolutionary time scales. We consider each of these behaviours in more detail below, beginning with the simpler case of evolutionarily static food webs.

7.3.2.1. Evolutionarily static food webs (Region II)

Evolutionarily static food webs dominate in an ellipsoid region of the parameter space, denoted Region II, at the higher end of feeding ranges where communities with trophic structure are likely and encompassing a relatively wide range of competition strengths. Figure 7.4 shows three characteristic examples, for different levels of the competition strengths c_0 . In all examples, the morph composition and network structure become static after the initial assembly phase, however the final morph positioning in the two dimensional trait space and the interaction network depend on c_0 .

For large values of the competition strength (left column in Fig. 7.4), the emerging food webs typically have a highly consistent trophic structure along the abstract trait axis, with chains of three regularly spaced morphs that keep a logarithmic bodysize distance of $\log(d)$ (see Fig. 7.4d). Adjacent chains display slight shifts in morph bodysize relative to each other and are irregularly spaced in the abstract trait. Consequently, the biomass distribution (Fig. 7.4g) exhibits small fluctuations. Neglecting the artificial extrema, the averaged distribution is nearly constant. This suggests that these fluctuations occur randomly and that there is no structure to the biomass distribution along the abstract trait. Plotting morphs by their logarithmic bodysize and trophic level (Fig. 7.4j) reveals three distinct clouds. For logarithmic bodysizes between 4 and 8 we see a strong positive correlation between trophic level and bodysize. In conjunction with the example network structure, this suggests that morphs are subject to a strict hierarchical ordering

7. A new dimension: evolutionary food web dynamics in two dimensional trait space

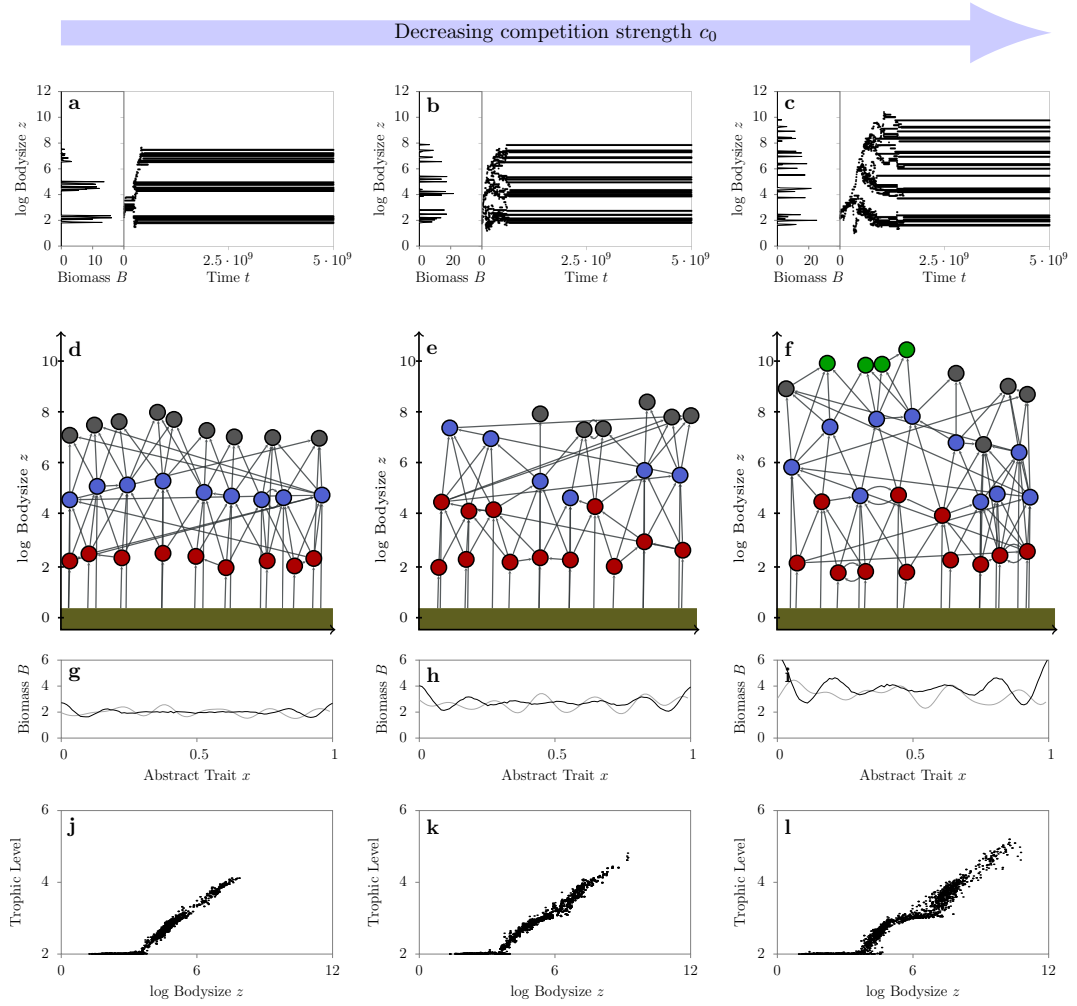


Figure 7.4.: Structure of evolutionary static food webs (Region II). Each column presents a different competition strength c_0 , decreasing from left to right (see Fig. 7.2 for position in parameter space). **Left column** ($c_0 = 0.012$): Static network with distinct bodysize layers. **Middle column** ($c_0 = 0.005$): Static network with slightly merged bodysize layers. **Right column** ($c_0 = 0.002$): Static network with intertwined bodysize layers. **a,b,c:** Temporal evolution of bodysizes (right panels) and bodysize-biomass histograms (left panels) of specific networks over the last $2.5 \cdot 10^9$ time units. **d,e,f:** Positioning of morphs in two dimensional trait space and interaction network. **g,h,i:** Biomass distribution of all morphs along the abstract axis of the network shown (grey) and the average over 100 aligned biomass distributions (see caption of Fig. 7.3 for more details). **j,k,l:** Morphs' trophic level against logarithmic bodysize for 100 simulated communities. In all simulations, the feeding range was fixed to $\sigma_z = 1$.

in bodysize, which determines their role in the food web. In contrast, morphs with trophic level 2 appear to have a relatively large range of bodysizes. This occurs because the ensemble of communities considered includes systems with and without trophic structure, each exhibiting different bodysize to trophic level distributions. In communities without a trophic structure, all morphs have a trophic level of two, but larger bodysizes (see Section 7.3.1), while morphs in communities with a trophic structure have a bodysize close to d , that is $\log(d) \approx 2$ for our parameters.

As competition strength decreases (middle column in Fig. 7.4), the bodysize layers become less distinct and the variance in bodysize of morphs in a given trophic level increases. In addition, morphs in adjacent trophic levels can have similar bodysizes, causing the trophic levels to merge. These losses in regularity extend to the network structure along the abstract niche. The repeating chain structure observed previously is replaced by an irregular network structure composed of a variety of motifs. While there is no noticeable change in the distribution of the smallest morphs along the abstract trait axis, larger morphs appear to cluster into denser patches separated by relatively large gaps. This is reflected in the biomass distribution (Fig. 7.4h) which displays larger fluctuations than were observed for higher competition strengths. These fluctuations persist in the average biomass distribution, which oscillates across the entirety of the abstract trait axis, although the difference between maxima and minima is small at its midpoint. This indicates the emergence of a regular pattern in the morph biomasses. The merging of trophic levels is also reflected in the logarithmic bodysize-trophic level plot (Fig. 7.4k). Whereas previously the relationship between logarithmic bodysize and trophic level was approximately linear, in these webs a concave shoulder appears for logarithmic bodysizes between 5 and 7.

These changes become more pronounced as the competition strength weakens further (right column in Fig. 7.4). In this case there are no distinct clusters of bodysizes, the trophic levels intertwine and morphs of equal bodysizes can have different trophic levels (see Fig. 7.4f). Thereby, network structure exhibits even larger variations and morphs of trophic level five can be found in some ranges of the abstract trait axis. The averaged biomass distribution (Fig. 7.4i) becomes increasingly inhomogeneous, with greater variation between maxima and minima and wider peaks. Additionally, the concave shoulder in the logarithmic bodysize-trophic level plot (Fig. 7.4l) becomes more pronounced. Within this range, trophic levels can hardly be predicted from bodysize. The varying shape of the logarithmic bodysize-trophic level relationship, from linear to almost stepped, provides a straightforward diagnostic of the regularity of the food web network structure.

7.3.2.2. Evolutionarily dynamic food webs (Region III)

Evolutionarily dynamic food webs dominate in a roughly triangular region of the parameter space, denoted Region III, at the lower end of feeding ranges and competition strengths where communities with trophic structure are likely. A characteristic example is shown in Fig. 7.5. Three distinct bodysize layers are present at all times, but the morph composition changes continuously. Occasionally an additional unstable bodysize layer emerges, temporarily increasing the number of morphs before it collapses again (see Figs. 7.5a-b). We refer to this phenomenon as an evolutionary outburst. As shown in Figs. 7.5d-e, the positioning of morphs in trait space strongly

7. A new dimension: evolutionary food web dynamics in two dimensional trait space

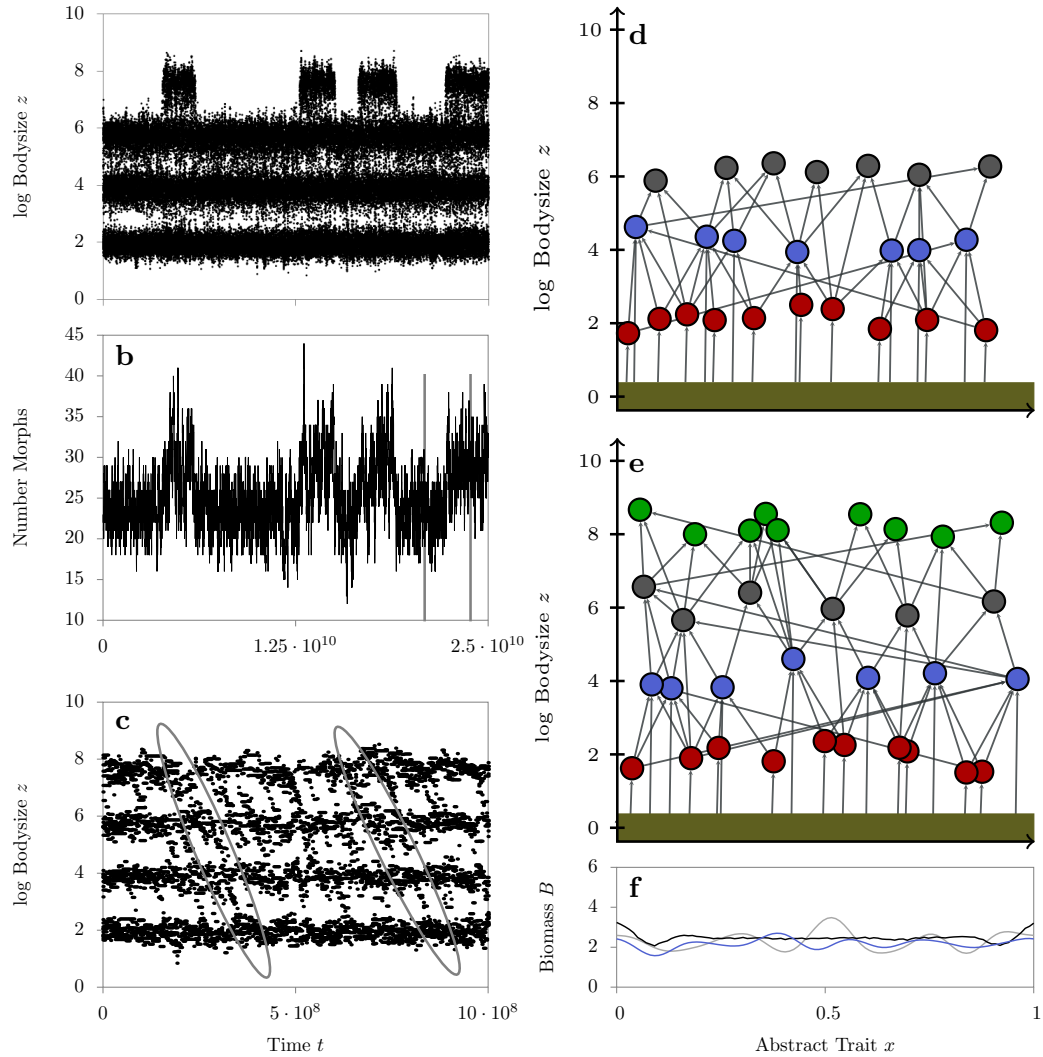


Figure 7.5.: Characteristics of an evolutionarily dynamic food web (Region III). **a:** Temporal behaviour of bodysizes, showing four evolutionary outbursts. **b:** Corresponding total number of morphs as a function of time. **c:** Close up of the temporal development of the bodysizes shown in (a), demonstrating the evolutionary downwards movement in bodysize (marked in grey). **d,e:** Positioning of morphs in trait space and interaction networks, before (d) and during (e) an evolutionary outburst. Time instances are marked by vertical lines in (a) and (b). **f:** Biomass distribution along the abstract trait axis of the networks shown in (d) (grey) and (e) (blue), and averaged over 100 simulation runs (black). Parameter values $c_0 = 0.005$ and $\sigma_z = 0.625$ (see also Fig. 7.2).

differs before and during an evolutionary outburst. The waiting times between outbursts and durations of outburst are described best by exponential distributions (Fig. 7.A.4). In addition to evolutionary outbursts, we also observe cases where morphs decrease their bodysize progressively, a phenomenon we refer to as evolutionary downwards movement. This movement can traverse several bodysize layers (Fig. 7.5c). The biomass distributions for individual networks exhibit small fluctuations, however the averaged distribution is nearly constant suggesting that these fluctuations do not reflect an underlying structure (Fig. 7.5f).

To gain more insight into the two evolutionary phenomena, outbursts and downward movements, we set up a system that can only contain a single predator and prey morph (Fig 7.A.2). In this small community it becomes relatively easy to disentangle population dynamics and evolutionary processes, leading in this case to the emergence of an evolutionary arms race. Assume that the predator in this system has bodysize z_1 and abstract trait value x_1 . The prey's fitness increases the further it is separated from the centre $(z_1 - d, x_1)$ of the predator's feeding range (see sketch in Fig. 7.A.2a). As such, over evolutionary time, the prey will evolve away from this centre due to a sequence of invasions by more fit mutants. This, in turn, decreases the predator's fitness, and consequently, the predator follows the prey by the same evolutionary process. This co-evolutionary process results in red-queen dynamics (Abrams, 2000; Rosenzweig et al., 1987; Dommar et al., 2008) between the predator and prey morph, as shown in Figs. 7.A.2b,c.

In larger systems with several morphs, this process can result in local compaction of morphs with similar bodysizes along the abstract trait axis. Morphs in the same layer generally optimize their pairwise distance along the abstract trait axis to avoid competition. However, if the losses of the prey morphs due to predation exceed the losses from increased competition, a coherent evolutionary motion of prey morphs along the abstract trait axis can be induced. As described above, predators will tend to follow this evolutionary movement, causing complex co-evolutionary dynamics (Dommar et al., 2008) and giving rise to transient density fluctuations of prey morphs in niche space.

This process can temporarily give rise to the formation of localised regions along the abstract trait axis with unusual high biomass density across all bodysize layers. Whenever, such localised regions are able to support larger morphs we observe the formation of an additional bodysize layer, i.e. an evolutionary outburst. However, predation from this higher trophic layer subsequently decreases the population density of the predators which drive compaction, which eventually causes the return to a more uniformly distributed biomass distribution. With this reduction in biomass density, larger morphs can no longer be supported and the evolutionary outburst collapses. Increasing morph densities along the abstract trait axis, i.e. by increasing resource availability, increases the duration of evolutionary outbursts and allows them to spread. Further increases eventually result in the permanent establishment of a larger bodysize layer, which itself may display evolutionary outbursts (not shown).

In a similar way, the phenomenon of evolutionary downwards movement can be explained by the emergence of density fluctuations along the trait axis. As an alternative to following its prey along the abstract trait axis, a predator can instead evolve downwards in bodysize to feed on lower bodysize layers.

7. A new dimension: evolutionary food web dynamics in two dimensional trait space

When this occurs in a region of lower biomass (due to compaction), the downwards drift may persist over a large number of evolutionary steps and traverse several trophic levels. If no other prey are found, the downward movement will terminate when the morph is able to feed optimally on the resource.

7.3.3. Transitions between community types

To study the transitions between community types in the different dynamic regions we now consider two cross sections of the parameter map (see Figs. 7.2 and 7.6), along which the parameters are varied separately. Along cross section I, the competition strength c_0 is varied, while the feeding range σ_z is fixed. Vice versa, for cross section II, σ_z is varied while c_0 stays the same. For each cross section we plot the frequency of occurrence of the community type (Figs. 7.6a,d), the structure of the biomass distribution along the abstract trait axis (Figs. 7.6b,e), and the bodysize distribution (Figs. 7.6c,f), each averaged over 100 realisations. We also include a key indicating which community type dominates for a given parameter range in Figs. 7.6c,f for ease of reference.

7.3.3.1. Cross section I: varying the competition strength

For small competition strength c_0 , the majority of communities are evolutionarily static and are evenly divided between those with trophic structure and those without (Fig. 7.6a). However a small increase in competition strength causes the frequency of occurrence for communities with trophic structure to increase sharply and Region II is entered. As competition strength increases further the frequency of such communities tends to decline and they are replaced with communities with no trophic structure. The transitions, first to a region dominated by static food webs, and then towards domination by communities without trophic structure appear to be relatively smooth.

As originally observed in Region II, see Section 7.3.2.1, the average biomass distribution undergoes a transition from heterogeneous to relatively homogeneous with increasing competition strength (Fig. 7.6b). The differences in biomass distribution for adjacent competition strengths are, for the most part, small, suggesting another smooth transition. The only exception is at the lower edge of Region II, where there appears to be a sharp change in the biomass distribution.

Finally, the bodysize spectrum displays a number of interesting features (Fig. 7.6c). In particular, for a given value of c_0 the spectrum exhibits a regular structure, corresponding to pronounced clusters of morphs at specific bodysize values. For varying values of c_0 these clusters form characteristic branches. We focus first on the branches that start at log bodysize values of 2 (bottom), 5 (middle) and 8 (top), reflecting the structure of a three trophic level network. All branches are relatively broad, suggesting that the network structure is irregular. This suggestion is corroborated by the weak (i.e. low frequency) branch that is emerging at a logarithmic bodysize value of 6, which suggests that a four-level trophic network is present in some areas. As the competition strength increases the top branch becomes weaker, the emerging branch becomes stronger, and the middle branch disappears almost entirely. These changes reflect the transition to a more regular network structure, see Section 7.3.2.1. Finally, at the upper boundary of Region II the top branch disappears and shortly thereafter the middle branch reappears.

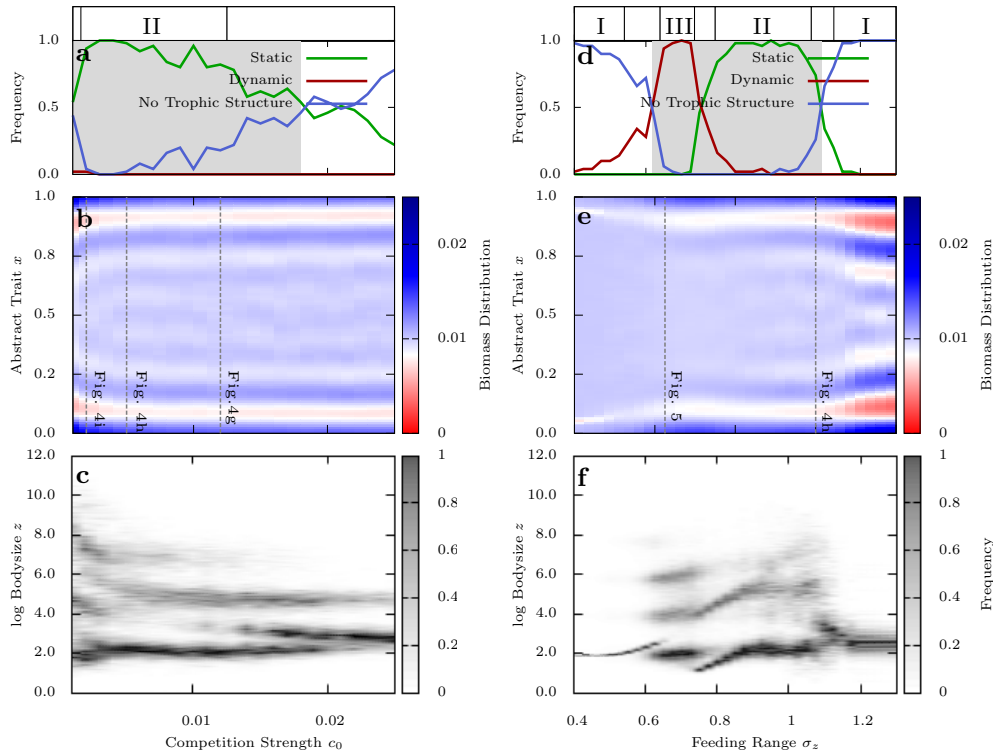


Figure 7.6.: Model outcome along the cross sections through parameter space, shown in Fig. 7.2. **Left column:** different values of competition strength c_0 for fixed $\sigma_z = 1$ (cross section I). **Right column:** different values of feeding range σ_z for fixed $c_0 = 0.005$ (cross section II). **a,d:** Frequencies of the different community types (indicated by colours) in repeated simulation runs. The grey area marks the regime in which at least 50% of all networks have a trophic structure (i.e., a maximum trophic level greater than 2.5). The bar above this plot indicates the region of parameter space (Roman numeral) in which the parameter combination lies. **b,e:** Average biomass distribution along the abstract trait axis, normalized by the total biomass. The averaging was done as explained in the caption of Fig. 7.3. Vertical lines indicate parameter values for which biomass distributions have been shown in Fig. 7.4 and Fig. 7.5. **c,f:** Probability density function of log bodysize. For each parameter we averaged over 100 simulation runs.

The middle branch now corresponds to morphs in communities with no trophic structure which can have relatively high bodysize, see Section 7.3.1. As competition strength increases further, the middle branch becomes stronger, indicating the increasing dominance of communities without a trophic structure (Fig. 7.A.5a).

7. A new dimension: evolutionary food web dynamics in two dimensional trait space

7.3.3.2. Cross section II: varying the feeding range

For small feeding ranges σ_z , the system is dominated by communities without a trophic structure (Region I) (Fig. 7.6d). As the feeding range increases, the frequency of occurrence of evolutionarily dynamic food webs increases until the system reaches Region III. Next, these communities become evolutionarily stable, and the system passes to Region II, as the feeding range increases further. Finally, for large feeding ranges these communities lose their trophic structure and the system returns to Region I.

Initially the average biomass distribution is homogeneous across the majority of the abstract trait (Fig. 7.6e). As the feeding range increases, periodic structures of biomass emerge, initially at the edges of the domain, but spreading with σ_z towards the centre. The differences between maxima and minima increase significantly with σ_z , and the width of the oscillations increases slightly. The transition from a nearly uniform to a structured biomass distribution is fairly smooth.

The bodysize spectrum shows fast transitions in the number of bodysize branches (Fig. 7.6f), which occur close to the boundaries between regions of the parameter space (Fig. 7.6d). The branches, corresponding to a single type of community, slowly become broader as σ_z increases. There is also a trend towards increasing morph bodysize, until the transition back to communities without trophic structure.

7.3.4. Drivers of variation in structure

We have observed that the communities generated by this model vary both in type and in their internal structure. The mechanisms responsible for these variations are explained briefly below.

7.3.4.1. Emergence of community structure

The evolutionary assembly of a community occurs in a bottom-up manner. Originating from the single initialized morph, new morphs with a similar bodysize spread by mutation events along the abstract trait axis. As explained in Section 7.3.1, the bodysize range of the morphs in the first bodysize layer depends on the feeding range σ_z and the competition strength c_0 . As the feeding range increases, so does the range of bodysizes, since morphs are less strongly specialised. Large competition strengths narrow the bodysize range, since morphs have to optimize the distance to their prey to compensate competition losses.

After the bodysize layer is established over a region along the abstract trait axis, a second layer can emerge if the competition strength and feeding range are in the right ranges. This occurs in a similar way to that described above, a single morph increases its bodysize until it can feed on a morph in the lower layer. The new layer then spreads across the abstract trait axis. The final bodysize of morphs in the higher layer depends on the bodysize of their prey in the lower layer. Therefore the variation in bodysize is passed from lower to higher bodysize layers.

Once all viable bodysize layers are occupied, the community can either become static or dynamic. Static denotes that morph bodysizes and abstract traits become fixed, indicating that no niches exist where a mutant can invade, while dynamic refers to a system with available niches for new mutants and thus the community does never become static. The latter occurs for small competition strengths and lower feeding ranges, invasions continue to occur, resulting

in evolutionarily dynamic food webs. In this parameter range, the sensitivity of the interaction kernels, $\alpha(\cdot)$ and $c(\cdot)$, to variations in bodysize is relatively large (in comparison to the rest of the parameter space).

7.3.4.2. Transitions in network structure and biomass distribution

The degree of order in the food web network is governed by the minimisation of competition, while maximising the feeding input. On the one hand, a morph evolutionarily tries to optimise its feeding input by maintaining an optimal logarithmic bodysize separation of $\log(d)$ and a minimal distance in the abstract trait from its prey. On the other hand, morphs within the same layer maximize their pairwise distance in trait space to avoid competition.

If the competition strength c_0 is high, competition losses exceed the feeding input, and morphs in the same layer increase their separation along the abstract trait. At the same time, optimization of the feeding input is important to compensate competition losses. As a consequence, ordered chainlike structures occur throughout the network. If the competition strength is lowered, feeding inputs outweigh competition losses, allowing morphs to approach each other. The fitness landscape is relatively flat close to a resident, a wide range of traits are viable, and, as such, the first invading morph fills the open niche and the network structure becomes irregular.

Increasing feeding range σ_z has a similar effect. For small σ_z , predators are highly specialised and thus only a narrow range of mutant bodysizes are viable, resulting in a distinct network structure. As σ_z increases predators become less specialised and the fitness landscape becomes flatter, allowing a more irregular network structure. This irregularity along the abstract trait axis spreads to higher bodysize layers, as described above.

When the trophic network structure is regular along the abstract trait axis the biomass in a given region of the abstract trait axis is also regular, since the morph composition of a given local region is consistent. However, the spacing of basal morphs can be slightly irregular, resulting in a uniform average biomass distribution. For more irregular networks, the morph composition of local regions varies, and consequently does the local biomass. This results in a structured biomass distribution, with large biomass maxima separated by a characteristic interval.

7.3.5. Comparison to empirical data

To justify our model, we compare the resulting food webs to empirical data, collected from 50 lakes in the Adirondack region (Sutherland and of Environmental Conservation, 1989). To compare food web topologies directly, we choose three common community characteristics for comparison: number of morphs, maximal trophic level, and food web connectance (Fig. 7.7). Since the model only considers a single resource, following Rossberg et al. (2006), we treated all species of trophic level one in the empirical data as a single species. For each parameter pair along the two cross sections described above (see Section 7.2.4) we collected 2000 simulated food webs. This ensemble includes communities with a trophic structure (trophic level larger than 2.5, Region II and III) and without (Region I). Therefore changes in the community characteristics could be due to either changes in the ratio of occurrences of these types or due to a transition in the food web structure itself. To separate these effects, we consider a sub-ensemble, consisting only of communities with trophic structure, in the parameter range where at least 50% of all

7. A new dimension: evolutionary food web dynamics in two dimensional trait space

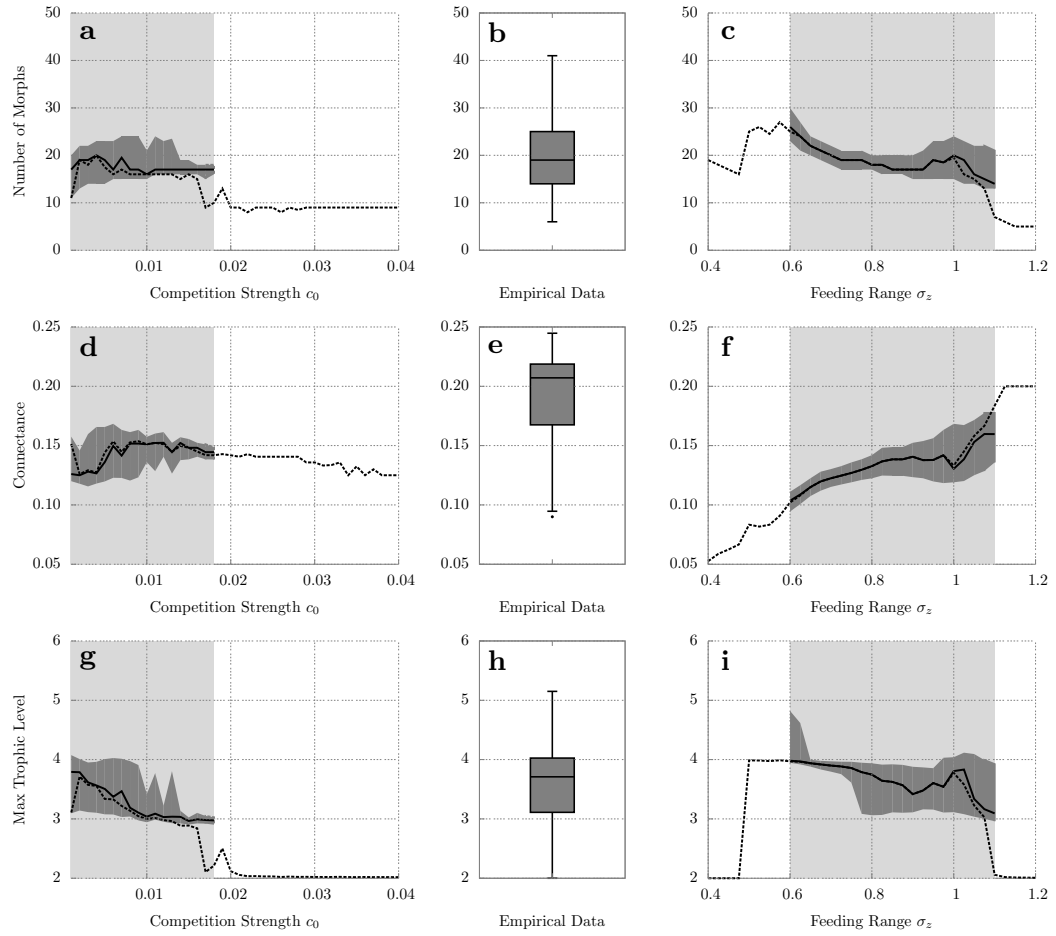


Figure 7.7.: Comparison of characteristics of empirical food webs with simulated networks along the two cross sections. **Left column:** different values of competition strength c_0 for fixed $\sigma_z = 1$ (cross section I). **Middle column:** empirical data, collected from the Adirondack lakes (Sutherland and of Environmental Conservation, 1989) using boxplots (whiskers extend to 1.5 times the interquartile range above and below the upper and lower quartiles.) **Right column:** different values of feeding range σ_z for fixed $c_0 = 0.005$ (cross section II). Along the cross sections the dashed lines represent the median over the complete ensemble of all 100 runs per parameter set. The grey area denotes the parameter regime in which at least 50% of all networks have a trophic structure (trophic level larger than 2.5). Within this area we considered the trophic ensemble, all networks with a trophic structure, and calculated the median (black curve) and the first and third quartile (represented by the dark grey area). **a,b,c:** Total number of morphs, **d,e,f:** connectance, and **d,e,f:** maximal trophic level. See text for further details.

communities have such a structure (light grey area, Fig. 7.7). The median values of the community characteristics chosen are plotted against the varied parameter values for the complete and trophic ensembles (dashed and solid lines in Fig. 7.7). The interquartile range for the trophic ensemble is plotted in dark grey and is directly comparable to the interquartile range (grey area) in the empirical values of these characteristics.

The empirical food webs contain a median of 19.1 species, with an interquartile range between 14 and 25. For both cross sections the trophic ensemble is in good agreement with these values, as is the complete ensemble for small feeding ranges (Fig. 7.7a-c). The median maximal trophic level for the empirical food webs is 3.7 with an interquartile range between 3.1 up to 4.0. The trophic ensembles along each cross section are also in good agreement with these values (Fig. 7.7g-i).

The median connectance of the empirical food webs is 0.20, with an interquartile range between 0.17 and 0.21. Along the parameter ranges shown here, our simulated communities have lower median connectance (Fig. 7.7d-f). Only communities with two trophic levels and a small number of morphs (see Fig. 7.3a) are in good agreement with the empirical values. However by combining the maxima of both cross sections (larger feeding ranges, low competition strength) one can gain networks with a higher connectance.

Finally, we note that the lower end of extreme values for each characteristic (the lower whisker) tends to be in good agreement with the complete ensemble at the upper end of competition strengths and feeding ranges. Empirical food webs with these features typically come from lakes which are relatively poor habitats which, as such, are unable to support a large number of species and high trophic levels. This situation would be most naturally represented by taking a lower value of the resource input I . However the resource limitation could also be expressed by high competition or a low feeding input (which results from relatively unspecialised feeding interactions), so this similarity is reasonable.

7.4. Discussion

Existing evolutionary food webs models typically produce either static or dynamic food webs (Loeuille and Loreau, 2005; Brännström et al., 2011; Allhoff et al., 2015a; Hartvig, 2011; Zhang et al., 2014). In contrast, our extended model produces both types of behaviour, dependent on the characteristics of morph interactions. Furthermore, even for food webs of a given evolutionary type, change in these interactions affects the structural properties of the emergent food webs, a phenomenon which has not been seen in many evolutionary food web models.

Our model framework allows us to describe a great variety of communities. This is important, because ecological food webs also display a significant degree of structural, and to a lesser degree dynamical, variety. Freshwater ecosystems have very distinct, hierarchical structures (Strong, 1992; Persson et al., 1992), while soil and marine ecosystems are often more amorphous (Polis, 1991). In addition, a variety of relationships between bodysize and trophic-level – or even the lack of a significant correlation – is reported in empirical studies (Riede et al., 2011; Jennings et al., 2002). While most empirical studies consider food webs to be constant over time, taxon cycles have been observed in small trophic communities (Roughgarden and Pacala, 1989). Thus, it is assumed that larger communities can also be dynamic (Ricklefs and Bermingham, 2002).

Since all of these behaviours are reproducible within our relatively simple model, it is possible

7. A new dimension: evolutionary food web dynamics in two dimensional trait space

to identify the model properties, and mechanisms, responsible for these differences. For example, our finding that the relative importance of predation and competition is a key determinant of food web regularity is supported by empirical observations (Holomuzki, 1986; Hebblewhite and Merrill, 2009). Our model suggests that, in highly competitive environments, the pressure to achieve optimal feeding relationships forces the formation of a very rigid food web structure. In contrast, when competition is weaker, the food web structure is looser as the niches within the community are less strictly defined. The degree of specialisation on a given prey type has a similar effect, for the same reasons; we are not aware of a study which has previously made this connection.

The primary technical difference between our model and its predecessors is the extension of the trait space into a second dimension. As such it follows that this second dimension is responsible for the increase in community diversity that we observe. We explain this as follows. In a one dimensional trait space, for instance in the model of Loeuille and Loreau (2005), morphs feed on all morphs in the lower trophic level (Allhoff and Drossel, 2013) and consequently the whole community is linked, directly or indirectly, by feeding interactions. In a two dimensional trait space this is no longer the case; if morphs are sufficiently far apart in the second dimension, then they have only negligible influence on each other. This allows the emergence of local variation in the food web structure. Additionally the expanded trait space provides morphs with a second evolutionary strategy; in addition to maximising feeding input they can now attempt to avoid predation (or equivalently search for higher densities of prey).

Previous work using evolutionary food web models has focused on the effects of trophic interactions on community structure. However, recent empirical studies have highlighted the influence of spatial factors on the structure of ecological communities (Amarasekare, 2008; Brose et al., 2004; Dunne, 2009). While we have not explicitly included space in our model, it would not be uncommon that the position on the abstract trait axis is associated to a spatial coordinate. This might describe situations where the trait value corresponds to habitat choice or preference for certain environmental characteristics, such as temperature, humidity, or altitude. In such cases, the abstract trait axis can be naturally interpreted as a spatial dimension (e.g. geographic latitude), with the abstract trait value corresponding to the spatial centre of a morph, around which the latter is distributed with a width of σ_x . Consequently, the effects attributed to the second trait dimension, localisation and avoidance, obtain a straightforward spatial interpretation.

On this basis, we can draw two conclusions about the dynamics of spatial community emergence, in particular considering large spatial scales. Firstly, the spatial assembly (horizontal) of food webs is faster than the trophic (vertical). We observe that a persistent predator can only emerge after a contiguous region of space has been occupied by their potential prey. Prey in the centre of this region can not avoid the predator evolutionarily, since it is confined by competition with other prey populations. For a non confined prey, an arms race emerges between predator and prey (Fig. 7.A.2) and the predator eventually focuses on the resource. Secondly, for evolutionary static food webs, propagation of similar morphs across space follows the principle of “First come, first served” (Munday, 2004; Burke et al., 2011). That is, the first viable morph introduced in a spatial region establishes and determines the local food web. This is supported by the observation that the lowest bodysize layer of our simulated food webs is irregular, even when morph feeding is specialised (low feeding range). Thus, the theoretically optimal morph, with bodysize d , does

not become established universally. This is a potential explanation for spatial species turnover, that is the empirical observation that the species filling a given ecological niche vary across a landscape (Gaston et al., 2007).

While the dynamics of community emergence are consistent for all food webs generated by our model, the structure of these communities is more variable. As noted above the food web structure is determined by the characteristics of morph interactions. However, in addition we also observe variation in the distribution of biomass across the habitat. Furthermore, the variation in trophic and spatial structures appear to be interdependent. Where the food web structure is consistent across the domain, the distribution of biomass is relatively uniform, i.e. unstructured. For varying food web structure however, the biomass concentrates into regularly spaced peaks. This can be explained relatively intuitively, consistent food web structures are constructed from similar subnetworks which consequently contain similar biomass. Where the food web structure varies spatially, subnetworks contain a greater variety in number, and size, of morphs, and thus in total biomass. Furthermore, as subnetworks increase in size, they impose greater competition pressure on morphs in the surrounding space, thus reducing the biomass of adjacent subnetworks. Spatial variation in food web structure and biomass distribution in homogeneous space have been observed in empirical studies (Berg and Bengtsson, 2007; Ettema and Wardle, 2002; Saetre and Bååth, 2000; Laverman et al., 2002), but the two phenomena have not previously been connected.

The dynamics of large communities are difficult to observe experimentally due to the time scales and sampling effort involved (Mercedes and Dunne, 2005). Consequently studies of such phenomena are largely theoretical. However, our results suggest that such dynamics arise from the cumulative effect of interactions between small groups of species which can be more easily studied. In particular, the primary driver of community dynamics in our model, is the coevolution of predator and prey, red-queen dynamics (Abrams, 2000; Rosenzweig et al., 1987; Dommar et al., 2008). In small communities this produces characteristic spatio-temporal patterns: bodysize oscillations and spatial chasing (Fig. 7.A.2) which are also observed in experimental studies (Holomuzki, 1986). In large communities these patterns combine to produce evolutionary outbursts, that is the recurring emergence of higher trophic levels for a limited period. These are similar to the trophic state cycling discovered by Takahashi et al. (2011, 2013) although, in our model, they are not terminated by evolutionary suicide. Instead when the outburst collapses, top predators reduce their bodysize until they are able to sustain themselves in an environment with lower prey density.

The presence of evolutionary outbursts in a community indicates that energy flows from the resource to the higher trophic levels are unstable. Note that the resources supplied are constant, the instability lies in the community structure itself. As such, the temporary collapse of a population of top predators is not necessarily an indication that a given community is endangered. Nonetheless, we note that changes in resource availability or in species interactions, say due to the introduction of an invasive species, can have similar effects.

One obvious criticism of the spatial interpretation of the second trait axis, is that species dispersal typically occurs on a different time scale to evolutionary adaptation. However, resolving these processes on separate time scales had little effect on the results obtained.

Other criticisms include the simplifying assumptions, such as the use of linear functional responses instead of a more realistic multi-species functional response (Holling, 1959), or the fact

7. A new dimension: evolutionary food web dynamics in two dimensional trait space

that competition leads to biomass losses instead of being described as a time consuming factor into the functional response (Beddington, 1975). As explained in the Model section, one major motivation for these simplifications was to preserve the elegance of the model. By keeping the model close to the original formulation in MacArthur and Levins (1967) and Loeuille and Loreau (2005), our model naturally unifies the two seminal models that describe species interactions, either competitive (MacArthur and Levins, 1967) or trophic (Loeuille and Loreau, 2005), from species positions in niche space. Future investigations should consider these factors and explore more realistic extensions, such as saturating functional responses. Nevertheless, the food webs generated by this model are in relatively good agreement with empirical data.

In summary, we have shown that, by adding a second trait dimension, with spatial properties, to the evolutionary food web framework, much more of the variety found in ecological communities can be described. Moreover, the framework remains simple enough to allow the factors determining the type of community obtained to be identified. As such this model represents a step towards a more general theory of ecological community assembly, structure and dynamics.

7.A. Appendix

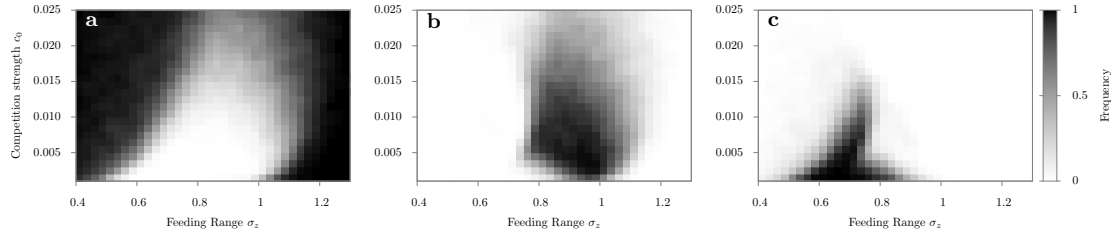


Figure 7.A.1.: Frequencies of occurrence (indicated in grey shading) of the different community types in repeated simulations, in dependency of the feeding range, σ_z , and competition strength, c_0 (compare to Fig. 7.2). **a:** Communities with no trophic structure, **b:** evolutionary static food webs, and **c:** evolutionary dynamic food webs. See Section 7.2.3 for more details.

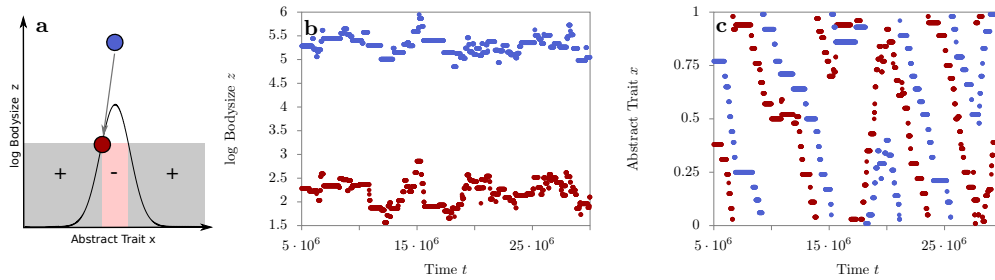


Figure 7.A.2.: Predator-prey arms race. The system was parametrised (by setting $I = 100$, $\sigma_x = 0.17$, $\sigma_z = 0.7$, $c_0 = 0.001$) so that it only contains a single predator (blue) and prey (red) morph. **a:** Positioning of predator and prey morphs (circles) in two-dimensional niche space and sketch of the feeding strength (solid line) and the prey's fitness landscape in dependence of the value of the abstract trait. Coloured shading indicates regions of negative (red) and positive (grey) fitness. **b,c:** Evolution of bodysize and abstract trait of the predator and prey morph, demonstrating the emergence of bodysize oscillations (**b**) and arms races (**c**). The predator is chasing the prey along the abstract trait axis. It is even possible for this movement to change directions: If the predator's and prey's abstract traits are similar, the mutational range can exceed the area of negative fitness (red area in **a**) and a mutant can occur on the other side of the predator.

7. A new dimension: evolutionary food web dynamics in two dimensional trait space

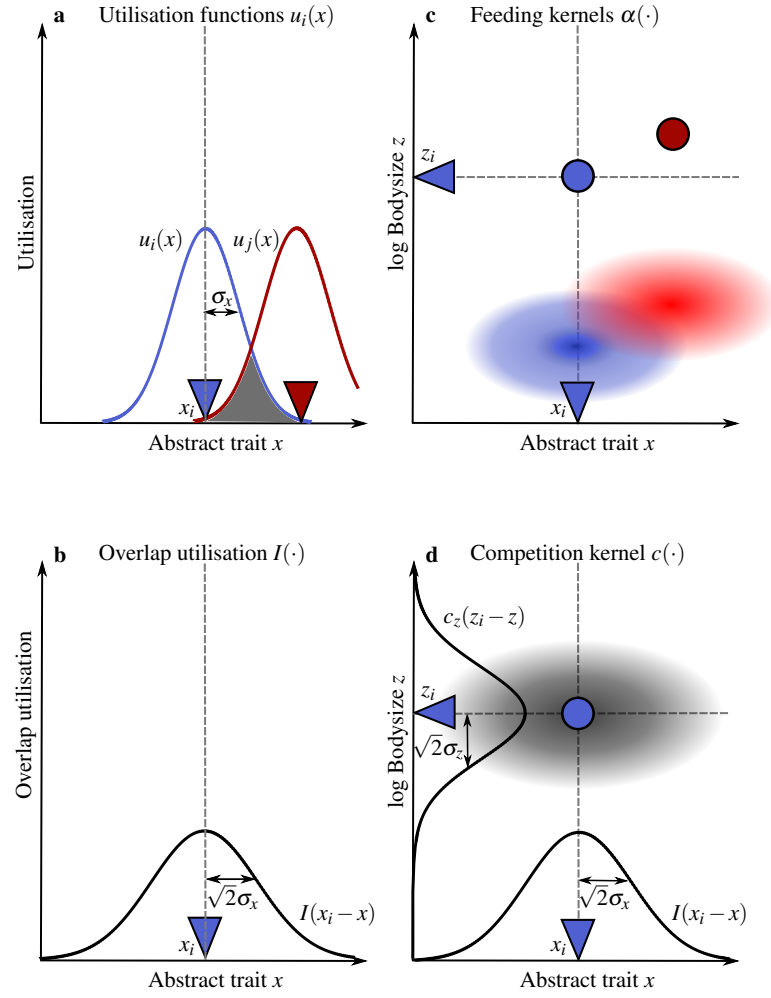


Figure 7.A.3.: Derivation of the interaction kernels. **Left Column:** Deduction of the utilisation overlap $I(\cdot)$, describing the interaction strength along the abstract trait dimension. **a:** Utilisation function $u_k(x)$, which can be interpreted as the distribution of morph k along the abstract trait axis. Following MacArthur and Levins (MacArthur and Levins, 1967), we assume that a morph k utilises a certain range around its abstract trait value x_k

$$u_k(x) = \frac{1}{\sigma_x \sqrt{2\pi}} \exp\left(-\frac{(|x_i - x|)^2}{2\sigma_x^2}\right),$$

which has a width of σ_x . **b:** The utilisation overlap $I(\cdot)$ between two morphs is given by the normalized overlap (Scheffer and van Nes, 2006) of their utilisation functions:

$$I(x_i, x_j) = \frac{\int_{-\infty}^{\infty} dx u_i(x) u_j(x)}{\int_{-\infty}^{\infty} dx u_i^2(x)} = \frac{1}{\sigma_x \sqrt{4\pi}} \exp\left(-\frac{(|x_i - x_j|)^2}{4\sigma_x^2}\right),$$

resulting in a Gaussian function with a width of $\sqrt{2}\sigma_x$. **Right Column:** Derivation of the competition kernel $c(\cdot)$ in two dimensional trait space. **c:** Feeding kernels $\alpha(\cdot)$ of two morphs in two dimensional trait space. **d:** Competition kernel $c(\cdot)$, given by the normalised overlap of the bodysize feeding kernel $c_z(\cdot) \sim \int_{-\infty}^{\infty} dx \alpha(z_i - z) \alpha(z_j - z)$, multiplied with the overlap $I(\cdot)$ of their utilisation functions. This results in a two dimensional Gaussian. The competition ranges are proportional to the width of the kernels of a single morph and are therefore no independent parameters.

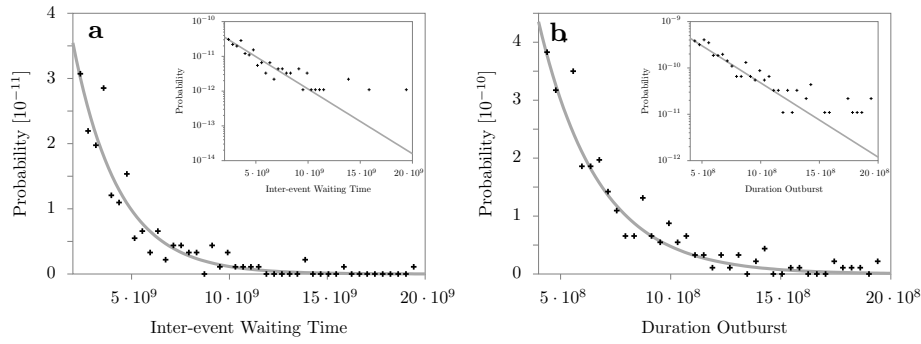


Figure 7.A.4.: Inter-event waiting time and duration of evolutionary outbursts. **a:** Probability density function of the inter-event waiting times between outbursts. **b:** Probability density function of the outburst duration. The insets in **a** and **b** show the same data in a semi-logarithmic plot. Solid lines show exponential functions fitted to the data, which yields typical time constants of $2.3 \pm 0.2 \cdot 10^9$ (inter-event waiting time) and $2.7 \pm 0.1 \cdot 10^8$ (outburst duration). The same parameters as in Fig. 7.5 were used. In total 2300 events were recorded.

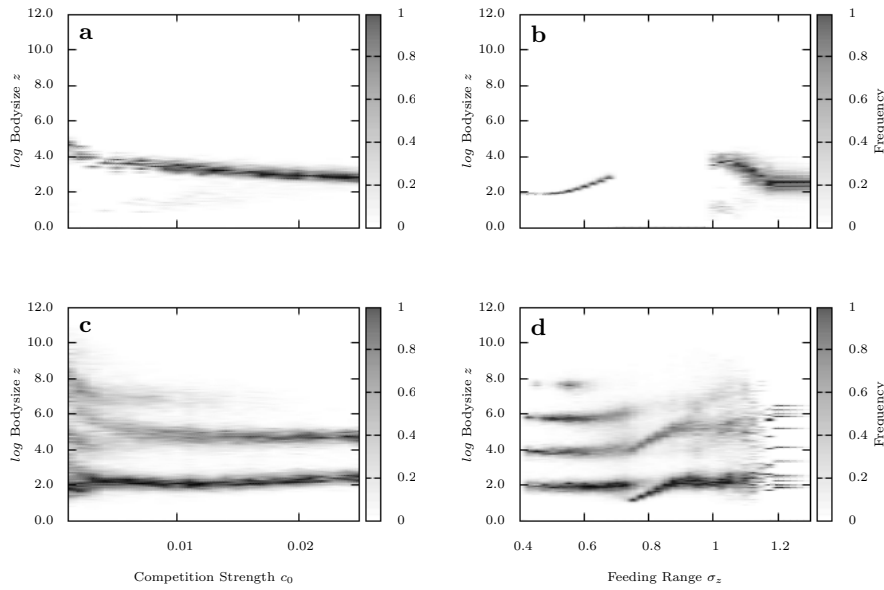


Figure 7.A.5.: Body size spectrum of communities with and without a trophic structure, along the cross sections of the parameter space, shown in Fig. 7.2. The first column shows cross section I (different values of competition strength c_0 , fixed $\sigma_z = 1$). The second column depicts cross section II (different values of feeding range σ_z , fixed $c_0 = 0.005$). For each parameter we averaged over 100 simulation runs. **a,b:** Body size probability density function of communities without a trophic structure. **c,d:** Body size probability density function of communities with a trophic structure.

Part III.

Discussion

8. Summary

“Your preparation for the real world is not in the answers you’ve learned, but in the questions you’ve learned how to ask yourself.”

— Bill Watterson —

We presented three independent studies each concentrating on different aspects of food web assembly. Each of these findings was already discussed in the corresponding chapter. However, we shortly summarise the main findings by answering the motivating questions of each chapter introduced in section 4 and afterwards, we refer them to each other.

1) Question: How static is static? The objective of chapter 5 was to study evolution in food webs, in particular evolutionary cycling. The latter seems to be a general phenomenon in evolutionary food web models and therefore these findings support the existence of continental taxon cycles (Ricklefs and Bermingham, 2002; Roughgarden and Pacala, 1989). In our study evolutionary cycling –of single morphs and of complete food webs – is driven by the interplay of trophic interactions, competition and feedback with the environment. Especially competition has proven to be an important determinant of the evolutionary behaviour of a food web and we found that strong competition between morphs can stabilise food webs evolutionary. Our results also imply that the network structures of evolutionarily static and dynamic food webs do not differ and therefore are not an indicator for the evolutionary behaviour of empirical food webs. However, evolutionarily dynamic and static food webs react differently to (evolutionary) perturbations.

Answer: Evolution seems to be a constant factor in food webs.

2) Question: How do resources of different sizes influence food webs? The objective of chapter 6 was to study the influence of multiple resources of different sizes on the assembly of food webs. We find that different sized resources give rise to partitions within a food web, which was also observed in empirical studies (Wardle et al., 2004; Fukami et al., 2006; Larios and Suding, 2014). These partitions influence the total food web in two ways: Firstly, they increase the variety of food web structures, since preimposed structures and hierarchical feeding relationships are softened. Secondly, partitions can destabilise the population dynamics by weak indirect interactions between predator and prey morphs. This leads to biomass oscillations and evolutionary intermittence. Due to these significant influences, we conclude that adequate resource descriptions, which are adapted to a specific food web type, are necessary to realistically describe food web assembly.

Answer: Size structure in resources can lead to partitions in food webs.

8. Summary

3) Question: How does a higher dimensional trait space influence food web assembly?

The objective of chapter 7 was to investigate food web assembly in two dimensional trait space and to study the phenomena that occur due to the higher dimensionality. We found that an additional dimension leads to a great variety in the evolutionary behaviour and also in the network structure. This is important, since ecological communities also display this high degree of variation. For instance, freshwater ecosystems have very distinct, hierarchical structures (Strong, 1992; Persson et al., 1992), while soil and marine ecosystems are often more amorphous (Polis, 1991). If the additional dimension is interpreted as space, our study has two additional implications: Firstly, trophic and spatial structure are intertwined. Secondly, it suggests the principle of “*First come, first served*” as an explanation for the high species turnover in space, which is observed in empirical studies (Gaston et al., 2007; Burke et al., 2011).

Answer: Higher dimensionality increases the variety of food webs.

Up to now, all research chapters are considered completely disconnected from each other. However, each chapter has implications, which affect the others. Chapter 5 implies that many food webs exhibit evolutionary dynamics, which is supported by the findings in chapter 7 and 6. They show that evolutionary dynamics can manifest in various ways.

In chapter 5, we find cycling of single morphs and also complete food webs. During these cycles the food web structure stays unchanged. In chapter 6, we observe two additional evolutionary states, which can co-occur. The first state exhibits predators that decrease their bodysize, since they lost their prey, until they are able to consume the resource. This behaviour is similar to single morph cycles and was also observed in empirical studies of taxon cycles (Taper and Case, 1992). The second state displays irregular cycling of the complete food web, which alters the network structure. Therefore, these cycles differ significantly from the cycling of the complete food web of chapter 5. The irregular cycling is more similar to predator-prey cycles, which are found in empirical (Holomuzki, 1986) and theoretical studies (Takahashi et al., 2011, 2013). Another, more subtle, kind of evolutionary state is found in chapter 6: evolutionary intermittence. Evolution slightly changes the network structure – the network structure barely changes – but it causes a transition in the population dynamics: the food web alternates between an static and an oscillatory fixpoint.

Throughout all chapters, hierarchical feeding relationships were embedded in the used model: morphs with a larger bodysize consume smaller sized morphs, which is supported by empirical data (Riede et al., 2011; Peters, 1986). Intuitively one can assume that this feeding relationship should result in food webs, in which the trophic level of morphs increases with bodysize. However, we find that an additional resource or an additional trait softens the effect of hierarchical feeding relationships on food web structure: in the same food web, morphs with smaller bodysize can have higher trophic levels than larger morphs, or morphs with bodysizes that differ considerably can be within the same trophic level. This results in a high variety of food webs structures, which can be also observed in empirical data. In addition, a variety of relationships between bodysize and trophic-level – or even the lack of a significant correlation – was reported in empirical studies (Riede et al., 2011; Jennings et al., 2002).

The aim of this work was to study food web assembly and in each research chapter, we applied different models to focus on conceptual questions. These models were kept minimalistic to be able to understand the underlying mechanisms, however we argued their generality. Despite their

simplicity, they revealed novel facts, which were interesting from an theoretical and also, more importantly, from an ecological point of view, since they can be linked to empirical observed behaviour. By combining these new insights, ecological more reasonable models can be set up, which are at the same time minimalistic and allow to investigate the mechanism that lead to the complex structures in nature.

In addition to this minimalistic approaches, conceptual ecological drawbacks, we developed a model that corrects for many of the ecological shortages of the Loeuille and Loreau (2005) model and incorporates additional evolutionary feeding traits for each morph (chapter appendix B). This relatively complex model is able to produce food webs that are in good agreement with empirical food web data. Thus, the model is a good candidate to investigate the conceptual questions in an ecological more accurate model.

9. Future work and open questions

“Like any good shaman, professional baseball player, or politician, my mother always answered questions with questions.”

— Sherman Alexie —
Ten Little Indians

To understand the assembly of food webs, additional work is necessary and each research chapter revealed new questions. Many were already addressed in length in each research chapter, which we are not going to repeat here. Instead, we focus on the spatial interpretation of the allometric evolutionary food web model introduced in chapter 7. First, we refer it to the spatial meta-community concept and point out open questions that arose in chapter appendix A. Second, we propose an extension of the allometric evolutionary food web model in two dimensional trait space. Afterwards, we introduce ecological questions that the developed models can help to answer.

Spatial interpretation: In chapter 7, we introduced an allometric evolutionary food web model with an additional abstract trait axis. By interpreting the latter as space, the model can be used to study the emergence of spatial food webs. This was done in chapter appendix A. Recent studies discretised the spatial dimension by patches: each patch contains a single food web, which are coupled via dispersal. This results in meta-communities (Leibold et al., 2004). Within this meta-community framework the stability of spatial food webs, regarding the dispersal function (Gramlich et al., 2015) and the patch topology (Ristl et al., 2014) was investigated and also the emergence of complexity in spatial food webs (Pillai et al., 2010, 2011).

Furthermore, Urban (2010) emphasised the importance of the interplay of evolution of migration. Allhoff et al. (2015b) studied the interplay in a chain of coupled patches with each patch

9. Future work and open questions

containing an evolving food web. Since metacommunities describe space only implicitly, while the continuous model (chapter 7) allows to describe space explicitly, one should compare both approaches with each other. Patch like structures can be produced by the continuous model, which then can be compared to the resulting metacommunities. This can be used to point out limitations of both approaches.

In chapter appendix A, it was shown that food web characteristics scale with spatial sampling size. Similar effects are known from habitat size (Brose et al., 2004; Connor and McCoy, 1979). In addition, we were able to show that a discrepancy between *perceived* and *real* food web can occur for spatial inhomogeneous structures if the sampling size or the number of samples are small.

The preliminary results also showed that one has to reconsider the morph definition in the spatial context: represent two morphs of similar bodysizes, but different spatial positions, two populations of the same morph, or are they fundamentally different? To answer this question, the spatial scale has to be considered. For smaller spatial ranges, for example a lake ecosystem, morphs of similar bodysizes can be identical, while on larger scales, for instance a continent, these morphs are different. Therefore, the answer depends on the considered spatial range, which changes the interpretation of the model.

Model Extension: Now, we are going to introduce a possible extensions of the allometric evolutionary food web model in two dimensional trait space. The second axis was originally introduced with the intention to describe space. We found that the single additional spatial dimension has a significant influence. However, it is necessary to increase the number, since food web habitats are either considered two dimensional, e.g. stream and terrestrial food webs, or three dimensional, such as lake communities (Brose et al., 2004).

A second step is to substitute spatial mutations by diffusion. The ordinary differential equations will become partial differential equations and the system turns into a reaction diffusion system. For a fixed number of morphs, this was studied in great detail (Cantrell and Cosner, 2003), but combined with adaptive networks approach (changing number of morphs), the behaviour of the system is mainly unknown.

The evolutionary algorithm in bodysize can also be replaced by a drift term, given by the master equation of adaptive dynamics (Dieckmann and Law, 1996). The set of partial differential equation, reduces to a single one of higher dimension. The drift term, representing evolution, would be anisotrop and dependent on the trait dimension. This system can be used to predict evolutionary spatial-temporal patterns of biodiversity.

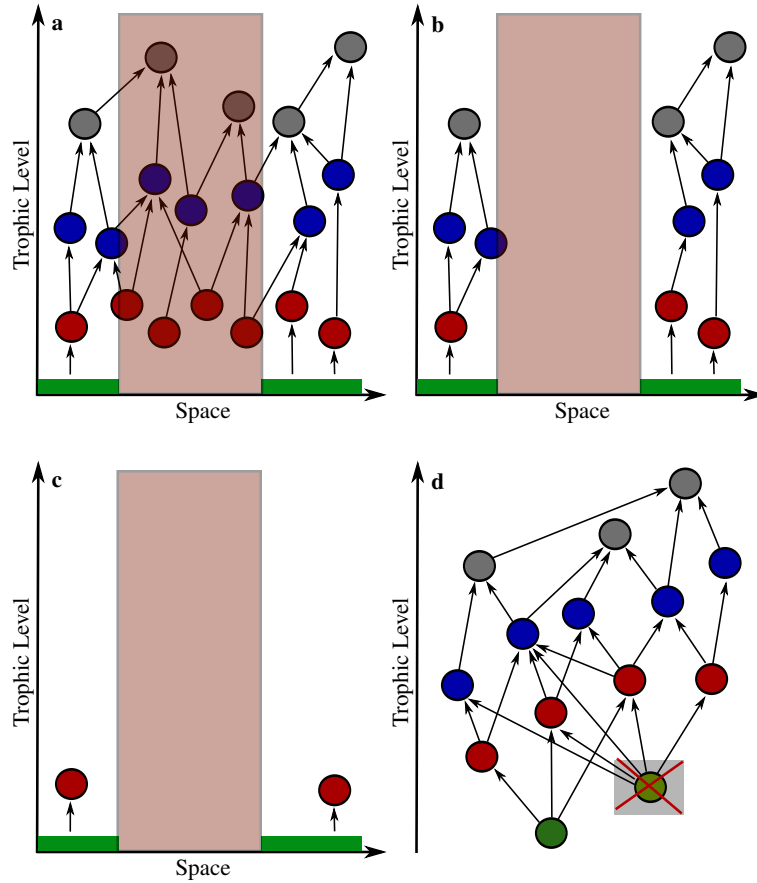


Figure 9.1.: Research questions regarding the influence of habitat fragmentation. Figure **a-c** consider the decrease of suitable habitat and possible ways to inflict food web assembly, while **d** studies the loss of resources due to habitat fragmentation.

Ecological questions One of the main drivers of ecological change is habitat destruction, due to human influence (Dirzo et al., 2014), leading to an immense loss in biodiversity. Habitat destruction can occur in several ways, for instance fragmentation of landscapes, or loss of suitable habitat and vital resources. Each motivates a different research question: how does fragmentation influence an existing food web (Fig. 9.1a), how does a partially destroyed ecosystem repair itself (Fig. 9.1b), how does a food web emerge in a fragmented landscape (Fig. 9.1c) and how does a food web react to the loss of a resource (Fig. 9.1d). The overall goal is to predict the necessary conservation action to keep the food web in its current state. All of these questions can be studied by applying the models introduced in chapter 6 or 7.

Curtain Call

The aim of this work was to study food web assembly and to do so we focused on three conceptual factors: evolution as a present element, influence of resources, and the effect of space; each studied in a minimalistic model. However, we were able to explain phenomena that are observed in empirical data. In addition, the resulting food web structures in chapter 7 were in good agreement with empirical food webs. Consequently, each of these factors seems to be important for food web assembly and therefore we conclude that these should be considered by future approaches.

With this I want to thank the reader for his/her patience to stick with me to the very end.

Part IV.

Appendix

A. Spatial sampling: Influence on the measured food web

In this chapter, we present preliminary results. They illustrate a useful application of the allometric evolutionary food web model in two dimensional trait space (chapter 3.2) and point out potential future work, which can build a bridge between theoretical and empirical studies of spatial food webs.

A.1. Introduction

Species within a habitat have an underlying spatial distribution. This fact is often neglected when considering food webs. Most empirical studies sample species over a certain habitat size and reduce the description of food webs to a single dimension, such as bodysize or trophic level (Dunne, 2009). Other studies neglect the trophic structure and focus on the influence of habitat size on network characteristics. That is, how number of species (Connor and McCoy, 1979) and number of links (Brose et al., 2004) scale with habitat size. However, studying network characteristics in small spatial food webs is often problematic, since a small spatial sampling size often corresponds to a decreasing sampling effort and therefore reduces the quality of the measured food web (Martinez et al., 1999). A discrepancy occurs between *perceived* and *real* food web.

To correct for this and to help to predict the spatial food web, theoretical models can be used. Many different model approaches exist to describe different aspects of spatial food webs: trophic meta-communities combined with patch occupancy models are used to study food web complexity in space (Pillai et al., 2010, 2011); spatial implicit models were applied to investigate the spatial influence on food web stability (McCann et al., 2005); and allometric evolutionary food web models on patches (Allhoff et al., 2015b) and in continuous space (chapter 7) were used to describe the assembly of spatial food webs. We refer to (Dunne, 2009; Amarasekare, 2008) for an extensive overview.

However, the influence of sampling size was neglected in many studies. Therefore, we use the allometric evolutionary food web model introduced in section 3.2 and interpret the abstract trait axis as a spatial dimension, to describe the assembly of spatial food webs. The objective of this chapter is, (i) to consider the spatial structure of large food webs and (ii) to investigate the influence of the sampling size on network characteristics.

A.2. Model

The considered model includes one resource R and a varying number of evolving morphs ($i = 1, \dots, N$). As stated in chapter 3, we use the term **morph** instead of species, since the speciation process is not considered. Each of the morphs is characterised by two evolutionary traits – logarithmic bodysize z_i and its abstract trait x_i – and a population biomass density B_i , which varies due to interactions with other morphs. Since only neutral assumption were made regarding the abstract axis, and more importantly interactions between morphs are stronger if their abstract trait values are similar, the abstract axis can be interpreted as space with the abstract trait value representing the **spatial position** \mathbf{x}_i of a morph. The spatial axis has a length of L , but periodic boundary conditions are used to simulate an infinite range. The resource is continuously distributed in space and has a bodysize $z_R = 0$. For further information about the evolutionary algorithm and the population dynamics, we refer to section 3.2.

A.3. Initialization and parameter values

The simulations are performed using the Sundials CVODE solver (Cohen and Hindmarsh, 1996) in C++ with absolute and relative errors per time step set to 10^{-12} . Most of the parameters are set according to chapter 7: $f_0 = 0.3$, $m_0 = 0.1$, $\theta = 10^{-10}$, $\Delta_z = \log(2)$, $I = 1000$, $e = 0.1$, $\sigma_x = 0.05$, $\Delta_x = 0.08$, $\alpha_0 = 1.0$. The spatial length L is set equal to 10, to produce larger spatial food webs. For comparison, in the previous chapter L was equal to 1. To accelerate the build up of the food web, we initialised each spatial unit length with one morph n of a logarithmic bodysize $z_n = \log(d)$ and a spatial position of $x_n = n - 0.5$ with $n \in (1, \dots, L)$, instead of initialising the system with a single morph. This does not change the resulting network structures, since the lowest bodysize compartment spreads faster than the higher bodysize compartments, which emerge upon these (chapter 7). In addition, we decrease the interval between mutations to a value of $t_m = 10^4$. This increases the number of mutations, which is still sufficiently small, so that the food web reaches a static fixpoint between two mutational steps.

A.4. Results

First, we consider the example spatial food web (Fig. A.1), which is used to investigate the influence of spatial sampling size. The parameter are chosen in a way that the food web is evolutionary static. The morph composition does not change after the initial build up (Fig. A.1a). It consists of three bodysizes compartments that are separated by gaps (see histogram). The compartments are blurred, since each contains a high number of morphs with similar bodysizes. Morphs in the same compartment can have different trophic levels (Fig. A.1c), therefore the trophic level does not strictly increases with bodysize (see chapter 7 for more details). Locally the food web consists of food chains, but for increasing spatial range these chains merge and the network complexity increases. The network structure differs along the spatial axis, since the maximal trophic level (Fig. A.1d) varies in different spatial regions. This irregularity is not visible in the biomass distribution (Fig. A.1e). Peaks occur, representing localised food chains, in

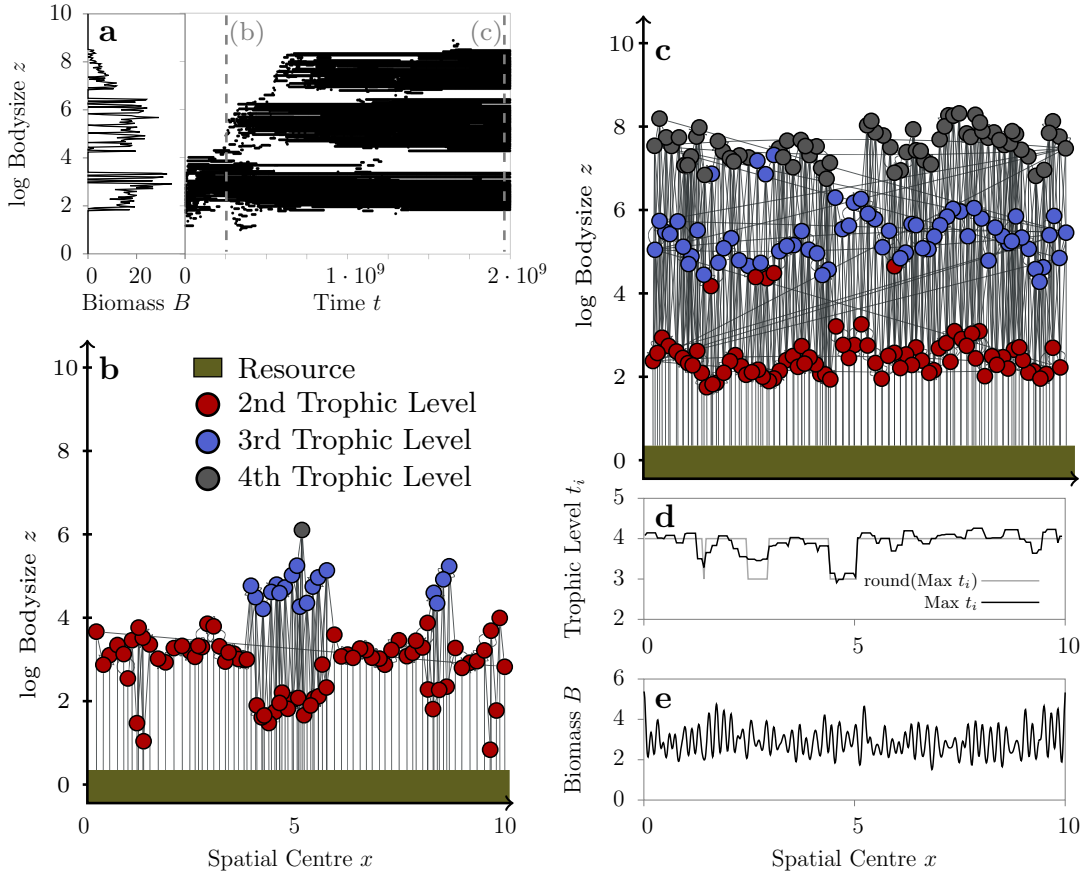


Figure A.1.: Considered spatial food web. **a:** Temporal evolution of bodysizes (right panel) and bodysize-biomass histograms (left panel). **b:** Temporal snapshot of the spatial food web during the assembly. The time point is marked in **a**. Morphs within the second trophic level (red circles) are distributed in space. Locally higher trophic level start to emerge. **c:** Final spatial food web. **d:** Float (black) and integer (grey) maximal trophic level of the local food web. The spatial sampling size Δx is equal to 0.01. The influence of the sampling size is discussed in Fig. A.2. The trophic level is calculated according to the flow-based trophic level (Williams and Martinez, 2004). **e:** Total spatial biomass distribution of all morphs. It is assumed that a morph's biomass is distributed around it spatial centre x_i , according to a Gaussian of width σ_x (see Fig. 3.4). The feeding range σ_z is set to 1.1 and the competition strength c_0 is equal to 0.005. All other parameters are set according to section A.3.

A. Spatial sampling: Influence on the measured food web

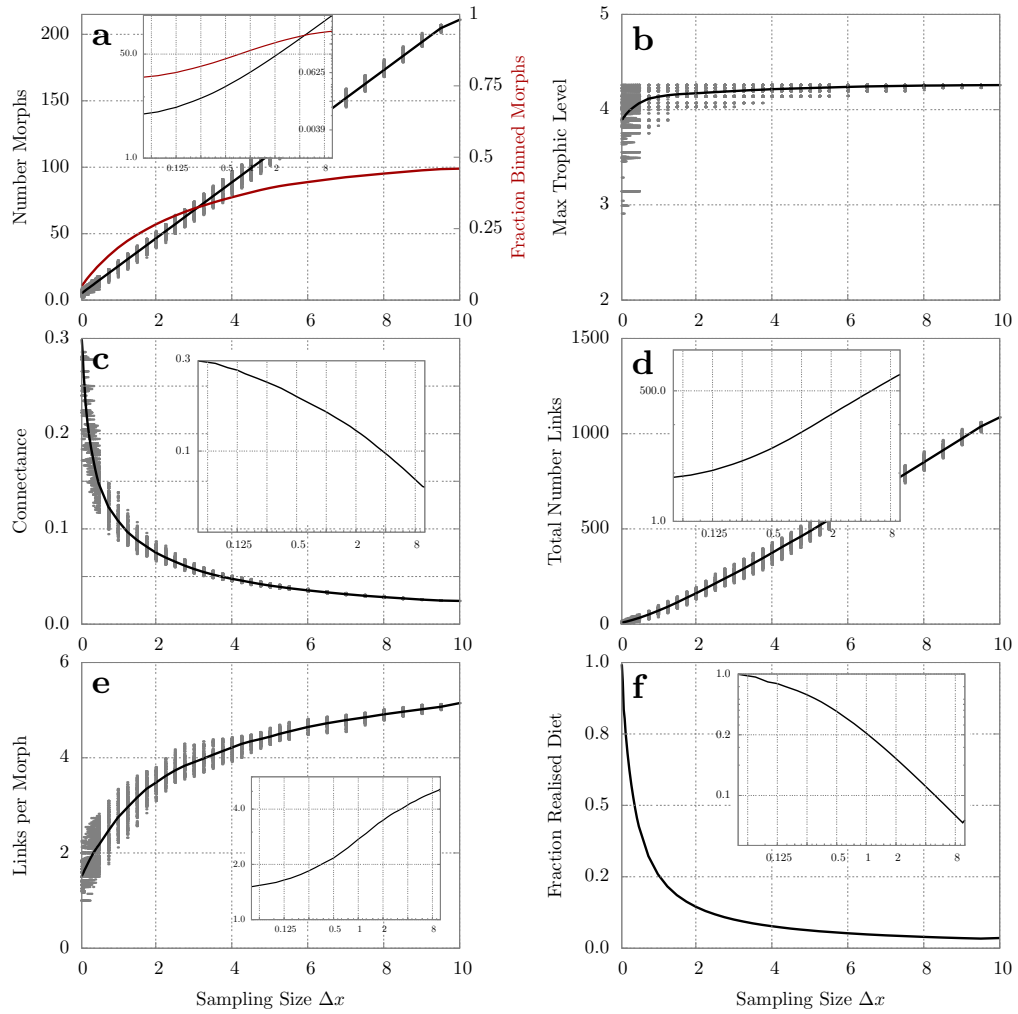


Figure A.2.: Influence of sampling size Δx on food web characteristics. The sampling size denotes the spatial range in which we collect morphs and construct the underlying food web. For each sampling size Δx , we collected 1000 networks from the food web shown in Fig A.1. The number of collected food webs is equal to the number of discretisation points of the spatial axis and we centred the sample intervals around these points. The network characteristics were averaged over the collected samples (black lines, insets show curves on a logarithmic scale) and in addition the characteristics of all sampled food webs are potted (grey). **a:** Total number of morphs and fraction of observed morphs. The latter was calculated by binning the bodysize axis (bin size $\Delta z = 0.01$, bodysize interval $[0 : 10]$). Morphs in the same bin were considered as identical, each bin presents therefore one possible morphs and the total number of possible morphs depends on the bin number. The fraction of observed morphs is calculated by dividing the occupied bins by the total number of bins. A fraction of one is not reached, since morphs only occur within the bodysize compartments and bins in between can not be filled. To calculate the following network characteristics the original morph definition was used (morphs that differ in at least one trait value are different). **b:** Maximal trophic level. **c:** Connectance **d:** Total number of links. **e:** Number of links per morph **f:** Fraction of realised diet: number of prey that is consumed divided by the potential number of prey if only bodysizes are considered and the spatial dimension is neglected.

a certain distance to each other, but the amplitude shows no correlation with trophic structure.

In addition to the final network structure, one temporal snapshot of the spatial network structure during the build up is shown (Fig. A.1b). In chapter 7, we already explained how food webs assemble in this model, but in larger spatial food webs the visibility of these processes increases. First, the lowest trophic level (red circles) spreads in space and only after the spatial region is colonised, a higher trophic level can emerge upon it (blue circles). This level also spread in space and higher trophic levels occur (grey circles).

Now we want to investigate the influence of the spatial sampling size Δx – the spatial range in which the food web is measured – on food web characteristics: number of morphs, maximal trophic level, connectance, total number of links, average number of links per morph and fraction of realised diet (Fig. A.2). Our findings show that all food web characteristics significantly vary with sampling size.

The total number of links and total number of morphs increase linearly with sampling size Δx , only for small sizes a deviation from this behaviour is visible. This is due to the fact that the presence or absence of predators strongly correlate to their prey (Brose et al., 2004). If the bodysize axis is binned and morphs within the same bin are considered as identical, the fraction of observed morphs saturates with increasing sampling size. The probability to include a new morph decreases with increasing sampling size.

The connectance and the fraction of realised diet decrease rapidly with sampling size, which has two implications. First, connectance is lower in larger food webs. Second, if the spatial axis is neglected and only bodysize is considered, as often done in empirical data, the bodysize gaps in a morphs diet increase with sampling size of the food web. However both effects are overestimated, due to the applied morph definition: Morphs in different spatial positions are not identical, even if their bodysizes are the same. Therefore, with increasing sampling range, new morphs are added constantly, which are due to the spatial distance not connected to previous morphs.

The variation in connectance and the average number of morphs is high in networks measured with small sampling sizes, while for larger sampling sizes the variance decreases. A similar behaviour occurs for the maximal trophic level, but with an asymmetric distributed around the mean value. This asymmetry reflects the spatial variation of the maximal trophic level (Fig. A.1d).

A.5. Discussion, shortcomings and future work

This study is by no means complete. However, first conclusions are possible and problems that have to be solved can be pointed out. We looked at a large spatial food web and sampled it in space. We found that sampling size influences network attributes, as emphasised in other studies (Brose et al., 2004; Connor and McCoy, 1979). In addition, our findings imply that for spatial inhomogeneous food webs, which are measured with a small sampling size (smaller than the spatial range of the variation) and a small number of samples, a discrepancy between *real* and *perceived* networks can occur (i.e. due to the asymmetric distribution of the maximal trophic level) (Martinez et al., 1999). To avoid this, either the sampling size, or the number of samples has to be increased.

In addition to the example network, we also considered food webs that were produced with different parameter values ($\sigma_z \in [0.7, 1.0, 1.1]$, $c_0 \in [0.001, 0.005, 0.01]$), with two simulation

A. Spatial sampling: Influence on the measured food web

runs per parameter value. The relationship between food web characteristics and spatial sampling size seems to be robust towards parameter variation. Only the absolute values change, as shown in chapter 7. Nevertheless, additional simulation runs for each parameter set are necessary, to show the generality of our findings.

One mayor point to consider in this study is the morph definition. Until now, morphs with similar bodysize but different spatial position are considered as different. This definition is valid for very large spatial scales, e.g. a continent. However on smaller spatial scales, for example lakes, two morphs with a similar bodysize can represent two populations of the same morph. The morph definition therefore depends on the interpretation of the model.

Applying one definition or another, significantly changes the dependency of the network characteristics on spatial sampling size. For instance, the non-binned (in bodysize) number of morphs increases nearly linearly with sampling size, while the binned number saturates (Fig. A.2a). The latter seems to be in better agreement with empirical studies (Connor and McCoy, 1979; Brose et al., 2004), but these studies also consider smaller habitat sizes. However, introducing binning, limits the maximal number of possible morphs and affects the value of all food web characteristics. Therefore, when applying this definition, one either has to adapt the binning to empirical data, which is to some extent artificial, or one has to normalise both. However, the functional relationship between food web characteristics and sampling size is not influenced by this.

To conclude, the presented study can be used to investigate the scaling of food web characteristics with sampling size. With this knowledge, food webs sampled over different habitat sizes can be compared, without limiting the comparison to size effects. In addition, it can help to avoid systematic errors, when measuring food webs with an unsuitable sampling size.

B. Evolutionary food web model based on body masses gives realistic networks with permanent species turnover

SCIENTIFIC REPORTS



OPEN

Evolutionary food web model based on body masses gives realistic networks with permanent species turnover

Received: 09 December 2014

Accepted: 12 May 2015

Published: 04 June 2015

K.T. Allhoff¹, D. Ritterskamp², B.C. Rall³, B. Drossel⁴ & C. Guillo⁵

The networks of predator-prey interactions in ecological systems are remarkably complex, but nevertheless surprisingly stable in terms of long term persistence of the system as a whole. In order to understand the mechanism driving the complexity and stability of such food webs, we developed an eco-evolutionary model in which new species emerge as modifications of existing ones and dynamic ecological interactions determine which species are viable. The food-web structure thereby emerges from the dynamical interplay between speciation and trophic interactions. The proposed model is less abstract than earlier evolutionary food web models in the sense that all three evolving traits have a clear biological meaning, namely the average body mass of the individuals, the preferred prey body mass, and the width of their potential prey body mass spectrum. We observed networks with a wide range of sizes and structures and high similarity to natural food webs. The model networks exhibit a continuous species turnover, but massive extinction waves that affect more than 50% of the network are not observed.

Classical models addressing the structure and stability of food webs are based on stochastic algorithms that produce structural patterns similar to empirically measured food webs¹, such as the niche model² or the cascade model³. A more recent approach is to use the empirically found allometries of body size and foraging behaviour of individual consumers to predict the links between species on a more biological basis⁴.

However, real food webs are not produced by a generative algorithm, but have been shaped by their evolutionary history and show an ongoing species turnover. New species in a food web occur by immigration and speciation, and species vanish due to extinction. Currently, the world faces one of the largest extinction waves ever, which is thought to be caused by anthropogenic drivers such as climate change and land use⁵. Even without human interference or other catastrophic causes, and apart from evolutionary suicide due to runaway selection⁶, biological extinctions occur due to intrinsic processes, i.e., the dynamic trophic and competitive interactions among species^{7,8}. The stability of food webs in terms of resistance to extinction waves after a perturbation (such as the removal or addition of a species), thus also depends on the network structure of these interactions between the species^{9,10}, and conversely the

¹Institute for Condensed Matter Physics, Technische Universität Darmstadt, Germany. ²Institute for Chemistry and Biology of the Marine Environment, Carl von Ossietzky University of Oldenburg, Germany. ³German Centre for Integrative Biodiversity Research (iDiv) Halle-Jena-Leipzig, Germany; Institute of Ecology, Friedrich Schiller University Jena, Germany; Netherlands Institute of Ecology (NIOO-KNAW), Wageningen, The Netherlands; J.F. Blumenbach Institute of Zoology and Anthropology, Georg-August-University Göttingen, Germany. ⁴Institute for Condensed Matter Physics, Technische Universität Darmstadt, Germany. ⁵Institute for Biodiversity and Ecosystem Dynamics, University of Amsterdam, The Netherlands; Institute of Biochemistry and Biology, University of Potsdam, Germany. Correspondence and requests for materials should be addressed to K.T.A. (email: allhoff@fkp.tu-darmstadt.de)

network structure results from species extinctions and additions. Understanding the interplay of food web structure and stability has therefore been identified as one of the most important questions in ecology¹¹.

Over the last decade, several models were introduced that include evolutionary rules on a longer time scale, in addition to population dynamics on shorter time scales: The former enables new species to enter the system, whereas the latter determines which species are viable and which go extinct. The newly emerging species can be modelled and interpreted either as invaders from another, not explicitly considered region or as “mutants” of existing species. The emerging network structures evolve in a self-organising manner, giving rise to complex, species-rich communities even when starting from initial networks with very few species¹.

A particularly simple and often cited evolutionary food web model was introduced in 2005 by Loeuille and Loreau¹² and subsequently modified by several other authors^{13–15}. Each species is characterised by its body mass, which is the only evolving trait. Feeding and competition interactions are determined via differences in body mass. The fact that body mass is an ecologically interpretable trait makes the results from this model easily comparable to empirical data. This major advantage has been pointed out in the review on large community-evolution models by Brännström *et al.*¹⁶. The evolutionary process in this model generates large networks that show an almost static behaviour, with clearly defined niches all of which are and remain occupied. Even if a newly emerging species is slightly better adapted to the resources and therefore displaces a species of similar body mass, it has the same feeding preferences and hence the same function in the food web, leading to a very low species turnover without secondary extinctions¹⁵. The network structure is robust with respect to various changes in the population dynamics rules, indicating that some simple, robust mechanism structuring these food webs is at work^{12,15}.

Complex networks with a less rigid structure emerge in the evolutionary version of the niche model¹⁷. The model allows for the evolution of three traits instead of just one, namely the niche value, the centre and the width of the feeding range. Other authors describe a species in a more abstract way by a vector of many traits, as implemented in the matching model^{18,19} and in the webworld model^{20,21}. Recently, also several individual-based models for evolving food webs were introduced^{22–24}. The emergence of complex food webs in these models is highly nontrivial. Some past attempts to set up an evolutionary model lead to repeated network collapse instead of persisting complex networks²⁵. Other attempts lead to trivial network structures, like simple food chains in the evolving niche model¹⁷ or a single trophic level in the webworld model²¹. In both models, adaptive foraging was required in order to obtain more complex networks.

Allhoff and Drossel¹⁵ suggested that an evolutionary food web model has to fulfil two conditions to be able to generate diverse and complex networks. First, it should allow for the evolution of more traits in addition to body mass in order to generate several possible survival strategies like for example specialists and omnivores. This idea is consistent with results from a recent empirical study by Rall *et al.*²⁶, who found that predators of similar body mass differ significantly in their feeding preferences. Second, the evolution of each trait has to be restricted in order to prevent unrealistic trends, for example towards extremely small or large body masses or towards extremely broad or narrow feeding ranges. In this context, the stabilising effect of adaptive foraging in previous models could be explained by the fact that a predator can focus on its most profitable prey without losing adaptation to other prey.

In this paper, we propose a new evolutionary food web model that includes the restriction of trait evolution in a more direct way. Similarly to the evolutionary niche model¹⁷ and supported by empirical data regarding the body-mass ratios of predator-prey pairs^{27,28}, we characterise a species by three traits with clear biological meaning: its own body mass (which determines its metabolic rates), its preferred prey body mass, and the width of its potential prey body mass spectrum. The evolutionary rules in our model confine the traits within certain boundaries, without the requirement to include adaptive foraging.

The model most similar to our model is the one by Loeuille and Loreau¹². It also has body mass as a key trait and a similar concept for setting the feeding preferences. Our model differs from the model by Loeuille and Loreau in the number of traits that characterize a species (3 instead of 1), the functional response (Beddington-deAngelis instead of linear), the competition rules (based on link overlap instead of body mass differences), the possibility of cannibalism and loops (included only in our model) and the resource dynamics. Moreover, we consider body mass ratios instead of body mass differences so that the body masses in our model spread over several orders of magnitude instead of only one. The bio-energetics of the species in our model follow well documented allometric scaling relationships²⁹, leading to networks with realistic body-mass scaling relations that can be tested directly against empirical data.

We demonstrate the capabilities of our model by evaluating 18 common food web properties and compare them to a data set of 51 empirical food webs from a large variety of different ecosystems. We further use the well-known evolutionary model by Loeuille and Loreau¹² as a benchmark to assess the quality of the predictions of our model. In principle, both models are able to produce diverse networks. However, we obtain a higher variability in the feeding preferences and survival strategies and therefore more realistic values for the corresponding network properties. Moreover, while the network structures of Loeuille and Loreau are static, species turnover and extinction avalanches occur naturally in our model.

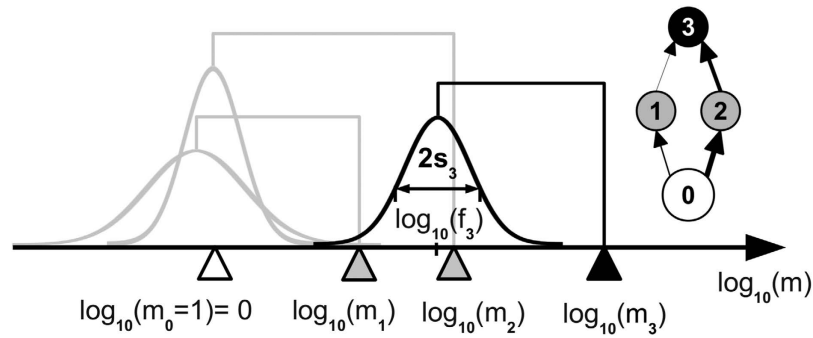


Figure 1. Model illustration using 4 species. Species 3 (black triangle) is characterised by its body mass m_3 , the centre of its feeding range f_3 , and the width of its feeding range s_3 . The Gaussian function (black curve) describes its attack rate kernel N_{3j} on potential prey species. Here, species 3 feeds on species 2 and 1 (grey triangles) with a high resp. low attack rate. Species 1 and 2 are consumers of the external resource, represented as species 0 with a body mass $m_0=1$ (white triangle). Also shown is the corresponding network graph.

The Model

The model includes fast ecological processes (population dynamics), which determine whether a species is viable in a given environment that is created by the other species, and slow evolutionary processes (speciation events), which add new species and enable the network to grow and produce a self-organised structure. A species i is characterised by its body mass, m_i , the centre of its feeding range, f_i , and the width of its feeding range, s_i . These traits determine the feeding interactions in the community (see Fig. 1) and thereby the population dynamics. A summary of all model parameters and variables is given in table 1.

Population dynamics. The population dynamics follows the multi-species generalisation of the bioenergetics approach by Yodzis and Innes^{30,31}. The rates of change of the biomass densities B_i of the populations are given by

$$\dot{B}_0 = G_0 B_0 - \sum_{j=\text{consumers}} g_{j0} B_j \quad (1)$$

for the external resource (species 0) and

$$\dot{B}_i = \sum_{j=\text{resources}} e_j g_{ij} B_j - \sum_{j=\text{consumers}} g_{ji} B_j - x_i B_i \quad (2)$$

for consumer species. $G_0 = R(1 - B_0/K)$ is the logistic growth rate of the external resource, e_j is the efficiency with which biomass of species j can be assimilated by its consumers, g_{ij} is the mass-specific rate with which species i consumes species j , and x_i is i 's mass-specific respiration rate. The mass-specific consumption rate is given by

$$g_{ij} = \frac{1}{m_i} \frac{a_{ij} B_j}{1 + \sum_{k=\text{res.}} h_i a_{ik} B_k + \sum_{l=\text{comp.}} c_{il} B_l}, \quad (3)$$

where

$$a_{ij} = a_i \cdot N_{ij} = a_i \cdot \frac{1}{s_i \sqrt{2\pi}} \cdot \exp \left[-\frac{(\log_{10} f_i - \log_{10} m_j)^2}{2s_i^2} \right] \quad (4)$$

is the rate of successful attacks of species i on individuals of species j , with the Gaussian feeding kernel N_{ij} as shown in Fig. 1. The parameter h_i is the handling time of species i for one unit of prey biomass, and c_{il} quantifies interference competition among predators i and l ^{32–34}. It depends on their similarity, as measured by the overlap $I_{il} = \int N_{ij} \cdot N_{lj} d(\log_{10} m_j)$ of their feeding kernels, via

$$c_{il} = c_{\text{food}} \cdot \frac{I_{il}}{I_{ii}} \text{ for } i \neq l. \quad (5)$$

parameter	meaning
resource	
$m_0 = 1$	body mass
$R = 1$	maximum mass-specific growth rate
$K = 100$	carrying capacity
B_0	biomass density
species i	
m_i	body mass
f_i	centre of feeding range
s_i	standard deviation of feeding range
B_i	biomass density
population dynamics	
$e_j = 0.85$ (0.45)	assimilation efficiency for animal (plant) resources
g_{ij}	functional response of predator i on prey j
a_{ij}	attack rate of predator i on prey j
$a_i = 1 \cdot m_i^{0.75}$	attack rate parameter
$h_i = 0.398 \cdot m_i^{-0.75}$	handling time of predator i
c_{il}	competition on species i from species l
c_{food}	competition parameter for food
c_{intra}	intraspecific competition parameter
$x_i = 0.314 \cdot m_i^{-0.25}$	respiration rate of species i
evolutionary rules	
$\omega = 10^{-4}$	mutation probability
$\varepsilon = \frac{2}{10^4}$	initial population density of a new species and extinction threshold

Table 1. A summary of all model parameters. The values of the population parameters are based on the work by Yodzis and Innes³⁰. If no value is given for a parameter, it is variable.

The normalisation of the competition with I_{ii} was proposed by Scheffer *et al.*³⁵ and accounts for the fact that the competition matrix is not symmetric. More specialised species exert a higher competition pressure than species with broad feeding ranges. The overlap I_{il} is similar to the niche overlap discussed by May³⁶.

We assume that interference competition is significantly higher within a species than between different species, e.g. due to territorial or mating behaviour. To account for this, we introduce an intraspecific competition parameter c_{intra} and set $c_{ii} = c_{\text{food}} + c_{\text{intra}}$.

Speciation events. Each simulation starts with a single ancestor species with body mass $m_1 = 100$ and feeding parameters $f_1 = 1$ and $s_1 = 1$, which is thus feeding on the external resource with its maximum attack rate. The initial biomass densities are $B_0 = K = 100$ for the resource and $B_1 = m_1 \cdot \varepsilon = 2 \cdot 10^{-2}$ for the ancestor species. The parameter ε is the extinction threshold, i.e., the minimum population density required for a population to survive. At each unit time step, species below this extinction threshold get removed from the system.

A speciation event occurs with probability $\omega = 0.0001$ per unit time. This is so rare that the system is typically close to a fixed point before the next mutation occurs. Then, one of the currently existing species (but not the external resource) is chosen randomly as parent species i for a “mutant” species j . Thus, every species has the same probability ω/S to “mutate”, where S is the number of currently viable species. The logarithm of the mutant’s body mass, $\log_{10}(m_j)$, is chosen randomly from the interval $[\log_{10}(0.5m_i), \log_{10}(2m_i)]$, meaning that the body masses of parent and mutant species differ at most by a factor of 2. The mutant’s initial biomass density is set to $B_j = m_j \cdot \varepsilon$ and is taken from the parent species.

The mutant’s feeding traits f_j and s_j are independent of the parent species. The logarithm of the feeding centre, $\log_{10} f_j$, is drawn randomly from the interval $[(\log_{10}(m_j) - 3), (\log_{10}(m_j) - 0.5)]$, meaning that the preferred prey body mass is 3 to 1000 times smaller than the consumer’s body mass, and following the results from Brose *et al.*²⁷. The width of the feeding range, s_j , is drawn randomly from the interval $[0.5, 1.5]$. A small value of s_j corresponds to a more specialised consumer, while a large value of s_j characterises a consumer with a broad feeding range and lower attack rates. A combination of large preferred prey mass f_j and a wide feeding range enables a consumer to prey on species with a larger body mass

than its own. This enables the emergence of cannibalism and feeding loops. The fixed intervals keep the evolving traits in reasonable ranges and prevent unrealistic trends, following the results by Allhoff and Drossel¹⁵.

When testing the robustness of the model predictions with respect to the model details, we used alternative rules, where the probability for choosing a parent species is proportional to its biomass (similar to the model by Loeuille and Loreau¹²) or to its inverse generation time $m_i^{-1/4}$ so that the mutation rate is proportional to the reproduction rate. Furthermore, we tested Gaussian distributions of mutant body masses around the parent with a standard deviation between 0.09 and 1. We used a cutoff at two standard deviations resulting in a maximum body mass factor between parent and daughter species between $10^{2 \cdot 0.09} \approx 1.5$ and $10^{2 \cdot 1} \approx 100$. The former describes local speciation events, whereas the latter describes species invasions from not explicitly modelled regions. We also compared the results to simulations where the mutants body mass is drawn randomly from the interval $[10^{-0.5}, 10^6]$. Finally, with a similar approach, we also included heredity into the feeding parameters s_i and f_i by combining Gaussian distributions around the parent's traits with the above given mutation intervals.

Methods

The computer code for our simulations was written in C. We used the Runge-Kutta-Fehlberg algorithm provided by the GNU Scientific library³⁷ for the numerical integration of the differential equations. Simulations were run for $5 \cdot 10^8$ time units. For comparison, the generation time of the initial ancestor species with body size $m_1 = 100$ is of the order of $\frac{1}{x_1} = \frac{100^{0.25}}{0.314} \approx 10$ time units.

The competition parameters c_{food} and c_{intra} have a strong effect on the diversity of the emerging food webs. To obtain the network variability observed in nature, we performed computer simulations with all four combinations of $c_{\text{food}} = 0.6$ or 0.8 and $c_{\text{intra}} = 1.4$ or 1.8 . The time series of these simulations are shown in the online supplementary material. From each simulation run, we collected 80 food webs obtained after every $5 \cdot 10^6$ time units from $t = 10^8$ to $t = 5 \cdot 10^8$, resulting in a total of 320 different networks. Due to the initial build-up of the network, the first 10^8 time units were not taken into account.

The structure of the emerging food webs is compared both to food webs produced with the model by Loeuille and Loreau¹² and to empirical food webs. For the empirical data, we re-evaluated 51 of the 65 food webs from different ecosystem types analysed by Riede *et al.*³⁸ for which we had body-mass data for all species in the network (for the complete list see online supplementary material). For the model by Loeuille and Loreau, we evaluated the final network structures obtained with 75 combinations of different parameter values. Due to the static network structure, we could not obtain different networks from one evolutionary simulation. The niche width was set to $nw = \frac{s^2}{d} = 0.5, 1.0, 1.5, 2.0, 2.5$ and the competition strength to $\alpha_0 = 0.1, 0.2, 0.3, 0.4, 0.5$, similar to the original work. To get networks of comparable size we decreased the competition range, $\beta = 0.025, 0.05, 0.075$.

Both models use Gaussian feeding kernels with in principle infinite width to describe the feeding interactions, meaning that each species can prey on every other species. Thus, for analysis, very weak links have to be cut off in order to obtain meaningful network structures. In our networks, we removed all links that contribute less than 75% of the average link to the total resources of a consumer. This criterion is weaker than it might seem, because most of the links of a predator are very weak, and so is the average link strength. Our cutoff measure depends on both the attack rate and the prey's biomass density. It thereby mimics unavoidable sampling limits in empirical food-web studies. For the networks produced by the algorithm of Loeuille and Loreau we used the cutoff criterion of the original work and removed all links with an attack rate that is smaller than 15% of the respective predator's potential maximum attack rate, disregarding the prey's biomass density. Since the value of the cutoff criterion is to some extent arbitrary, we report its effects on the predicted network properties in the online supplementary material. There we also show results obtained for the model by Loeuille and Loreau with our cutoff rule.

Results

A typical simulation run. A typical simulation run with the competition parameters $c_{\text{intra}} = 1.4$ and $c_{\text{food}} = 0.8$ is shown in Fig. 2. After an initial period of strong diversification, the system reaches a size of approximately 60 species (panel (a)) on 3 to 4 trophic levels above the resource (panel (c)). The species form clusters of similar body masses, as shown in panel (b). New predator and prey species emerge preferentially within these clusters: A prey species in a cluster experiences less predation pressure due to the saturation of the functional response of the predator, and the predation input of a predator is larger if its feeding preferences match such a cluster. Therefore, we observe a trend towards strong specialisation on these clusters, resulting in the following network structure. Species in the first cluster have a body mass of approximately 10^1 , specialise on the resource and represent most of the second trophic level. Species in the second cluster with a body mass of approximately $10^2 - 10^3$ feed either on the resource ($TL \approx 2$) or on the first cluster ($TL \approx 3$). Species in the top cluster with a body mass greater than 10^3 specialise either on the first or on the second cluster and therefore have intermediate trophic positions ($3 \leq TL \leq 4$). Some species have even higher trophic positions due to cannibalism and loops.

The initial build-up of the network continues until the species in the top cluster are close to the extinction threshold. Once all clusters have emerged, the system shows a continuous turnover of species. We suppose the following turnover mechanism. Mutants with very few predators can occur occasionally

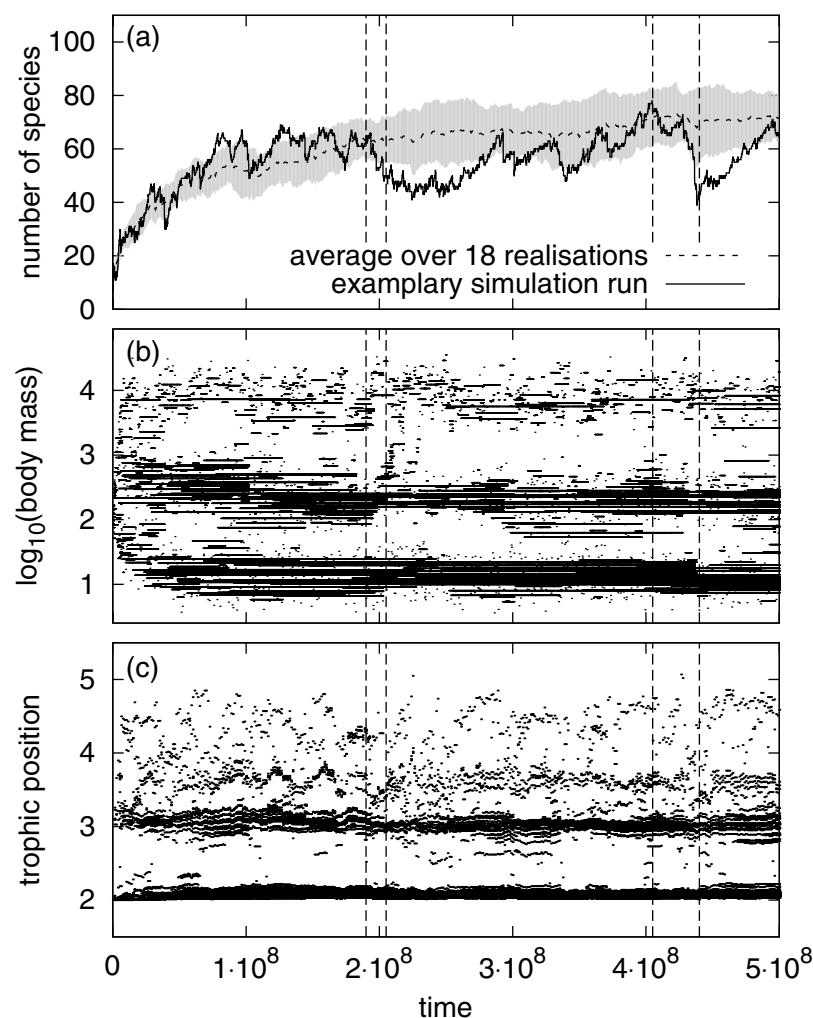


Figure 2. Network size, body masses and flow-based trophic positions⁶⁰ of all species occurring during one exemplary simulation run with competition parameters $c_{\text{intra}} = 1.4$ and $c_{\text{food}} = 0.8$. Panel (a) also shows the average network size and its standard deviation for 18 simulations with identical parameters but different random numbers. Body masses and trophic positions were plotted at every 25th mutation event. Network visualisations for the time points indicated by vertical lines are shown in the online supplementary material.

if their body mass is between two clusters and if the other species are specialised on the clusters. If such a mutant has viable feeding parameters, it can grow a large population and displace many other species at once, potentially even causing secondary extinctions. Examples for such extinction events are visible at $t \approx 2 \cdot 10^8$ and $t \approx 4.3 \cdot 10^8$. After an extinction event, the network rearranges, and temporally also species with broader feeding ranges appear, before the trend towards specialisation followed by an extinction event starts again.

Network evaluation and comparison. We compared 320 networks from our model with 51 empirical networks and 75 networks from the model by Loeuille and Loreau¹², see Fig. 3. Panels (a)–(c) show the distributions of body masses of all three data sets. The observed peaks in our simulated data correspond to the body mass clusters mentioned before. The distance between the peak maxima is determined by the upper boundary of the mutation interval of the feeding centre. Single empirical food webs show a similar peak pattern (not shown). In contrast, the body mass distribution of the model by Loeuille and Loreau looks blurred, due to our choice of the niche width $nw = \frac{s^2}{d}$. With smaller values of the feeding range s , the network structure is strongly layered and clusters of body masses that are multiples of the feeding distance d occur, where each species feeds on those in the cluster below and is prey to those in the cluster above¹⁵. We also observed that because we based the network structure on predator-prey body-mass ratios instead of body-mass differences, the resulting community-size spectra from our model

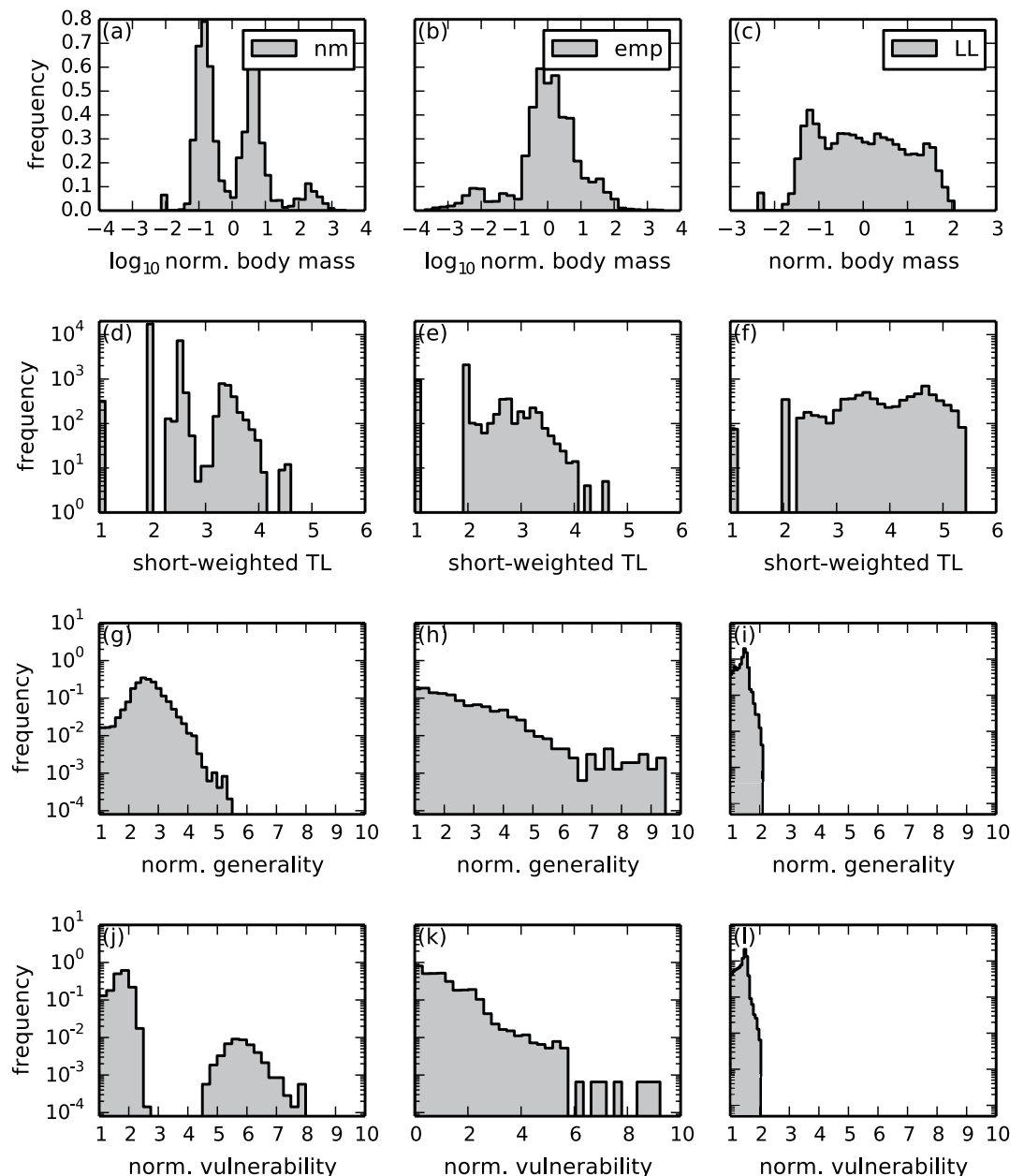


Figure 3. Frequency distributions of body masses and short-weighted trophic level⁶⁰, as well as the distributions of generality (number of prey species) and vulnerability (number of predators). The latter two are normalised by the average number of links per species. **nm**: 320 networks from 4 simulations of our new model with all four combinations of $c_{\text{food}} = 0.6$ or 0.8 and $c_{\text{intra}} = 1.4$ or 1.8 . **emp**: Average over 51 empirical food webs. **LL**: Average over 75 simulations of the model by Loeuille and Loreau¹². Note that panel (c) shows absolute body masses, since in this model all body masses are in the same order of magnitude. See *Methods* for more information.

follow empirical observations and theoretical predictions more closely than those from the model by Loeuille and Loreau, as shown in the online supplementary material.

Panels (d)–(f) show the distributions of trophic levels of all three data sets. Here, we use the short-weighted instead of the flow-based trophic level. This allows for better comparison with the empirical data for which the population sizes are often not available. The comparison between the two models reveals the main difference between the two different cutoff rules. A link with intermediate attack rate to a small prey population represents only a small proportion of the predator's diet, and is therefore neglected when using our cutoff threshold (75% of the average link). However, it is not recognised as a weak link with the cutoff rule by Loeuille and Loreau (15% of the maximum attack rate). On the other hand, a link with small attack rate to a big prey population (especially to the resource) is deleted in their

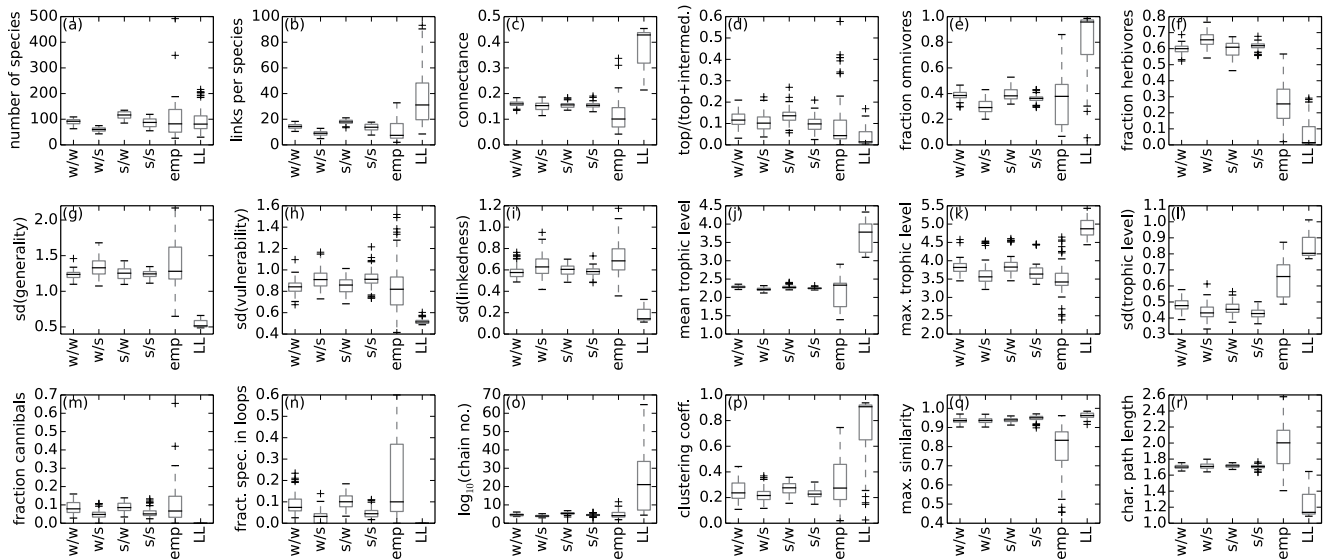


Figure 4. Network properties of four realisations with different values of the competition parameters. **w/w:** Weak competition, $c_{\text{intra}} = 1.4 / c_{\text{food}} = 0.6$. **w/s:** Weak intraspecific competition and strong competition for food, $c_{\text{intra}} = 1.4 / c_{\text{food}} = 0.8$. **s/w:** Strong intraspecific competition and weak competition for food, $c_{\text{intra}} = 1.6 / c_{\text{food}} = 0.6$. **s/s:** Strong competition, $c_{\text{intra}} = 1.6 / c_{\text{food}} = 0.8$. **emp:** Average over 51 empirical food webs. **LL:** Average over 75 simulations of the model by Loeuille and Loreau¹². See *Methods* for more information. Details on the calculation of these network characteristics can be found in the online supplementary material.

model. Thus, trophic levels are overestimated, whereas our model with our cutoff rule results in a quite realistic distribution.

Both models have difficulties reproducing the empirical distributions of generality (number of prey species) and vulnerability (number of predators), which are much broader than the distributions produced by the models (panels (g)–(l)). For the model by Loeuille and Loreau, the distribution results from the fact that the species in the model feed only on prey with smaller body masses. The situation is similar to the cascade model³, which also constrains predators to feed only on prey with a lower rank. Consequently, both generality and vulnerability cannot be larger than twice the average number of links per species. In our new model, the distribution of the vulnerability shows two humps. The first hump contains the carnivores in the higher trophic levels that feed on herbivores or on other carnivores. They have a high generality and a small vulnerability. The second hump contains the herbivores that feed on the resource. They are prey to many other species and hence have a high vulnerability.

We ascribe the differences between the models and the empirical distributions to the fact that both models have only one resource, which means that all herbivores feed on the same resource, whereas in empirical networks herbivores can have more than one resource. Furthermore, both models ignore the within-species body-mass distribution by assigning to each species a precise value of the body mass. This also narrows down the range of body sizes a species can feed on or is vulnerable to.

By analysing the 320 networks from the 4 simulations separately (see Fig. 4), we found two trends concerning the network size (panel (a)): First, the stronger the intraspecific competition c_{intra} , the smaller are the population sizes and the more populations can survive on the same amount of energy provided by the resource. Second, the stronger the competition for food c_{food} is, the sooner species can displace others resulting in rather small networks with fast evolutionary species turnover.

Both models are able to produce networks of realistic sizes, but tend to overestimate the number of links per species (panel (b)) and hence the connectance (panel (c)). The effect is much larger in the model by Loeuille and Loreau due to their original cutoff rule. This also explains the high fraction of omnivores and the low fraction of top and herbivorous species (panels (d)–(f)), as well as the high values of the number of chains and the clustering coefficient (panel (o) and (p)) and the small value of the characteristic path length (panel (r)). In the online supplementary material, we show that the model by Loeuille and Loreau provides more realistic predictions when using our cutoff rule.

Both models fail to reproduce the maximum similarity (panel (q)), due to the same reasons that also lead to the narrow distributions of generality and vulnerability. For the remaining panels, the model by Loeuille and Loreau performs worse than our model regardless which cutoff rule is used. For example, the short-weighted trophic levels (panel (j)–(l)) are not only overestimated due to the cutoff rule, but also reflect the regular network structure. As mentioned above, these networks are layer-like structures,

where each cluster represents one trophic level. Since all clusters accommodate a similar number of species instead of heaving more species on lower levels like in our model, the mean trophic level is overestimated. Moreover, the model does not include cannibalism (panel (m)) and loops (panel (n)), for which our model provides good predictions.

Due to the evolution of three instead of one trait, we obtain more diverse network structures than Loeuille and Loreau. We observe a higher standard deviation of the generality, the vulnerability and the linkedness (panel (g)–(i)), reflecting different feeding preferences and survival strategies.

Robustness of the results against variations of the evolutionary rules. In order to ensure that our findings are no artefacts of the specific choice of evolutionary rules, we tested the robustness of our results against the changes outlined at the end of the model section. We found that making mutation probabilities dependent on biomass or body mass influences the time dependency of the network development but leaves the averaged network properties, like the total network size, the distribution of body masses and the fraction of species or biomasses per trophic level, mostly unchanged. Also the trend towards strong specialisation with subsequent extinctions still occurs in these variants.

When changing the degree to which the parent's body mass is inherited by the mutant, the main effect was that species turnover became slower with stronger inheritance. In this case it is less likely that mutants with body masses between two clusters occur, which have few predators and cause extinction avalanches. The probability for such mutants increases with a decreasing degree of inheritance, which is consistent with our observation that the body mass clusters appear to be blurred in case of a very low degree of inheritance. The same is true for randomly chosen body masses. However, we still obtain large, complex networks.

If the parent species i and the mutant j have similar feeding centres, $f_i \approx f_j$, the initial build-up of different trophic levels and their recovery after an extinction avalanche is also slowed down. With very strong inheritance of the feeding centre, all species will focus on the resource and no mutant emerges with a feeding centre matching the first body mass cluster, leading to trivial structures with only one trophic level. If parent and mutant have a similar degree of specialisation, $s_i \approx s_j$, all species exert and experience a similar competition pressure. Thus, instead of one species displacing another, both populations stay small and hence more populations per trophic level can survive. However, small or intermediate degrees of inheritance in the feeding traits leave the network characteristics again mostly unchanged. The situation is different, when either the feeding range or the feeding centre is chosen from an interval around the parent's trait without any body mass dependent constraint. In consistency with the predictions of Allhoff and Drossel¹⁵, these variants lead to unrealistic trends and trivial instead of complex network structures.

Discussion

We introduced a new evolutionary food web model where the feeding links are based on body mass, and where species differ by body mass, feeding centre, and feeding range. By iterating population dynamics and speciation events for a sufficiently long time, we obtained complex networks, which show a high degree of commonality with empirical food webs. The new model is able to produce more realistic and more diverse network structures than the model by Loeuille and Loreau¹².

Both models use a very similar approach of Gaussian feeding kernels to determine the interactions between the species, which by construction leads to perfectly interval networks. Following the results of Stouffer *et al.*³⁹, we assume this to be a reasonable approximation. In contrast to the model by Loeuille and Loreau, the new model allows for cannibalism and loops, since the feeding range can extend to body masses larger than that of the predator. The species in our model can have different feeding preferences and survival strategies, due to the larger number of evolving traits in our model. This leads to a higher variability in network characteristics such as linkedness, generality and vulnerability, even though natural variability is still larger, which we ascribe to the facts that our model has only one basal resource and no body-size structure within species. We showed that an appropriate choice of the cutoff rule for weak links is essential for obtaining realistic results for connectance and trophic structure.

The increased number of evolving traits compared to the model by Loeuille and Loreau has also a large effect on the evolutionary trends. The networks show an ongoing species turnover and are subject to constant restructuring. The species in our model form body mass clusters and the evolutionary process is characterised by a trend towards increased specialisation on these clusters. Similar specialisation trends have also been observed in other studies^{15,17}. We assume the following explanation for the continuous species turnover. The evolved specialists gradually replace less efficient species with broader feeding ranges that cover also the gaps between the body mass clusters. Those broad ranged species have the role of keystone species that stabilise the networks against the occurrence of large extinction avalanches^{40,41}. In the absence of control by such predators, new mutants (or invaders) can find niches between two clusters with very little predation pressure, where they can grow to high abundance and cause extinction avalanches propagating from lower to higher trophic levels. After such extinction events, the empty niches can be reoccupied also by species with broader feeding ranges, before the speciation process starts again.

This corresponds to the results of Binzer *et al.*⁸, who identified specialised species on high trophic levels to be prone to secondary extinctions, and to the results of Rossberg⁴², who suggested a very similar turnover mechanism for the results of his model. In consistence with the described mechanism, also

Mellard and Ballantyne⁴³ reported that co-evolution of species does not necessarily lead to high levels of resilience for the ecosystem as a whole. However, such a turnover mechanism is missing in the model by Loeuille and Loreau. There, a displaced species is always replaced by a new species of a very similar body mass. And since the body mass is the only evolving trait, the new species has automatically the same predators and the same prey, excluding the possibility of secondary extinctions or major changes in the network structure¹⁵. The same is true for the model version by Brännström *et al.*, which led to evolutionary equilibria, where no more mutants are able to invade the system¹⁴. Ingram *et al.* reported that also their model extension with evolving feeding ranges, but with fixed predator-prey body mass ratios, tends to reach dynamically stable configurations with little structural change¹³.

However, real ecosystems do show extinction events of different sizes, and their distribution evaluated over geological times resembles a power law⁴⁴. For this reason, it has been suggested that ecosystems show self-organised criticality (SOC)⁴⁵, which means that the intrinsic dynamics of the systems is responsible for the power-law size distribution of extinctions. However, the question remains open due to sparse and ambiguous data^{46,47}. Some previous evolutionary food web models, for example the evolutionary niche model¹⁷, exhibit SOC, whereas other models like the webworld model²⁰ or the model by Loeuille and Loreau¹² do not. The size distribution of extinction avalanches in our model is a power law with an exponent around 4 (not shown). Because of its steepness, this power law covers only approximately one decade, meaning that extinction events of more than 10 species are extremely rare. This is not the type of SOC required to explain the large extinction events in earth history, where up to 90 percent of all species went extinct. Regarding the time span a species is present in the system, our model is consistent with paleobiological data concerning the fact that higher trophic level species stay in the system for a shorter time span than lower level species⁴⁶, although it should be mentioned that the exact distribution of these time spans in our model depends on the relation between a species' body mass and its mutation probability.

The evolutionary rules implemented in our model are simplified and to some extent artificial. To make sure that our results do not depend on these simplified rules, we tested several variations concerning the mutation and inheritance rules. Our general finding is that minor changes in the evolutionary algorithm have only minor effects on the results. The overall mechanism with a trend towards specialisation followed by an extinction event as explained above is robust to changes in the evolutionary rules. Also the time averaged network structures remain mostly unchanged. However, the typical time period for a specialisation-extinction cycle can change with extinction events being triggered sooner or later.

The fact that our networks show realistic patterns concerning many common food web properties suggests that our model provides a valuable tool to discuss urgent topics in ecological research. For example, the allometric equations are extendable by temperature terms (e.g.^{48–51}). This approach would allow to model how warming might change evolution and extinction waves, in order to discuss current global change questions.

Another idea would be to address habitat loss and habitat fragmentation as a prominent example of an external driver of extinction events^{52,53}. Recently, various approaches have been made to study the influence of the spatial environment on the food web composition and stability. If space has the structure of discrete habitats, these food webs can be interpreted as “networks of networks”^{54,55}. However, most of the studies on such metacommunities so far focus on spatial aspects under the assumption that the species composition is static, although it has been emphasised that combining the spatial and the evolutionary perspective is essential for a better understanding of ecosystems^{56–58}. Recently, Allhoff *et al.* studied a spatial version of the model by Loeuille and Loreau⁵⁹. However, their findings were associated with the applied competition rules and the remarkable stability of the original model, highlighting the assumption that a more dynamic species turnover as in our new model would lead to a better understanding of the interplay between evolving food web structure and spatial structure.

References

- Drossel, B. & McKane, A. J. *Handbook of Graphs and Networks: From the Genome to the Internet*, Ch. 10, 218–247 (Wiley-VCH Verlag GmbH & Co. KGaA, Weinheim, 2005).
- Williams, R. J. & Martinez, N. D. Simple rules yield complex food webs. *Nature* **404**, 180–182 (2000).
- Cohen, J. & Newman, C. A stochastic theory of community food webs: I. models and aggregated data. *Proceedings of the Royal Society of London. Series B. Biological sciences* **224**, 421–448 (1985).
- Petchey, O. L., Beckerman, A. P., Riede, J. O. & Warren, P. H. Size, foraging, and food web structure. *Proceedings of the National Academy of Sciences* **105**, 4191–4196 (2008).
- Barnosky, A. D. *et al.* Has the earth's sixth mass extinction already arrived? *Nature* **471**, 51–57 (2011).
- Parvinen, K. Evolutionary suicide. *Acta Biotheoretica* **53**, 241–264 (2005).
- Riede, J. O. *et al.* Size-based food web characteristics govern the response to species extinctions. *Basic and Applied Ecology* **12**, 581–589 (2011).
- Binzer, A. *et al.* The susceptibility of species to extinctions in model communities. *Basic and Applied Ecology* **12**, 590–599 (2011).
- May, R. M. Will a large complex system be stable? *Nature* **238**, 413–414 (1972).
- Otto, S. B., Rall, B. C. & Brose, U. Allometric degree distributions facilitate food-web stability. *Nature* **450**, 1226–1229 (2007).
- May, R. Unanswered questions in ecology. *Philos. Trans. R. Soc. London B Biol. Sci.* **354**, 1951–1959 (1999).
- Loeuille, N. & Loreau, M. Evolutionary emergence of size-structured food webs. *PNAS* **102**, 5761–5766 (2005).
- Ingram, T., Harmon, L. J. & Shurin, J. B. Niche evolution, trophic structure, and species turnover in model food webs. *The American Naturalist* **174**, 56–67 (2009).
- Brännström, Å., Loeuille, N., Loreau, M. & Dieckmann, U. Emergence and maintenance of biodiversity in an evolutionary food-web model. *Theoretical Ecology* **4**, 467–478 (2011).

15. Allhoff, K. T. & Drossel, B. When do evolutionary food web models generate complex structures? *Journal of Theoretical Biology* **334**, 122–129 (2013).
16. Brännström, Å. *et al.* Modelling the ecology and evolution of communities: a review of past achievements, current efforts, and future promises. *Evolutionary Ecology Research* **14**, 601–625 (2012).
17. Guill, C. & Drossel, B. Emergence of complexity in evolving niche-model food webs. *Journal of Theoretical Biology* **251**, 108–120 (2008).
18. Rossberg, A., Matsuda, H., Amemiya, T. & Itoh, K. Food webs: Experts consuming families of experts. *Journal of Theoretical Biology* **241**, 552–563 (2006).
19. Rossberg, A., Ishii, R., Amemiya, T. & Itoh, K. The top-down mechanism for body-mass-abundance scaling. *Ecology* **89**, 567–580 (2008).
20. Drossel, B., Higgs, P. G. & McKane, A. J. The influence of predator-prey population dynamics on the long-term evolution of food web structure. *Journal of Theoretical Biology* **208**, 91–107 (2001).
21. Drossel, B., McKane, A. J. & Quince, C. The impact of nonlinear functional responses on the long-term evolution of food web structure. *J. Theor. Biol.* **229**, 539–548 (2004).
22. Bell, G. The evolution of trophic structure. *Heredity* **99**, 494–505 (2007).
23. Yamaguchi, W., Kondoh, M. & Kawata, M. Effects of evolutionary changes in prey use on the relationship between food web complexity and stability. *Popul. Ecol.* **53**, 59–72 (2011).
24. Takahashi, D., Brännström, Å., Mazzucco, R., Yamauchi, A. & Dieckmann, U. Abrupt community transitions and cyclic evolutionary dynamics in complex food webs. *Journal of Theoretical Biology* **337**, 181–189 (2013).
25. Takahashi, D., Brännström, Å., Mazzucco, R., Yamauchi, A. & Dieckmann, U. Cyclic transitions in simulated food-web evolution. *J. Plant. Interact.* **6**, 181–182 (2011).
26. Rall, B. C., Kalinkat, G., Ott, D., Vucic-Pestic, O. & Brose, U. Taxonomic versus allometric constraints on non-linear interaction strengths. *Oikos* **120**, 483–492 (2011).
27. Brose, U. *et al.* Consumer-resource body-size relationships in natural food webs. *Ecology* **87**, 2411–2417 (2006).
28. Riede, J. O. *et al.* Stepping in elton's footprints: a general scaling model for body masses and trophic levels across ecosystems. *Ecology Letters* **14**, 169–178 (2011).
29. Brown, J. H., Gillooly, J. F., Allen, A. P., Savage, V. M. & West, G. B. Toward a metabolic theory of ecology. *Ecology* **85**, 1771–1789 (2004).
30. Yodzis, P. & Innes, S. Body size and consumer-resource dynamics. *The American Naturalist* **139**, 1151–1175 (1992).
31. Brose, U., Williams, R. J. & Martinez, N. D. Allometric scaling enhances stability in complex food webs. *Ecol. Lett.* **9**, 1228–1236 (2006).
32. Beddington, J. R. Mutual interference between parasites or predators and its effect on searching efficiency. *Journal of Animal Ecology* **44**, 331–340 (1975).
33. DeAngelis, D. L., Goldstein, R. A. & O'Neill, R. V. A model for trophic interaction. *Ecology* **56**, 881–892 (1975).
34. Skalski, G. T. & Gilliam, J. F. Functional responses with predator interference: viable alternatives to the holling type ii model. *Ecology* **82**, 3083–3092 (2001).
35. Scheffer, M. & van Nes, E. H. Self-organized similarity, the evolutionary emergence of groups of similar species. *Proceedings of the National Academy of Sciences* **103**, 6230–6235 (2006).
36. May, R. M. On the theory of niche overlap. *Theoretical Population Biology* **5**, 297–332 (1974).
37. Galassi, M. *et al.* *GNU Scientific Library Reference Manual* (Network Theory Ltd, 2009).
38. Riede, J. O. *et al.* Scaling of food-web properties with diversity and complexity across ecosystems. *Advances In Ecological Research* **42**, 139–170 (2010).
39. Stouffer, D. B., Camacho, J. & Amaral, L. A. N. A robust measure of food web intervality. *Proceedings of the National Academy of Sciences* **103**, 19015–19020 (2006).
40. Power, M. E. *et al.* Challenges in the quest for keystones. *Bioscience* **46**, 609–620 (1996).
41. Eklöf, A. & Ebenmann, B. Species loss and secondary extinctions in simple and complex model communities. *Journal of Animal Ecology* **75**, 239–246 (2006).
42. Rossberg, A. G. *Food webs and biodiversity: foundations, models, data*, Ch. 22, 287–309 (John Wiley & Sons, 2013).
43. Mellard, J. P. & Ballantyne IV, F. Conflict between dynamical and evolutionary stability in simple ecosystems. *Theoretical Ecology* **7**, 273–288 (2014).
44. Raup, D. Biological extinction in earth history. *Science* **231**, 1528–1533 (1986).
45. Snepken, K., Bak, P., Flyvbjerg, H. & Jensen, M. H. Evolution as a self-organized critical phenomenon. *Proceedings of the National Academy of Sciences* **92**, 5209–5213 (1995).
46. Newman, M. E. & Palmer, R. G. *Modeling extinction* (Oxford University Press, 2003).
47. Drossel, B. Biological evolution and statistical physics. *Advances in Physics* **50**, 209–295 (2001).
48. Vasseur, D. A. & McCann, K. S. A mechanistic approach for modeling temperature-dependent consumer-resource dynamics. *The American Naturalist* **166**, 184–198 (2005).
49. Binzer, A., Guill, C., Brose, U. & Rall, B. C. The dynamics of food chains under climate change and nutrient enrichment. *Philosophical Transactions of the Royal Society B: Biological Sciences* **367**, 2935–2944 (2012).
50. Norberg, J., Urban, M. C., Vellend, M., Klausmeier, C. A. & Loeuille, N. Eco-evolutionary responses of biodiversity to climate change. *Nature Climate Change* **2**, 747–751 (2012).
51. Stegen, J. C., Ferriere, R. & Enquist, B. J. Evolving ecological networks and the emergence of biodiversity patterns across temperature gradients. *Proceedings of the Royal Society of London B: Biological Sciences* **279**, 1051–1060 (2012).
52. Hagen, M. *et al.* Biodiversity, species interactions and ecological networks in a fragmented world. *Advances in Ecological Research* **46**, 89–210 (2012).
53. Gonzalez, A., Rayfield, B. & Lindo, Z. The disentangled bank: How loss of habitat fragments and disassembles ecological networks. *American Journal of Botany* **98**, 503–516 (2011).
54. Amarasekare, P. Spatial dynamics of foodwebs. *Annual Review of Ecology, Evolution, and Systematics* **39**, 479–500 (2008).
55. Leibold, M. A. *et al.* The metacommunity concept: a framework for multi-scale community ecology. *Ecology letters* **7**, 601–613 (2004).
56. Logue, J. B., Mouquet, N., Peter, H. & Hillebrand, H. Empirical approaches to metacommunities: a review and comparison with theory. *Trends in Ecology & Evolution* **26**, 482–491 (2011).
57. Urban, M. C. *et al.* The evolutionary ecology of metacommunities. *Trends in Ecology & Evolution* **23**, 311–317 (2008).
58. Loeuille, N. & Leibold, M. Ecological consequences of evolution in plant defenses in a metacommunity. *Theoretical population biology* **74**, 34–45 (2008).
59. Allhoff, K. T., Weiel, E. M., Rogge, T. & Drossel, B. On the interplay of speciation and dispersal: An evolutionary food web model in space. *Journal of Theoretical Biology* **366**, 46–56 (2014).
60. Williams, R. J. & Martinez, N. D. Limits to trophic levels and omnivory in complex food webs: Theory and data. *The American Naturalist* **163**, 458–468 (2004).

Acknowledgements

This work was supported by the DFG under contract number Dr300/12-1 and 13-1. C.G. was supported by the Leopoldina Fellowship Program under contract number LPDS 2012-07. We thank Markus Schiffhauer and Jannis Weigend, who analysed several model variants concerning the mutation and heredity rules in the context of their bachelor theses. Moreover, we thank Christoph Digel and Jens Riede for providing empirical data and Sebastian Plitzko and Bernd Blasius for very helpful discussions.

Author Contributions

All authors designed the model. K.T.A. performed the simulations. K.T.A. and C.G. analysed the results. K.T.A. wrote the manuscript with minor contributions from the other authors. All authors reviewed the manuscript.

Additional Information

Supplementary information accompanies this paper at <http://www.nature.com/srep>

Competing financial interests: The authors declare no competing financial interests.

How to cite this article: Allhoff, K.T. *et al.* Evolutionary food web model based on body masses gives realistic networks with permanent species turnover. *Sci. Rep.* **5**, 10955; doi: 10.1038/srep10955 (2015).



This work is licensed under a Creative Commons Attribution 4.0 International License. The images or other third party material in this article are included in the article's Creative Commons license, unless indicated otherwise in the credit line; if the material is not included under the Creative Commons license, users will need to obtain permission from the license holder to reproduce the material. To view a copy of this license, visit <http://creativecommons.org/licenses/by/4.0/>

Bibliography

- Abrams, P. A., 2000. The evolution of predator-prey interactions: Theory and evidence. *Annual Review of Ecology and Systematics* 31:pp. 79–105.
- Allesina, S., D. Alonso, and M. Pascual, 2008. A general model for food web structure. *Science* (New York, N.Y.) 320:658–61.
- Allhoff, K. T. and B. Drossel, 2013. When do evolutionary food web models generate complex networks? *Journal of Theoretical Biology* 334:122 – 129.
- Allhoff, K. T., D. Ritterskamp, and B. G. C. Rall, B. C. Drossel, 2015a. Evolutionary food web model based on body masses gives realistic networks with permanent species turnover. *Scientific Report* 5.
- Allhoff, K. T., E. M. Weiel, T. Rogge, and B. Drossel, 2015b. On the interplay of speciation and dispersal: An evolutionary food web model in space. *Journal of Theoretical Biology* 366:46 – 56.
- Amarasekare, P., 2008. Spatial dynamics of foodwebs. *Annual Review of Ecology, Evolution, and Systematics* 39:pp. 479–500.
- Beddington, J. R., 1975. Mutual interference between parasites or predators and its effect on searching efficiency. *Journal of Animal Ecology* 44:pp. 331–340.
- Berg, M. P. and J. Bengtsson, 2007. Temporal and spatial variability in soil food web structure. *Oikos* 116:1789–1804.
- Binzer, A., U. Brose, A. Curtsdotter, A. Eklöf, B. C. Rall, J. O. Riede, and F. de Castro, 2011. The susceptibility of species to extinctions in model communities. *Basic and Applied Ecology* 12:590 – 599.
- Brännström, A. and J. Johansson, 2012. Modelling the ecology and evolution of communities: a review of past achievements, current efforts, and future promises. *Evolutionary Ecology Research* 14:601–625.
- Brännström, A., N. Loeuille, M. Loreau, and U. Dieckmann, 2011. Emergence and maintenance of biodiversity in an evolutionary food-web model. *Theoretical Ecology* 4:467–478.
- Brose, U., R. B. Ehnes, B. C. Rall, O. Vucic-Pestic, E. L. Berlow, and S. Scheu, 2008. Foraging theory predicts predator–prey energy fluxes. *Journal of Animal Ecology* 77:1072–1078.

Bibliography

- Brose, U., A. Ostling, K. Harrison, and N. D. Martinez, 2004. Unified spatial scaling of species and their trophic interactions. *Nature* 428:167–171.
- Brose, U., R. J. Williams, and N. D. Martinez, 2006. Allometric scaling enhances stability in complex food webs. *Ecology Letters* 9:1228–1236.
- Burke, C., P. Steinberg, D. Rusch, S. Kjelleberg, and T. Thomas, 2011. Bacterial community assembly based on functional genes rather than species. *Proceedings of the National Academy of Sciences* 108:14288–14293.
- Caldarelli, G., P. G. Higgs, and A. J. McKane, 1998. Modelling coevolution in multispecies communities. *Journal of Theoretical Biology* 193:345 – 358.
- Cantrell, R. S. and C. Cosner, 2003. *Spatial Ecology via Reaction-Diffusion Equations*. Wiley.
- Cohen, J. E., 1977. Food webs and the dimensionality of trophic niche space. *Proceedings of the National Academy of Sciences* 74:4533–4536.
- Cohen, J. E., 1997. Ratio of prey and predators in community food webs. *Nature* 270:165–167.
- Cohen, J. E. and C. M. Newman, 1985. A stochastic theory of community food webs: I. models and aggregated data. *Proceedings of the Royal Society of London. Series B, Biological Sciences* 224:pp. 421–448.
- Cohen, S. D. and A. C. Hindmarsh, 1996. CVODE, A Stiff/Nonstiff ODE Solver in C. *Computers in Physics* 10:138–143.
- Connell, J. H., 1980. Diversity and the coevolution of competitors, or the ghost of competition past. *Oikos* 35:pp. 131–138.
- Connor, E. F. and E. D. McCoy, 1979. The statistics and biology of the species-area relationship. *The American Naturalist* 113:pp. 791–833.
- Cope, E. D., 1896. *The primary factors of organic evolution*, by E. D. Cope. Chicago, The Open Court Publishing Company,.
- Darwin, C., 2011. *The Origin of Species by Means of Natural Selection: Or, the Preservation of Favored Races in the Struggle for Life*. Unabridged ed. Blackstone Audio, Inc.
- Dieckmann, U. and R. Law, 1996. The dynamical theory of coevolution: a derivation from stochastic ecological processes. *Journal of Mathematical Biology* 34:579–612.
- Dirzo, R., H. S. Young, M. Galetti, G. Ceballos, N. J. B. Isaac, and B. Collen, 2014. Defaunation in the anthropocene. *Science* 345:401–406.
- Dobson, A., D. Lodge, J. Alder, G. S. Cumming, J. Keymer, J. McGlade, H. Mooney, J. A. Rusak, O. Sala, V. Wolters, D. Wall, R. Winfree, and M. A. Xenopoulos, 2006. Habitat loss, trophic collapse, and the decline of ecosystem services. *Ecology* 87:1915–1924.

- Dommar, C., A. Ryabov, and B. Blasius, 2008. Coevolutionary motion and swarming in a niche space model of ecological species interactions. *The European Physical Journal Special Topics* 157:223–238.
- Downing, A. S., S. Hajdu, O. Hjerne, S. A. Otto, T. Blenckner, U. Larsson, and M. Winder, 2014. Zooming in on size distribution patterns underlying species coexistence in baltic sea phytoplankton. *Ecology Letters* 17:1219–1227.
- Drossel, B., P. G. Higgs, and A. J. Mckane, 2001. The influence of predator–prey population dynamics on the long-term evolution of food web structure. *Journal of Theoretical Biology* 208:91 – 107.
- Dunbar, M., 1953. Arctic and subarctic marine ecology: Immediate problems. *ARCTIC* 6.
- Dunne, J. A., 2009. Food webs. Pp. 3661–3682, *in* R. A. Meyers, ed. *Encyclopedia of Complexity and Systems Science*. Springer.
- Egerton, F. N., 2007. Understanding food chains and food webs, 1700–1970. *Bulletin of the Ecological Society of America* 88:50–69.
- Eklöf, A., U. Jacob, J. Kopp, J. Bosch, R. Castro-Urgal, N. P. Chacoff, B. Dalsgaard, C. de Sassi, M. Galetti, P. R. Guimarães, S. B. Lomáscolo, A. M. Martín González, M. A. Pizo, R. Rader, A. Rodrigo, J. M. Tylianakis, D. P. Vázquez, and S. Allesina, 2013. The dimensionality of ecological networks. *Ecology Letters* 16:577–583.
- Ettema, C. H. and D. A. Wardle, 2002. Spatial soil ecology. *Trends in Ecology & Evolution* 17:177 – 183.
- Fukami, T., D. A. Wardle, P. J. Bellingham, C. P. H. Mulder, D. R. Towns, G. W. Yeates, K. I. Bonner, M. S. Durrett, M. N. Grant-Hoffman, and W. M. Williamson, 2006. Above- and below-ground impacts of introduced predators in seabird-dominated island ecosystems. *Ecology Letters* 9:1299–1307.
- Fussmann, G. F., S. P. Ellner, K. W. Shertzer, and N. G. Hairston Jr., 2000. Crossing the hopf bifurcation in a live predator-prey system. *Science* 290:1358–1360.
- Fussmann, G. F. and G. Heber, 2002. Food web complexity and chaotic population dynamics. *Ecology Letters* 5:394–401.
- Fussmann, G. F., M. Loreau, and P. A. Abrams, 2007. Eco-evolutionary dynamics of communities and ecosystems. *Functional Ecology* 21:465–477.
- Gaston, K. J., R. G. Davies, C. D. L. Orme, V. A. Olson, G. H. Thomas, T.-S. Ding, P. C. Rasmussen, J. J. Lennon, P. M. Bennett, I. P. Owens, and T. M. Blackburn, 2007. Spatial turnover in the global avifauna. *Proceedings of the Royal Society of London B: Biological Sciences* 274:1567–1574.
- Geritz, S., E. Kisdi, G. Mesze, and J. Metz, 1998. Evolutionarily singular strategies and the adaptive growth and branching of the evolutionary tree. *Evolutionary Ecology* 12:35–57.

Bibliography

- Gough, B., 2009. GNU Scientific Library Reference Manual - Third Edition. 3rd ed. Network Theory Ltd.
- Gramlich, P., S. J. Plitzko, L. Rudolf, B. Drossel, and T. Gross, 2015. The influence of dispersal on a predator-prey system with two habitats. ArXiv e-prints .
- Guo, Z., L. Zhang, and Y. Li, 2010. Increased dependence of humans on ecosystem services and biodiversity. PLoS ONE 5:e13113.
- Hartvig, M., 2011. Food web ecology: individual life-histories and ecological processes shape complex communities. Ph.D. thesis.
- Hebblewhite, M. and E. H. Merrill, 2009. Trade-offs between predation risk and forage differ between migrant strategies in a migratory ungulate. Ecology 90:pp. 3445–3454.
- Heckmann, L., B. Drossel, U. Brose, and C. Guill, 2012. Interactive effects of body-size structure and adaptive foraging on food-web stability. Ecology Letters 15:243–250.
- Holling, C. S., 1959. The components of predation as revealed by a study of small-mammal predation of the european pine sawfly. The Canadian Entomologist 91:293–320.
- Holomuzki, J. R., 1986. Predator avoidance and diel patterns of microhabitat use by larval tiger salamanders. Ecology 67:pp. 737–748.
- Holt, R. D., 2002. Food webs in space: On the interplay of dynamic instability and spatial processes. Ecological Research 17:261–273.
- Hone, D. W. and M. J. Benton, 2005. The evolution of large size: how does cope's rule work? Trends in Ecology & Evolution 20:4 – 6.
- Huisman, J., A. M. Johansson, E. O. Folmer, and F. J. Weissing, 2001. Towards a solution of the plankton paradox: the importance of physiology and life history. Ecology Letters 4:408–411.
- Huisman, J. and F. J. Weissing, 1999. Biodiversity of plankton by species oscillations and chaos. Nature Pp. 407–410.
- Ingram, T., L. J. Harmon, and J. B. Shurin, 2009. Niche evolution, trophic structure, and species turnover in model food webs. The American naturalist 174:56–67.
- Jennings, S., J. K. Pinnegar, N. V. C. Polunin, and K. J. Warr, 2002. Linking size-based and trophic analyses of benthic community structure. Marine Ecology Progress Series 226:77–85.
- Kingsolver, J. G. and D. W. Pfennig, 2004. Individual-level selection as a cause of cope's rule of phyletic size increase. Evolution 58:pp. 1608–1612.
- Larios, L. and K. N. Suding, 2014. Competition and soil resource environment alter plant-soil feedbacks for a native and exotic grass. AoB Plants .
- Laverman, A., P. Borgers, and H. Verhoef, 2002. Spatial variation in net nitrate production in a n-saturated coniferous forest soil. Forest Ecology and Management 161:123 – 132.

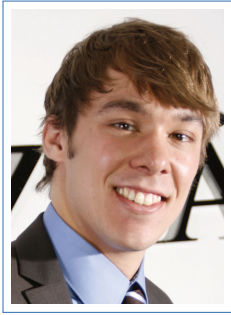
- Leibold, M. A., M. Holyoak, N. Mouquet, P. Amarasekare, J. M. Chase, M. F. Hoopes, R. D. Holt, J. B. Shurin, R. Law, D. Tilman, M. Loreau, and A. Gonzalez, 2004. The metacommunity concept: a framework for multi-scale community ecology. *Ecology Letters* 7:601–613.
- Loeuille, N. and M. Loreau, 2005. Evolutionary emergence of size-structured food webs. *Proceedings of the National Academy of Sciences of the United States of America* 102:5761–5766.
- Loeuille, N. and M. Loreau, 2006. Evolution of body size in food webs: does the energetic equivalence rule hold? *Ecology Letters* 9:171–178.
- Loeuille, N. and M. Loreau, 2009. Emergence of complex food web structure in community evolution models. *in* H. A. Verhoef and M. P. J., eds. *Community Ecology: Processes, Models, and Applications*. Oxford University Press.
- Lurgi, M., N. Galiana, B. C. López, L. Joppa, and J. M. Montoya, 2014. Network complexity and species traits mediate the effects of biological invasions on dynamic foodwebs. *Frontiers in Ecology and Evolution* 2.
- MacArthur, R. and R. Levins, 1967. The limiting similarity, convergence, and divergence of coexisting species. *The American Naturalist* 101:pp. 377–385.
- MacArthur, R. H., 1957. On the relative abundance of bird species. *Proceedings of the National Academy of Sciences of the United States of America* 43:pp. 293–295.
- MacDonald, N., 1976. Time delay in simple chemostat models. *Biotechnology and Bioengineering* 18:805–812.
- Martinez, H. B. A., Neo D. and, H. A. Dawah, and B. P. Feifarek, 1999. Effects of sampling effort on characterization of food-web structure. *Ecology* 80:1044–1055.
- Matsuda, H. and P. A. Abrams, 1994. Runaway evolution to self-extinction under asymmetrical competition. *Evolution* 48:1764–1772.
- May, R. M., 1972. Will a large complex system be stable? *Nature* 238:413–414.
- McCann, K., A. Hastings, and G. R. Huxel, 1998. Weak trophic interactions and the balance of nature. *Nature* 395:pp. 794–798.
- McCann, K. S., 2000. The diversity-stability debate. *Nature* 405:228–233.
- McCann, K. S., J. B. Rasmussen, and J. Umbanhowar, 2005. The dynamics of spatially coupled food webs. *Ecology Letters* 8:513–523.
- Mercedes, P. and J. A. Dunne, 2005. From small to large ecological networks in a dynamic world. Pp. 3–24, *in* M. Pascual and J. A. Dunne, eds. *Ecological Networks: Linking Structure to Dynamics in Food Webs* (Santa Fe Institute Studies on the Sciences of Complexity). Oxford University Press.

Bibliography

- Millennium Ecosystem Assessment, 2003. Ecosystems and human well-being: A framework for assessment (millennium ecosystem assessment series).
- Mortlock, R. (ed.) 2012. Microorganisms as Model Systems for Studying Evolution (Monographs in Evolutionary Biology). Softcover reprint of the original 1st ed. 1984 ed. Springer.
- Munday, P. L., 2004. Competitive coexistence of coral-dwelling fishes: The lottery hypothesis revisited. *Ecological Society of America* 85:623–628.
- Novick, A. and L. Szilard, 1950. Description of the chemostat. *Science* 112:715–716.
- Persson, L., S. Diehl, L. Johansson, G. Andersson, and S. F. Hamrin, 1992. Trophic interactions in temperate lake ecosystems: A test of food chain theory. *The American Naturalist* 140:pp. 59–84.
- Peters, R. H., 1986. *The Ecological Implications of Body Size* (Cambridge Studies in Ecology). Cambridge University Press.
- Pillai, P., A. Gonzalez, and M. Loreau, 2011. Metacommunity theory explains the emergence of food web complexity. *Proceedings of the National Academy of Sciences* 108:19293–19298.
- Pillai, P., M. Loreau, and A. Gonzalez, 2010. A patch-dynamic framework for food web metacommunities. *Theoretical Ecology* 3:223–237.
- Polis, G. A., 1991. Complex trophic interactions in deserts: An empirical critique of food-web theory. *The American Naturalist* 138:pp. 123–155.
- Press, W. H., S. A. Teukolsky, W. T. Vetterling, and B. P. Flannery, 2007. *Numerical Recipes 3rd Edition: The Art of Scientific Computing*. Cambridge University Press.
- Ricklefs, R. E. and E. Bermingham, 2002. The concept of the taxon cycle in biogeography. *Global Ecology and Biogeography* 11:353–361.
- Ricklefs, R. E., G. W. Cox, S. The, A. Naturalist, and N. M. Apr, 2014. *The University of Chicago Taxon Cycles in the West Indian Avifauna* 106:195–219.
- Riede, J. O., U. Brose, B. Ebenman, U. Jacob, R. Thompson, C. R. Townsend, and T. Jonsson, 2011. Stepping in elton's footprints: a general scaling model for body masses and trophic levels across ecosystems. *Ecology Letters* 14:169–178.
- Ristl, K., S. J. Plitzko, and B. Drossel, 2014. Complex response of a food-web module to symmetric and asymmetric migration between several patches. *Journal of Theoretical Biology* 354:54 – 59.
- Ritterskamp, D., D. Bearup, and B. Blasius, 2015a. Evolutionary cycles in an evolutionary food web model. in preparation .
- Ritterskamp, D., D. Bearup, and B. Blasius, 2015b. A new dimension: Evolutionary food web dynamics in two dimensional trait space. under Review .

- Rosenzweig, M. L., J. S. Brown, and T. L. Vincent, 1987. Red queens and ess: the coevolution of evolutionary rates. *Evolutionary Ecology* 1:59–94.
- Rossberg, A., M. H. T. Amemiya, and K. Itoh, 2006. Food webs: Experts consuming families of experts. *Journal of Theoretical Biology* 241:552 – 563.
- Rothstein, S. I., 1990. A model system for coevolution: Avian brood parasitism. *Annual Review of Ecology and Systematics* 21:pp. 481–508.
- Roughgarden, J., 1972. Evolution of niche width. *The American Naturalist* 106:pp. 683–718.
- Roughgarden, J. and S. Pacala, 1989. Taxon cycle among anolis lizard populations: review of evidence. *Speciation and its consequences* Pp. 403–432.
- Ruan, S. and G. S. Wolkowicz, 1996. Bifurcation analysis of a chemostat model with a distributed delay. *Journal of Mathematical Analysis and Applications* 204:786 – 812.
- Rummel, J. D. and J. Roughgarden, 1983. Some differences between invasion-structured and coevolution-structured competitive communities: A preliminary theoretical analysis. *Oikos* 41:477–486.
- Rummel, J. D. and J. Roughgarden, 1985. A Theory of Faunal Buildup for Competition Communities. *Evolution* 39:1009–1033.
- Saetre, P. and E. Bååth, 2000. Spatial variation and patterns of soil microbial community structure in a mixed spruce–birch stand. *Soil Biology and Biochemistry* 32:909 – 917.
- Scheffer, M. and E. H. van Nes, 2006. Self-organized similarity, the evolutionary emergence of groups of similar species. *Proceedings of the National Academy of Sciences of the United States of America* 103:6230–5.
- Schwarz Müller, F., N. Eisenhauer, and U. Brose, 2015. 'trophic whales' as biotic buffers: weak interactions stabilize ecosystems against nutrient enrichment. *Journal of Animal Ecology* 84:680–691.
- Sommer, U., H. Stibor, A. Katechakis, F. Sommer, and T. Hansen, 2002. Pelagic food web configurations at different levels of nutrient richness and their implications for the ratio fish production:primary production. *Hydrobiologia* 484:11–20.
- Stomp, M., J. Huisman, E. Mittelbach, and C. A. Klausmeier, 2011. Large-scale biodiversity patterns in freshwater phytoplankton. *Ecology* 92:2096–2107.
- Stouffer, D. B., J. Camacho, and L. A. N. Amaral, 2006. A robust measure of food web intervality. *Proceedings of the National Academy of Sciences* 103:19015–19020.
- Stouffer, D. B., J. Camacho, W. Jiang, and L. A. Nunes Amaral, 2007. Evidence for the existence of a robust pattern of prey selection in food webs. *Proceedings of the Royal Society of London B: Biological Sciences* 274:1931–1940.

- Strong, D. R., 1992. Are trophic cascades all wet? differentiation and donor-control in speciose ecosystems. *Ecology* 73:pp. 747–754.
- Sutherland, J. and N. Y. S. D. of Environmental Conservation, 1989. Field surveys of the biota and selected water chemistry parameters in 50 adirondack mountain lakes .
- Takahashi, D., A. Brännström, R. Mazzucco, A. Yamauchi, and U. Dieckmann, 2011. Cyclic transitions in simulated food-web evolution. *Journal of Plant Interactions* 6:181–182.
- Takahashi, D., A. Brännström, R. Mazzucco, A. Yamauchi, and U. Dieckmann, 2013. Abrupt community transitions and cyclic evolutionary dynamics in complex food webs. *Journal of Theoretical Biology* 337:181 – 189.
- Taper, M. and T. Case, 1992. Models of character displacement and the theoretical robustness of taxon cycles. *Evolution* 46:317–333.
- Turchin, P., 2003. Complex population dynamics: a theoretical/empirical synthesis, vol. 35. Princeton University Press.
- Urban, M. C., 2010. Microgeographic adaptations of spotted salamander morphological defenses in response to a predaceous salamander and beetle. *Oikos* 119:646–658.
- Vucic-Pestic, O., B. C. Rall, G. Kalinkat, and U. Brose, 2010. Allometric functional response model: body masses constrain interaction strengths. *Journal of Animal Ecology* 79:249–256.
- Wardle, D. A., R. D. Bardgett, J. N. Klironomos, H. Setälä, W. H. van der Putten, and D. H. Wall, 2004. Ecological linkages between aboveground and belowground biota. *Science* 304:1629–1633.
- Williams, R. J. and N. D. Martinez, 2000. Simple rules yield complex food webs. *Nature* 404:180–183.
- Williams, R. J. and N. D. Martinez, 2004. Limits to trophic levels and omnivory in complex food webs: Theory and data. *The American Naturalist* 163:pp. 458–468.
- Williams, R. J. and N. D. Martinez, 2008. Success and its limits among structural models of complex food webs. *Journal of Animal Ecology* 77:512–519.
- Wilson, E. O., 1961. The nature of the taxon cycle in the melanesian ant fauna. *The American Naturalist* 95:169–193.
- Wolkowicz, G. S. K. and H. Xia, 1997. Global asymptotic behavior of a chemostat model with discrete delays. *SIAM Journal on Applied Mathematics* 57:1019–1043.
- Yodzis, P. and S. Innes, 1992. Body size and consumer-resource dynamics. *The American Naturalist* 139:pp. 1151–1175.
- Zhang, L., M. Hartvig, K. Knudsen, and K. Andersen, 2014. Size-based predictions of food web patterns. *Theoretical Ecology* 7:23–33.



Daniel Ritterskamp

Curriculum Vitae

Personal Details

Name: Daniel Ritterskamp
Address: Lindenallee 12
26122 Oldenburg
Germany
Born: 30/07/1987
Email: daniel.ritterskamp@outlook.de

Education

- 30/09/2015: **Disputation: Evolutionary Dynamics in Food Webs: Influence of Resources and Space.**
- 1/08/2012: **PhD candidate in the group of Prof. B. Blasius. Embedded in the graduate school "Environmental Sciences and Biodiversity", Carl von Ossietzky University in Oldenburg, Germany .**
- 27/02/2012: **Diploma Degree in Physics (1.0, very good), Westfälische Wilhelms University in Münster, Germany.**
- 10/2010-1/2012: **Diploma thesis "A Neural Network with Synaptic Plasticity: Applications to Epileptic Seizures" in the group of Prof. R. Friedrich, Westfälische Wilhelms University in Münster, Germany.**
- 9/2009-9/2010: **Erasmus exchange, University of Strathclyde in Glasgow, United Kingdom.**
- 09/2008: **"Intermediate Diploma" (1.3, very good), Westfälische Wilhelms University in Münster, Germany.**
- 8/2006: **A-Level (2.3, good), Liebfrauenschule Mülhausen in Grefrath, Germany .**

Conferences and Summer schools

- 3/2015: **Invitation to the group Seminar of Frank Hilker**, Talk, *Osnabrück, Germany*.
3/2015: **DPG Spring Meeting 2015**, Talk, *Berlin, Germany*.
10/2014: **Workshop "Networks on Networks"**, Talk, *Goettingen, Germany*.
10/2014: **Dynamic Days Europe 2014**, Talk, *Bayreuth, Germany*.
9/2014: **Models in Population Dynamics and Ecology 2014**, Talk, *Turin, Italy*.
5/2014: **Workshop "Modelling and Analysis of Innovation and Competition Processes" (Adaptive Dynamics)**, *Milan, Italy*.
10/2013: **Workshop on the Structure and dynamics of meta-food webs**, Talk, *Bielefeld, Germany*.
9/2013: **Models in Population Dynamics and Ecology 2013**, Talk in Minisymposium, *Osnabrück, Germany*.
9/2013: **11th INTECOL 2013**, Talk, *London, United Kingdom*.
8/2012: **Summer School "Modern computational science: Optimization"**, *Oldenburg, Germany*.
9/2011: **Dynamic Days 2011**, Poster contribution, *Oldenburg, Germany*.
6/2011: **Summer School "Computational Neuroscience"**, *Ottawa, Canada*.

Honors and scholarship

Promos scholarship, 2011.

Germany Scholarship, 2011-2012.

Erasmus scholarship, 2009-2010.

Entry in the Dean's List of the University of Strathclyde Glasgow for outstanding marks, 2010.

Publications

In Preparation:

Paper I **D Ritterskamp, D Bearup and B Blasius**. Evolutionary cycles in an evolutionary food web model, in preperation

Paper II **D Ritterskamp, D Bearup, C Feenders and B Blasius**. Evolutionary food web models: effects of an additional resource, in preperation

Submitted:

Paper III **D Ritterskamp, D Bearup and B Blasius**. A New Dimension: The Influence of Two Dimensional Niche Space on Evolutionary Food Web Models, submitted

Published:

Appendix Paper **KT Allhoff, D Ritterskamp, BC Rall, B Drossel and C Guill**. Evolutionary food web model based on body masses gives realistic networks with permanent species turnover, *Scientific Reports* **5**, 2015, doi: 10.1038/srep10955

Danksagung

“So long and thanks for all the fish.”

— Douglas Adams —

The Hitchhiker's Guide to the Galaxy

Ich schreibe diese Danksagung am Vorabend der Abgabe mit einem Glas Whisky in der Hand. Beides habe ich mir bis zum Schluss aufgehoben: Dieses Kapitel, weil es am angenehmsten ist und den Whisky zur Belohnung. Ich hätte es nicht alleine bis hierhin geschafft und deswegen möchte ich mich bei allen bedanken, die mich während meiner Dissertation unterstützt haben.

Zuerst möchte ich meinem Doktorvater Bernd meinen Dank aussprechen. Seine Art der Betreuung habe ich sehr geschätzt, da ich das Gefühl, hatte meinen eigenen wissenschaftlichen Interessengebieten nachgehen zu dürfen und dabei unterstützt zu werden. Er hatte immer eine offene Tür, um bei Problemen zu helfen und einen Input an Ideen zu geben, der wirklich unerschöpflich war. Auch für die Gelegenheit diverse Tagungen zu besuchen, möchte ich mich bedanken, da dies nicht immer selbstverständlich ist.

Auch bei Frank möchte ich mich bedanken. Nicht nur dafür, dass er sich bereit erklärt hat, das Zweitgutachten meiner Arbeit zu übernehmen, sondern auch für die Einladung in sein Gruppenseminar und was noch wichtiger ist für die Unterstützung meines Eiskonsums in Turin, als auch für den anschließenden Lauf, um die angesammelte Energie wieder los zu werden.

Des weiteren möchte ich Jörg-Olaf Wolff dafür danken, dass er sich so spontan dazu bereit erklärt hat, als Prüfer zu fungieren, als auch für seine ruhige und freundliche Art während der Prüfung.

If I have to state two situations that characterise our working group, I would name our coffee meetings after lunch and the preparation for a conference talk. I would have never expected that one can discuss a fifteen minute talk for nearly two hours. I do not want to miss this input and it really helped me preparing for conferences! Therefore, I want to thank all members of our working group for the support, the advice and the nice atmosphere. Special thanks go to the following members that accompanied me for the better part of the last three years:

Alexey möchte ich für die vielen Diskussionen, seine Geduld und für die Einführung in russische Spitznamen danken. Leider habe ich es nicht mehr geschafft, das Wort “Löffel” in kyrillisch zu schreiben. Ein außerordentlich großes Dankeschön gebührt Cora. Für die Hilfe bei moralischen Programmierfragen, für das Bekanntmachen mit dem Känguru, was mich wohl mein Leben lang verfolgen wird, und für das offene Ohr bei Problemen in jeglicher Hinsicht. Ich glaube, ohne sie hätte ich nur halb so viel Spaß gehabt! Auch Christoph gebührt mein Dank für die Hilfe bei Computerproblemen, als auch für die Hilfe beim Schreiben. In beiden Dingen habe ich viel von ihm gelernt. Christoph, ich genieße gerade übrigens einen Deanston, der

die Frechheit besitzt mit "Virgin Oak Casks" zu werben. Special thanks go to Daniel, for his patience regarding my writing, for supporting me in research questions but also for the time spent together. I really enjoyed it and so did he, even if he won't admit it. He is officially invited to visit me in Bristol. Ich möchte mich auch bei Hanno bedanken, unter anderem für die vielen guten Ratschläge bzgl. der Übungsgruppen. Er kann sicher sein, dass ich mich an ihn wenden werde, wenn ich jemals ein Fachwerkhaus kaufe. Besonderer Dank gebührt Lena, mit der ich ein Büro teile, da sie mir in der Endphase sehr geholfen hat, wie zum Beispiel durch regelmäßiges Kaffetrinken oder beim einstellen der Bindekorrektur. Ebenso möchte ich mich bei Siri bedanken, die leider den ein oder anderen schlechten Witz aufgrund ihres Namens von meiner Seite ertragen musste. Sie hat mir vor allem die Ankunft in Oldenburg sehr erleichtert.

Nicht zu vergessen sind auch Johannes und Benjamin, die zwar nicht zu unserer Arbeitsgruppe gehören, aber mit denen ich mir für fast drei Jahre ein Büro geteilt habe. Vielen Dank für die schöne Atmosphäre. Außerdem möchte ich Florian und Korinna danken, die Teil der selben Forschergruppe waren und sich durch meine Arbeit quälen mussten. Lautes Piratengeschrei ist an sie gerichtet.

Natürlich möchte ich mich auch bei Leuten außerhalb des universitären Umfeldes bedanken. Ich möchte mit meiner WG beginnen: Luana, Max, Henning, Nico und Dominik. Ihr habt mir die Ankunft in Oldenburg erleichtert und unsere Wohnung für mich zu einem Zuhause gemacht. Vielen Dank für das immer offene Ohr und die vielen guten Zeiten, die ich in Erinnerung behalten werde. Ohne euch hätte ich die letzten drei Jahre nicht so genießen können. Zusätzlicher Dank geht nochmals an Dominik, Henning und Max für das Korrekturlesen. Nicht zu vergessen ist auch mein alter Mitbewohner Marc aus Münster, da er sich ebenfalls durch die Arbeit quälen musste. Bedanken möchte ich mich auch bei Oliver für seine Ratschläge, die ich schätze und immer schätzen werden: Viel Glück euch dreien!

Auch bei meiner Schwester möchte ich mich für das Korrekturlesen bedanken. Natürlich geht mein Dank an sie darüber hinaus, da sie und meine restliche Familie mir immer den nötigen Rückhalt gegeben haben und mich in jeglicher Lebenslage unterstützt haben. Ich freue mich schon darauf, wieder mehr Zeit für diese zu haben!

Ein Dank geht auch an viele Andere, die hier nicht namentlich erwähnt werden: Alle Leute in Oldenburg, die diese Stadt für mich zu einer Heimat gemacht haben, Zeit für mich hatten, wenn ich sie brauchte und großes Verständnis mit mir in der Endphase meiner Abgabe hatten. Zuletzt möchte ich mich noch bei den Mensamitarbeitern bedanken, da sie meiner Meinung nach zu wenig bedacht werden. Sie haben mir die nachmittäglichen Pausen sprichwörtlich versüßt.

Vielen Dank für alles